DOI: 10.31891/2079-1372

THE INTERNATIONAL SCIENTIFIC JOURNAL

PROBLEMS OF TRIBOLOGY

Volume 27 ***No 3/105-2022***

МІЖНАРОДНИЙ НАУКОВИЙ ЖУРНАЛ

ПРОБЛЕМИ ТРИБОЛОГІЇ

PROBLEMS OF TRIBOLOGY

INTERNATIONAL SCIENTIFIC JOURNAL

Published since 1996, four time a year

Volume 27 No 3/105-2022

Establishers:
Khmelnitskiy National University (Ukraine)
Lublin University of Technology (Poland)

Associated establisher:
Vytautas Magnus University (Lithuania)

Editorial board address:
International scientific journal "Problems of Tribology",
Khmelnitsky National University,
Institutskaia str. 11, Khmelnitsky, 29016, Ukraine
phone +380975546925

Indexed: CrossRef, DOAJ, Ulrichsweb, Google Scholar, Index Copernicus

E-mail: tribosenator@gmail.com

Internet: http://tribology.khnu.km.ua

ПРОБЛЕМИ ТРИБОЛОГІЇ

МІЖНАРОДНИЙ НАУКОВИЙ ЖУРНАЛ

Видається з 1996 р. ***Виходить 4 рази на рік***

Том 27 **№ 3/105-2022**

Співзасновники:
Хмельницький національний університет (Україна)
Університет Люблінська Політехніка (Польща)

Асоційований співзасновник:

Університет Вітовта Великого (Литва)

Адреса редакції:
Україна, 29016, м. Хмельницький, вул. Інститутська 11, к. 4-401
Хмельницький національний університет, редакція журналу "Проблеми трибології"
тел. +380975546925, **E-mail**: tribosenator@gmail.com

Internet: http://tribology.khnu.km.ua

Зареєстровано Міністерством юстиції України
Свідоцтво про держреєстрацію друкованого ЗМІ: Серія КВ № 1917 від 14.03. 1996 р.
(перереєстрація № 24271-14111ПР від 22.10.2019 року)

Входить до переліку наукових фахових видань України
(Наказ Міністерства освіти і науки України № 612/07.05.19. Категорія Б.)

Індексується в МНБ: CrossRef, DOAJ, Ulrichsweb, Google Scholar, Index Copernicus

Рекомендовано до друку рішенням вченої ради ХНУ, протокол № 2 від 29.09.2022 р.

Problems of Tribology, *V. 27, No 3/105-2022*

Problems of Tribology

Website: http://tribology.khnu.km.ua/index.php/ProbTrib
E-mail: tribosenator@gmail.com

CONTENTS

***Problems of Tribology**, V. 27, No 3/105-2022*

Problems of Tribology

Website: http://tribology.khnu.km.ua/index.php/ProbTrib

E-mail: tribosenator@gmail.com

ЗМІСТ

***Problems of Tribology**, V. 27, No 3/105-2022, 6-26*

Problems of Tribology
Website: http://tribology.khnu.km.ua/index.php/ProbTrib
E-mail: tribosenator@gmail.com

DOI: https://doi.org/10.31891/2079-1372-2022-105-3-6-26

Extrusion and rarefaction of lubricant in boundary layer is the key processes of adhesive wear of highly loaded tribocontacts

Oleksandr Stelmakh[1], Hongyu Fu[1], Yiqiao Guo[1], Xinbo Wang[1], Hao Zhang[1*], Pavlo Kaplun[2]

[1]School of Mechanical Engineering, Beijing institute of technology, Beijing 100081, China
[2]Khmelnitskyi National University, Ukraine
**E-mail: hao_zhang@bit.edu.cn*

Received: 18 June 2022: Revised: 20 July 2022: Accept: 29 July 2022

Abstract

A comprehensive analysis of the Adhesion-Deformation, Elasto-hydrodynamic and Hydrodynamic friction models is presented, which describe different modes of lubrication in accordance with the Stribeck curve. The main provisions of these models are considered in conjunction with the Langmuir-BET theory of adsorption and Hertz's elastic-deformation theory of curvilinear contacts. It is shown that the revealed contradictions require their resolution, and the discovered multiple effects need a scientifically based interpretation. It is proposed to develop a more generalized model of friction and wear based on naturally occurring processes that have been hidden from direct observations for a long time. These are: Extrusion of lubricating layers in the convergent elastically deformed and Rarefaction in divergent elastically deformed regions of tribo-contacts. Understanding these processes makes it possible to predict the localization sites and causes of the occurrence of primary subsequent acts of adhesion of friction surfaces and their wear in the following cycle: “rarefaction and desorption of lubricating layers, which leads to deformation destruction of oxide films and adhesion of juvenile surface areas, after which to tearing of a fragment material from the bearing and the neoplasm of the protrusion on the shaft - in the divergent elastically deformed areas of the contact. Then microcutting by this fragment of the bearing surface occurs with the release of the wear product in the convergent elastically deformed region, which accordingly leads to a change in the actual geometry and tension of the tribo-contact. Further, in other areas of the renewed contact, adhesive interaction occurs in other divergent areas according to the same mechanism. A deep understanding of the reasons for the desorption of lubricating layers will make it possible to develop and apply new highly efficient technological and material science methods in order to increase the resource of highly loaded tribo-systems of machines and mechanisms.

Keywords: Macro-friction models; adhesive wear; pressure gradient; cavitation

1. Introduction

One of the main fundamental tasks of modern tribology is a deep and comprehensive understanding of the relationship of all regular phenomena and processes occurring in tribo-contact. Solving this problem will effectively increase the reliability and service life of civil and military equipment, an integral part of which are highly loaded curvilinear tribo-contacts of power plants and other mechanisms.

Highly loaded modern tribo-contacts are elastically deformed curvilinear discrete micro- and macro-contacts of solid surfaces with layers of active components (surfactants and others) adsorbed on them that are present in modern oils. Obviously, increasing the efficiency of their work is a complex physical-mechanical and physico-chemical problem, the key issue in which is to elucidate the role of hydrodynamic processes in a wide range of tribo-contact operation. The solution of this problem is impossible without understanding the physical model of the key processes that cause wear.

Modern tribology does not consider these key processes and is based on the three most popular models that describe the corresponding load-speed ranges and tribo-contact lubrication modes:

(1) The mode of "boundary" lubrication or boundary friction at low speeds and high loads is described in terms of the Adhesion-deformation model of friction and wear. This model covers the left descending branch of

the Striebeck curve (Fig. 1) in the friction range from starting off, at ultra-low, low speeds to medium. At the same time, the Adhesion-deformation model denies any hydrodynamic processes in the boundary layers, which are visually observed and predetermine the occurrence of quasi-dry friction conditions, adhesive interaction of friction surfaces and their wear [1–10].

(2) The mode of "liquid" non-contact friction at high sliding speeds and low loads is described by the classical Hydrodynamic friction model [11-14] without wear, which reflects the operation of a radial plain bearing in the range of the right ascending branch of the Stribeck graph (Fig. 1). In this friction mode, in contrast to the Adhesion-Deformation model, elastic-deformation processes in tribo-contacts are unfairly ignored. It should be emphasized that in modern highly loaded tribo-systems, the implementation of the hydrodynamic effect of the "oil wedge" at high loads, at low sliding speeds is unlikely and practically unrealizable. Within the framework of the Hydrodynamic model, the regular processes of extrusion and rarefaction of lubricating layers were not identified and were not taken into account.

(3) Friction under conditions of mixed or transient lubrication between "boundary" and liquid lubrication modes is described by the elasto-hydrodynamic friction model [15-19], which reflects the transition region of the Stribeck curve between the left and right branches. In the elasto-hydrodynamic model, as well as in the hydrodynamic model of friction, the tribo-system is theoretically wear-free. Within the framework of this model, the elastic-deformed state of curvilinear tribo-contacts during friction and elasto-hydrodynamic processes in the lubricating elasto-hydrodynamic layer, which is endowed with a bearing capacity during friction, are considered. However, a number of the main provisions of the elasto-hydrodynamic model directly contradict the theory of adsorption–desorption of mono- and multimolecular layers on the surfaces of solids by Langmuir and BET [20–22], and also directly contradict the fundamental physical laws of Hooke and Pascal. In particular, it is incorrect to consider the pressure in the elasto-hydrodynamic film as identical to the contact stresses, which is fundamentally wrong from the standpoint of the BET theory. Moreover, it is assumed that no hydrodynamic processes occur during friction of the elasto-hydrodynamic tribo-contact in the elasto-hydrodynamic film; the elasto-hydrodynamic film is a kind of glassy substance in a highly compressed state [15–16]. In addition, the discontinuity of the continuity of the lubricating layer is fundamentally denied in the elastohydrodynamic model, and the natural phenomenon of EXTRUSION, hidden from the eyes, was not detected and was not studied.However, cavitation that occurs in the outlet region of tribocontacts in recent decades, as an effect, has become a research trend in modern tribology [23–46].

The choice of a friction model plays a leading role in understanding the processes that determine the efficiency of the friction unit [47]. An analysis of the adhesion-deformation, hydrodynamic, and elasto-hydrodynamic friction models leads to the conclusion that each of these models lacks important information about the hydrodynamic processes that naturally occur in the elastically deformed regions of the tribocontact. These are the extrusion of lubricating layers in a converging and their extrusion in an expanding elastically deformed contact area [48].

The purpose of the work is to establish, based on the analysis of existing phenomenological models of tribo-contact friction, the relationship between elastic-deformation and hydrodynamic processes of lubricant boundary layers and the primary adhesion of friction surfaces in order to develop a promising new tribocontact friction model, which takes into account the key processes of extrusion and rarefaction of lubricating layers in elastically deformed contact areas.

The Stribeck curve (Fig. 1) — perhaps the only fundamental experimental dependence recognized in tribology, which connects the friction force with the external friction parameters (load, speed) and lubrication conditions (lubricating medium viscosity) simultaneously.

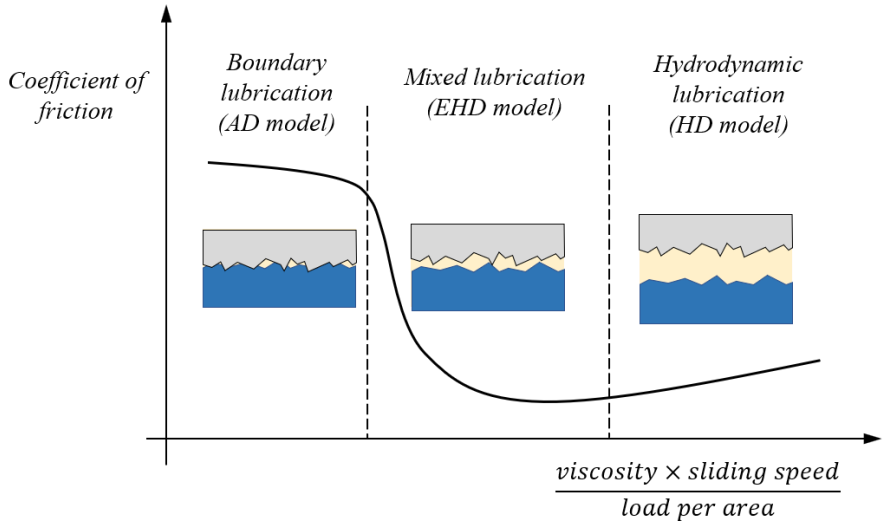

Fig. 1 Graphical illustration of different types of lubrication depending on friction modes

This remarkable dependence qualitatively illustrates the behavior of the tribo-system, covering the entire range of its friction during operation: from the starting stage of switching on to operating speeds and subsequent shutdown at each cycle of the entire machine. The generally recognized three characteristic regions of the Striebeck curve (Fig. 1) describe the corresponding modes of friction and lubrication by three phenomenological models: 1. contact "boundary" lubrication (the left descending branch of the Striebeck curve) is considered within the framework of the adhesion-deformation model of friction and wear at high loads and low speeds [2-5]; 2. Theoretically, non-contact "hydrodynamic" lubrication is described by the hydrodynamic friction model, respectively - the right ascending branch of the Stribeck curve [6-10]; 3. Theoretically, contactless "mixed" lubrication, including "boundary" and "hydrodynamic" types of lubrication in an elastically deformed friction contact at moderate speeds and loads, is described by the elasto-hydrodynamic friction model - the transition region of the Striebeck curve [15-19].

Adhesive interaction of friction surfaces with adsorbed lubricant layers and adhesive wear of surfaces, as the main negative process during friction, is considered only within the framework of the adhesion-deformation model. Adhesive interaction of surfaces, their submicro- and microsetting, the formation of secondary structures during friction, and wear kinetics are the main issues studied within the adhesion-deformation model.

Within the framework of Elasto-hydrodynamic and Hydrodynamic, the theoretically direct interaction of friction surfaces is prevented by a lubricating layer, the minimum thickness of which should exceed the sum of roughnesses. Therefore, Hydrodynamic and Elasto-hydrodynamic models are non-contact and wear-free. Therefore, the adhesion-deformation model of friction and adhesive wear of friction surfaces, which determines the resource and reliability of the entire mechanism, is of the greatest interest among designers and machine builders.

Depending on the operating mode of the tribosystem, the graph (Fig. 1) shows the contact patterns of two rough friction surfaces separated by a lubricant layer, the smallest thickness of which, in comparison with the roughness, characterizes one or another lubrication mode during friction. However, the minimum thickness of the lubricating layer in tribocontact is not reliably determined by direct measurement methods today, which prevents the establishment of clear boundaries between friction modes, types of lubricant and, accordingly, between the adhesion-deformation, elasto-hydrodynamic and hydrodynamic models that describe them.

Thus, the same bearing, depending on the friction rate, load and rheological properties of the lubricating medium (viscosity), is considered from the standpoint of these different phenomenological models and the corresponding basic provisions: from contact boundary friction at low speeds and high Amonton-Coulomb contact loads [47] to hydrodynamic non-contact friction at high speeds and low loads (classical hydrodynamic friction model with lubrication by O. Reynolds [11].

In practice, all critical and highly loaded friction units, which are usually enclosed in one lubrication system (lubrication systems for internal combustion engines, gas-turbine engines, transmissions and other power plants and mechanisms), as well as the entire machine, are periodically stopped and cyclically restarted for the duration of operation. to perform the following tasks. After parking for different durations in different conditions, when starting the machine, starting from the moment of starting, with acceleration, bypassing ultra-low speeds, all friction units reach operational speed, load and thermal conditions. When stopping, each tribosystem goes back: from operational load-speed and thermal modes of operation to a complete stop.

It turns out that completely different friction models are applied to the same tribosystem with lubrication operating in different speed, load and thermal conditions: Adhesion-Deformation, Elasto-hydrodynamic and Hydrodynamic, which have a limited area of use and do not have clear boundaries and applicability criteria. This indicates the need to search for those underlying dominant and key processes that occur during friction that have not come to the attention of tribologists in order to create a more complete and universal model of friction and wear. This work is aimed at such a search, and the presented results and conclusions can sufficiently meet the criterion of scientific novelty of this article.

2. Analysis of theoretical positions, experimental phenomena and effects of Adhesion-Deformation, Hydrodynamic and Elasto-hydrodynamic models of friction.

The left descending branch of the Stribeck curve (Fig. 1), when friction occurs at ultra-low-low-medium speeds and high loads, reflects the so-called friction mode under “boundary lubrication” conditions, which is described by the Adhesion-Deformation model of friction and wear (Bowden, Tabor, Kragelsky, Demin and others [1-10]). The beginning of the curve on the Stribeck diagram corresponds to the maximum value of the friction force that occurs at the moment the tribosystem leaves the state of rest at the very beginning of the relative movement of the surfaces at the points of contact - “rest friction”. The law of friction, originally formulated by Leonardo da Vinci in 1508 in an implicit form as “Friction requires doubling the effort if the weight is doubled”, 200 years later Amonton was proposed in a quantitative form [47]:

$$F_{friction} = f \cdot N \quad (1)$$

where the friction force $F_{friction}$ is directly proportional to the load or downforce (normal reaction) N,

multiplied by the dimensionless friction coefficient *f*.

In 1875, Coulomb proposed a refinement of formula (1):

$$F_{friction} = A + f \cdot N \tag{2}$$

where *A* - a constant component that occurs in the process of adhesion microseizure of surfaces and is one of the reasons for the mismatch between static friction and sliding friction, that is, the presence of a jump at the beginning of sliding (Fig. 1).

The adhesion-deformation or molecular-mechanical model of friction is based on the concept of the dual nature of friction and the corresponding two-term friction force formula, which is essentially the Amonton-Coulomb law (Eq. (2)), where A is the adhesive or molecular component of the friction force, and the second term $\left(f \cdot N \right)$ reflects the deformation or mechanical component.

The study of the contribution of each of these components of the friction force to its total value according to the Eq. (2), carried out by V. Hardy [50] showed the following relationship: $\left(f \cdot N \right) : A = 1:10000$, while I. V. Kragelsky [1,10,50] values this ratio as 1:100. Consequently, the adhesive interaction of friction surfaces, which leads to adhesive wear, generates the most significant 99% component of the total friction force *A*, the reduction of which is the most important task of boundary friction tribology. Noteworthy is the absence in Eq. (1) and Eq. (2) of the friction velocity ***υ***, which is the main condition for the friction process itself, as well as the compression force *N*.

2.1 Adhesion-Deformation model of friction and wear

The main provisions of the Adhesion-Deformation model:

(1) The main position of the Adhesion-Deformation model of friction and wear is based on the concept of the discreteness of the actual contact of rough elastically deformed surfaces compressed by an external force, which are visualized by the classic schemes (Fig. 2(a)). Since the surfaces of real solids always have irregularities, the nature of which depends on the material of the contacting surfaces and the method of their processing, the contact of such surfaces is discrete at relatively low compression forces. It is believed that in the elastic contact of the rough surfaces of a friction pair, only a small part of the protrusions of these surfaces is elastically deformed - up to 0.001 fraction of the contour area according to [2].That is, the contact area of the surfaces is a set of locally loaded curvilinear quasi-point and quasi-linear microcontacts, which, during friction, interact with each other according to the deformation and adhesion mechanisms, dynamically replacing one contact zone with another.

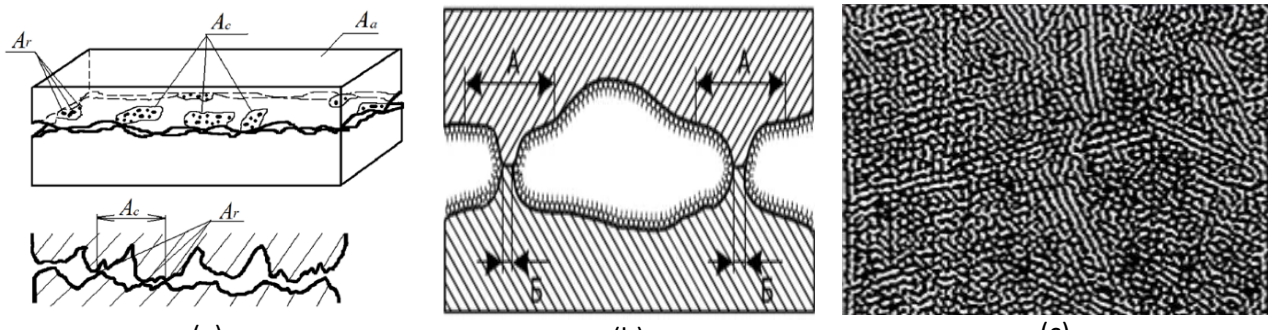

Fig. 2. Classical schemes of the adhesion-deformation model of friction of surfaces based on the concept of discreteness of actually contacting protrusions of real rough surfaces: 3D-scheme and 2D-scheme (I.V. Kragelsky, A.M. Demkin) [1,2] - (a); a schematic representation of the appearance of mutually elastically deformed sections A and the formation of adhesion sites of setting B after the destruction of the boundary monomolecular lubricant layer on the protrusions of rough surfaces (Bowden) [3] - (b); cellular structure of nanorough surfaces when the vertices merge into closed cells like honeycombs along the contour (dark areas) with multimolecular lubricant layers inside the contours (light areas) [48] - (c).

During the friction of such elastic discrete contacts of two surfaces with layers of lubricant adsorbed on them, between the contacting areas of the surfaces, adhesive interaction forces arise in the form of welding bridges (Fig. 2(b)) [3,5], which manifest themselves as microseizure, microseizing, tearing of fragments of a less durable material and neoplasms on a more durable one, followed by their cyclic cutting and formation of wear products.

This position is limited to reflect the contact of highly rough surfaces or the contact of polished surfaces under low compressive load. The fact is that the Adhesion-Deformation model of friction and wear originated in the USSR in the first half of the last century in 1939 (A. M. Ertel [15]) and was further developed in the USSR

(A. N. Grubin, 1947; A I. Petrusevich, 1951; Kragelsky, 1965 [1,16,18]), and in England (D. Dawson 1963, 1966, Bowden 1968, Tabor 1978) [3]. It should be noted that, at that time (1930-1970s), the metalworking industry was at the initial stage of its development and, accordingly, the parts of friction units were manufactured with large errors and deviations, and the surfaces themselves had a relatively large roughness with the parameter R_a = 0.25 ... 0.5 microns and more.

At the same time, a hypothesis arose about the process of running in new parts as a self-formation of a certain "optimal roughness" in the process of running in machines and mechanisms (at present, a fashionable name is often used - self-organization). Its essence lies in the fact that smooth polished friction surfaces should not be made, for example, a shaft and a radial plain bearing, since during their running-in the roughness will increase due to adhesive destruction with characteristic tears in the bearing and subsequent microcutting. Conversely, a large shaft roughness during friction will somewhat decrease due to deformation shearing, microcutting and adhesive wear. Losses for such self-formation of optimal roughness during running-in are inevitable - increased friction and high wear intensity with known negative consequences at the initial stage of product operation.

Currently, in the course of the revolutionary development of machine tool building, materials science, metalworking technologies, as well as methods for finishing friction surfaces in production, nanometer roughness is achieved with a parameter of R_a<0.1…0.02 mkm and even with Ra<10 nm. A constant increase in contact stresses and an increase in the nanometer quality of surfaces leads to a logical conclusion that with an increase in the compression force of the initially discrete contact areas of nanoprotrusions, their elastic deformation occurs and the dimensions of these actual compression areas will naturally increase. Therefore, the generally recognized discrete model of contacting highly polished nano-rough surfaces at constantly increasing contact stresses (for example, 1000 MPa and more in aviation tribo-contacts) should be supplemented with logical processes for increasing not only their actual contact areas, but also their natural and inevitable merging with the subsequent emergence of common for two surfaces of closed cavities (Fig. 2(c)).

That is, under static compression, in the course of deformation of the protrusions of surfaces with monomolecular layers adsorbed on them, closed contours will appear, inside which there are cavities common to two surfaces, such as many lakes with multimolecular layers of lubricant of different amounts (two, three, and more) according to the type of Fig. 2(b)) and 2(c)). Therefore, precision engineering is of particular interest to the behavior of boundary layers of lubricant between highly polished nano-rough surfaces with monomolecular boundary layers located on them with a comparable nanometer thickness both under static compression and friction.

(2) Within the framework of the Adhesion-Deformation model, the definition of the process of adhesive wear is given as a consequence of the atomic-molecular interpenetration of juvenile contact areas of friction surfaces with subsequent tearing out and transfer of a material fragment from one surface to another and its subsequent cutting with the formation of a free wear particle [1-6].

A prerequisite for the occurrence of adhesive wear is the absence of any films on friction surfaces such as oxides, secondary structures, including mono- or multimolecular lubricant layers [48]. It is believed that in real friction units, adhesive wear always manifests itself under the condition that the rate of attrition of various films on the friction surface exceeds the rate of its recovery due to the physical adsorption of the lubricant, or chemisorption, or oxidative processes.

Depending on the extensiveness of the contact of molecular interaction, adhesive wear is distinguished at the microlevel and macrolevel. At the micro level, the process of molecular adhesion develops on elastically deformable rubbing protrusions of microroughness of rough friction surfaces. Depending on the strength of the emerging molecular bonds, destruction is observed both in thin near-surface layers and deep tearing of the metal. In this case, processes of material transfer from one friction surface to another often occur, for example, technological methods of copper plating or friction brassing. The metal particles torn out and stuck to the friction surface are partially cut off or peeled off in subsequent interactions, forming adhesive wear products. The composition of the wear particles is in most cases identical to the base material. Adhesive wear at the macrolevel manifests itself in friction units in the form of seizing, deep tearing and seizing. This type of wear, as a rule, manifests itself at high contact stresses, with large tangential and normal forces in the contact zones, leading to desorption of the boundary layers.

The intensity of wear during adhesive wear is quite high, and the process itself is accompanied by high values of the friction coefficient, its oscillations with large amplitude and frequency, as well as significant heating of the parts of the friction unit.

(3) The third position is related to the ideas about the structure and properties of the boundary layers of lubricant on friction surfaces: the surfaces of solids are always in interaction with the environment, the nature of which depends on the physicochemical properties of the material of the solid and the medium. Boundary layers always appear on all lyophilic surfaces of solids wetted with a lubricating hydrocarbon medium, which traditionally contains both surfactants and dissolved molecules of environmental gases (from 8 to 12%) [49].

Within the framework of the Adhesion-Deformation theory, it is believed that mono- and multimolecular layers of lubricant with a thickness of 0.01...0.10 μm [1-10] are always formed on the oxide films of the friction surfaces of real parts according to the mechanism of physical and chemical adsorption. It is believed that when the boundary layers of the lubricant are strongly compressed by two surfaces, they acquire the properties of some

kind of amorphous “glassy” or “third body” [16-17]. These properties are different from what they would have in an unlimited volume of lubricant. It is also generally accepted that the thinner the layer, the higher its elasticity. The strength of such layers in compression is very high, their modulus of elasticity exceeds the modulus of elasticity of structural materials of friction surfaces and even diamond, which is noted in the works of V. Hardy [50] and A.S. Akhmatov [10]. A schematic representation of the process of static compression of surfaces with such multimolecular layers of an Epitropic- Liquid Crystal structure [51] is shown in Fig. 3.

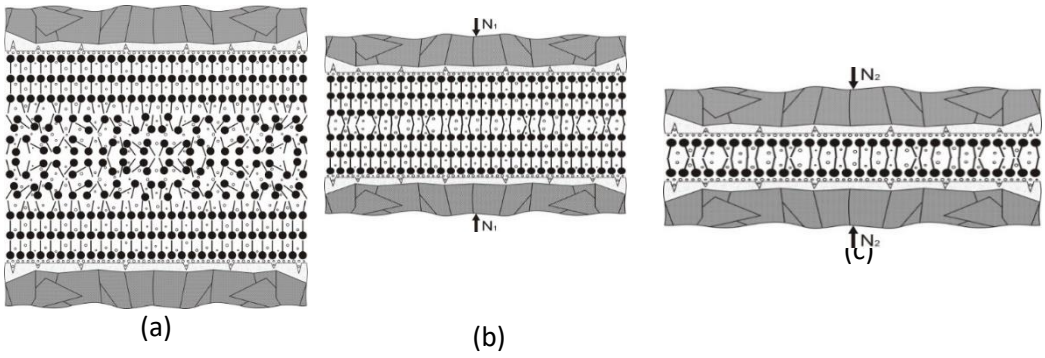

Fig. 3. Schemes of the structure of Epitropic-Liquid-Crystalline oil layers, taking into account active molecules adsorbed on the surfaces (plates with circles) and gases dissolved in oil (transparent circles) between two surfaces with a gap (a); layer-by-layer desorption of supra-monomolecular layers during their static compression by force N1 (b); as well as a diagram of the uniaxial stress state of monomolecular layers adsorbed on friction surfaces at higher compression loads N2 >> N1 (c) [10,50,51].

Fig. 3 shows a diagram of the appearance of contact between surfaces and monomolecular layers during compression in accordance with the concept of the epitropic liquid crystal structure of boundary layers of oils on lyophilic friction surfaces [51]. Such a representation is consistent with the theories of Langmuir and BET, namely: all multimolecular liquid crystal layers located above the monomolecular layer behave like fluid fragments of a liquid in a volume. Accordingly, when these fragments are deformed, they flow into the bulk phase in the region of lower pressure, under laboratory conditions, these are regions with ambient pressure - atmospheric pressure p_0.

(4) Since the monomolecular lubricant layer is capable of withstanding, without collapsing, significant compression pressures [10], it is believed that at ultra-low friction velocities and high loads in the contact zone of surfaces with boundary layers of lubricant adsorbed on them, there are no hydrodynamic processes.

This dubious position is too categorical, it is not sufficiently substantiated, and here's why. In accordance with the well-known Langmuir and BET adsorption theories [20–22], monomolecular and polymolecular lubricant layers on lyophilic friction surfaces indeed have a high bond strength with the active centers of the surfaces and high elasticity under static compression. However, as extensive research results show, during friction with relatively small loads and low speeds, areas of adhesive setting of surfaces always appear, material is pulled out, which obviously must be preceded by the destruction of monomolecular adsorbed lubricant layers, that is, their desorption. Therefore, it is quite logical that the first act of adhesive interaction of surfaces with lubricant layers adsorbed on them or primary adhesion during friction of lubricated surfaces should be preceded by desorption of both multi- and monomolecular layers.

There is a main hypothesis about the tangential force destruction of lubricating layers at the tops of discrete contacts of rough surfaces under the action of tangential shear stresses [1-3] (Bowden, Tabor, Kragelsky, etc.), which is experimentally insufficiently confirmed. Moreover, A.S. Akhmatov in his famous work “Molecular physics of boundary friction” [10] focused on the fact that no one has reliably observed the destruction of boundary layers by such a tangential mechanism and is a very controversial point of view. Another hypothesis of thermal desorption of boundary layers [9] is based on the concept of local temperature flashes that occur at discrete contact areas during friction and can reach 600...1200°C. However, in the initial period of starting from a place, when primary adhesion of friction surfaces occurs, such flashes are not observed and are also insufficiently confirmed experimentally.

(5) The maximum contact stresses are calculated according to the Hertz formulas [56-57] without taking into account the roughness so that they do not exceed the yield strength of the material. In practice, this situation is extremely rare, in real friction units, as a rule, the maximum contact stresses of tribo-contacts are an order of magnitude less than the yield strength of structural materials.

Since the primary adhesive interaction of the surfaces of solids and their wear is possible only if there are no multi- and monomolecular layers of lubricant on them, as well as any oxidizing [4] and other films, it is obvious that the primary adhesive interaction of "juvenile" surfaces friction must be preceded by desorption of the boundary layer of the lubricant [58-59].

The cause-and-effect relationship between desorption of boundary layers and adhesion of friction surfaces is a key moment for understanding the mechanism of the occurrence of primary, secondary, and so on acts of adhesion in local areas of contacting friction surfaces.

Primary adhesion when the shaft rubs against the plain bearing leads to tearing out of a fragment of material from the surface of the bearing, then the formed build-up (new formation) on the shaft is cut off when it comes into contact with the formation of a free particle - a wear product, and the remaining build-up on the shaft is micro-cutting the bearing. Thus, it becomes obvious that it is the desorption of the boundary layers that causes the occurrence of conditions for local quasi-dry friction, as a process preceding the primary adhesive setting of the friction surfaces.

Primary adhesion leads to an instantaneous change in all contact conditions and violation of all initial friction conditions, which sharply reduces the possibilities of modeling within the Adhesion-Deformation model. And if we take into account the fundamentally random places of localization of adhesion during friction, as well as the fundamentally random behavior of the friction force due to adhesive wear, then the modeling of tribosystems becomes very far from practice.

Thus, from the above analysis of the Adhesion-Deformation model, it follows that a clear understanding of all the phenomena and patterns in the relationship that determine the desorption of lubricating layers during friction under boundary lubrication conditions is extremely necessary. The mechanism of the appearance of primary adhesion during friction of lubricated surfaces is an extremely urgent problem of modern tribology, the solution of which will largely determine the success in creating advanced technology for various purposes. Prevention of primary adhesion of friction surfaces requires a deep understanding of all the elementary processes that occur during friction in combination to create effective technological methods in the manufacture of tribosystems in order to reduce or completely prevent their wear during long-term operation.

(6) Adhesive wear is based on the concepts of molecular adhesion of friction surfaces or “welding”, therefore it is quite obvious that this process must be preceded by the destruction of sufficiently strong mono- and multi-molecular lubricant layers, as well as oxidative layers of surfaces. Consequently, the organization of adsorption of boundary layers of lubricant on friction surfaces, the creation of frictional contact, the friction of boundary layers and their desorption, followed by adhesion of surface materials, are successive fast processes that can be represented as Fig. 4 shows:

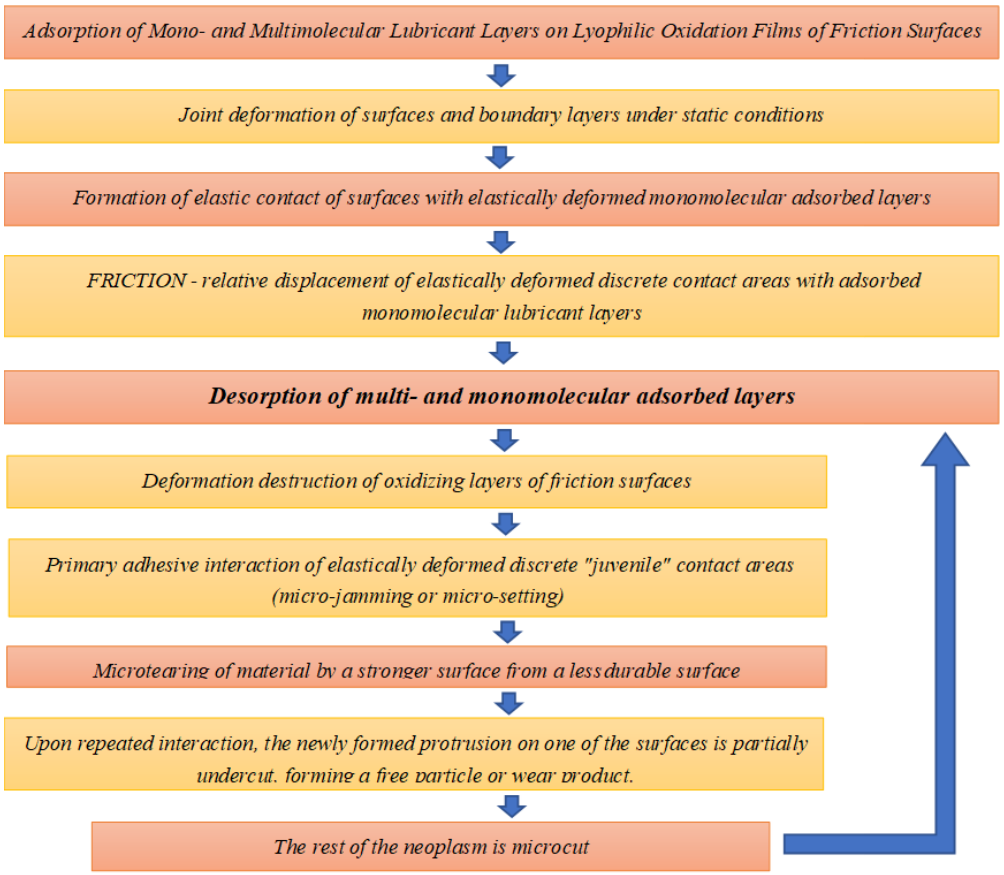

Fig. 4 Process of the destruction of lubricant layers and oxidative layers on surfaces

According to the authors, unreasonable ignoring the occurrence of any hydrodynamic processes during friction of surfaces with sufficiently strong mono- and multimolecular layers of a lubricating medium adsorbed on them at ultra-low and low speeds is the main obstacle to the further development of the Adhesion-

Deformation model.

Meanwhile, the Adhesion-Deformation model of friction and wear covers a number of well-known theories, phenomena and effects, among which the following stand out: the theory of oxidative wear of friction surfaces by B.I. Kostetsky [4], "The phenomenon of selective transfer of copper" or "the effect of wearlessness" and the theory of hydrogen wear by D. Garkunov and others [52-53], "The phenomenon of abnormally low friction" by Silin and others [54]. Also of interest is the effect of abnormally high wear resistance of a sliding friction pair: a polished shaft - a highly rough bearing (I.V. Kragelsky) [1]. The question of why rubbing a polished shaft against a highly rough lubricated bearing results in less wear on the latter than rubbing against a similarly polished surface also needs to be explained. In addition, the mechanism of the regular behavior of tribocontacts when starting from a place, when at the moment of the beginning of the movement of richly lubricated surfaces the static friction force significantly exceeds the motion friction force, is not fully disclosed, which also needs a deeper experimental and theoretical substantiation and interpretation.

The main drawback of the Adhesion-Deformation model of friction and wear is the denial of hydrodynamic processes in the boundary layers during friction. Therefore, there is no relationship between the elastic-deformation processes of curvilinear discrete micro-contacts and hydrodynamic processes in the lubricant adsorbed on them by mono- and multimolecular boundary layers during friction. Below [2-5] it will be shown that at the slightest displacement of such contacts, the extrusion of boundary layers immediately occurs in narrowing (converging in the direction of friction - the input contact area) and their rarefaction in expanding (divergent in the direction of friction - the output contact area) elastically - deformed contact areas.

2.2. Hydrodynamic model of lubrication without wear

The right ascending branch of the Striebeck curve (Fig. 1), when friction occurs at high sliding speeds in a viscous medium, and with a small radial load *N*, is referred to as a hydrodynamic or "liquid" friction mode, when smooth surfaces are completely separated by an oil layer of thickness *h* due to the occurrence it has a sufficiently high hydrodynamic pressure and the so-called "oil wedge" effect is realized. Such a friction mode is described by the Hydrodynamic friction model [11-14], the classical scheme of which is presented on the example of a radial plain bearing (Fig. 5). In accordance with the Hydrodynamic model of friction, surface wear is not considered in principle.

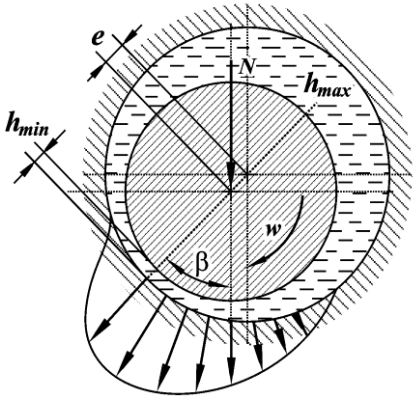

Fig. 5. Classical representation of the Hydro-Dynamic model of friction of a radial plain bearing, which illustrates the occurrence of pressure in the lubricating film (pressure diagram is shown as radial arrows, reflecting the effect of the "oil wedge"), at high shaft speeds ω, at low or moderate radial load *N* , where it is shown how the rotating shaft "floats up" and shifts in the direction of friction by the eccentricity *e*, and the axis of the shaft centers, on which the minimum $h_{\min}$ and maximum $h_{\max}$ clearances of the radial bearing are located, is shifted by an angle β.

Friction within the framework of the Hydrodynamic model is described by the equation of O. Reynolds (1886) [11] using various boundary conditions and algorithms in order to determine the load capacity of the lubricating film in the minimum gap between the rubbing surfaces $h_{\min}$. At the same time, the friction coefficient has significantly lower values compared to the "boundary" friction mode within the framework of the Adhesion-Deformation model. The basic equation of the Osborne Reynolds Hydrodynamic theory allows you to determine the pressure distribution in the lubricating film along the gap of a radial plain bearing according to the formula:

$$\frac{\partial p}{\partial x} = 6\mu\upsilon\frac{\left(h - h_{\min}\right)}{h^3} \tag{3}$$

where x – the coordinate in the direction of the shaft movement, h – the value of the current

clearance, $h_{\min}$ – the minimum clearance between the shaft and the bearing; p - the pressure in the oil film, μ – the viscosity of the oil, υ – the peripheral speed of the shaft sliding along the bearing [11].

Noteworthy is the absence of load N in Eq. (2), which is usually taken into account through the minimum thickness of the lubricating film $h_{\min}$. In this case, any deformation of the surfaces is also not taken into account, as well as their stressed state: the bearing capacity of the lubricating film under pressure is estimated by the excess of the pressure in it, multiplied by the friction area, over the value of the radial load applied to the bearing. The main criterion of the Hydrodynamic model of friction is the value of the minimum thickness of the lubricating layer in the bearing clearance $h_{\min}$, which should not exceed the sum of the roughness of the shaft and bearing surfaces $\left(R_{a1}+R_{a2}\right)$. Unfortunately, today the minimum thickness of lubricating layers $h_{\min}$, as the most important criterion for their non-contact bearing capacity, is not reliably measured and in most cases is a hypothetical speculative value.

2.2.1 The main provisions of the Hydrodynamic model of friction of lubricated surfaces

(1) The gap of the radial bearing is completely filled with lubricant, there are no end flows of the lubricant, the viscous lubricating layer implements a laminar layer-by-layer Newtonian flow. O. Reynolds voiced this position at the very beginning of his work, analyzing the Beauchamp Tower experiments on the instructions of the Institute of Mechanical Engineers in 1883-1884[11-14];

(2) The surfaces do not come into contact, since the minimum thickness of the lubricating layer $h_{\min}$ exceeds the sum of the surface roughness $\left(R_{a1}+R_{a2}\right)$, therefore, wear of the surfaces is not assumed and is not considered;

(3) The bearing implements friction immediately at sufficiently high speeds, which is contrary to practice: all friction units, like all machines, go through the natural stages of starting off, accelerating to operating speeds and operating for the required time, followed by stages of deceleration to a complete stop.

(4) When the shaft rubs against the radial bearing, the pressure in the lubricating layer **p(x)** always exceeds the ambient pressure p_0;

2.2.2 Actual experimental and theoretical problems of the Hydrodynamic model of friction

(1) The mechanism of occurrence of the hydrodynamic effect of the “oil wedge” has not been fully disclosed, probably due to the lack of reliable and complete information about the regular extrusion flows of boundary layers, which O. Reynolds mentioned at the very beginning of his well-known work [11];

(2) Adhesive interaction of surfaces, their wear, as well as their contact, the Hydrodynamic model is not provided, although in practice all bearings wear out. It is believed that wear occurs only at the starting and stopping stages of operation. This assumption has not been experimentally proven;

(3) Calculations of the bearing capacity of lubricating layers based on Eq. (3) are not widely used in the design bureaus of machine-building enterprises - new friction units are created by improving tribosystems of previous generations using new structural and lubricant materials, coatings and additives, as well as by improving existing manufacturing technologies;

(4) In the main equation of hydrodynamic lubrication of the Hydrodynamic model (Eq. (3)), there is a sliding speed, medium viscosity, minimum thickness of the lubricating layer, but there is no load, which, like speed, is the second main condition for the implementation of the process of friction of solids. The absence in Eq. (3) of the value of contact stresses σ(x) of the surfaces in the area of the elastically deformed state of the contact $\left[-b;+b\right]$, which are set by the designer and are quite well calculated by the formulas of G. Hertz, is the main problem of the Hydrodynamic model. The fact is that bearings with a small contact load in modern mechanical engineering are of no practical value, just like a bearing without relative movement of compressed surfaces, that is, without speed (Amonton-Coulomb Eq. (2)).

(5) Problem of “negative pressure loop” by O. Reynolds and half Sommerfeld solution (half solution of A. Sommerfeld of hydrodynamic friction).

In the well-known works of O. Reynolds, when describing Fig. 10 [11, p. 275], it is noted that in the direction of rotation of the shaft relative to the minimum gap filled with oil, with a flat surface, two symmetrical regions arise: narrowing to the minimum gap - convergent, and subsequent expanding - divergent. O. Reynolds notes that "... if the load (on the liner with a rotating shaft) continues to increase, then the pressure at point A ([11, Fig. 1, p. 256]) decreases or even becomes negative." “Since the amount of negative pressure that the oil can withstand depends on unexplained reasons, then the ultimate load that provides complete lubrication should be considered one at which the smallest distance between the pin and the liner is equal to half the difference in radii.” Further, O. Reynolds notes: “fluid pressure on the right side removes the surfaces” (we are talking about the convergent area), but since “the pressure on the left side is negative” (divergent gap area), then “a moment is

obtained that rotates towards the surface" shaft. Further, when considering Fig. 11 in [11], it is indicated that "the pressure is everywhere positive ... therefore, the pressure everywhere tends to push the surfaces apart." In further reasoning, starting from the description of Fig. 12, O. Reynolds, based on the experiments of B. Tower, only a few times mentions "negative pressure in the lubricating layers", which then leads to "rupture of the oil layer" [11], p. 284, it is interpreted as follows: "whether this negative pressure occurs or not depends on whether the lower end of the insert is completely immersed in the oil bath or not. Usually, such a case does not occur. If this happens, it still remains unclear how far the negative pressure can go ... we can only say that it is not lower than atmospheric pressure. Such reflections of the great O. Reynolds regarding the "negative pressure" in the divergent areas have not received a clear interpretation to this day.

Brilliant calculations of the pressure in the lubricating layer of a radial plain bearing by A. Sommerfeld [11] also indicate the occurrence of a "negative pressure" in the lubricating film in the divergent contact area. However, the categorical, initially introduced by O. Reynolds, the main position of the Hydrodynamic model of friction about a completely filled gap between the trunnion and the bearing, led to the beautiful centrally symmetric pressure distribution curve in the lubricating layer of A. Sommerfeld, with positive and "negative" values, the scientific community has recognized only half of this curve, where the pressures are always not "negative", that is, greater than "zero". Then the "negative" part of the local pressure distribution curve in the lubricating layers was equated to constant values of ambient pressure, that is, to atmospheric pressure.

The problem of the "negative friction loop in the lubricating layer" of Reynolds-Sommerfeld (according to A. Cameron [55]) remains relevant, as well as the accepted terms "half Sommerfeld solution" [11].

Looking ahead, the authors believe that the resolution of these issues lies in the absence of a connection between the stress state of the surfaces and the local pressure in the lubricating layers between them with the ambient pressure p_0. The fact is that the microvolume state of lubricating layers of real droplet liquids in contact under compression is naturally characterized by flow properties due to their practical incompressibility. Also, in accordance with the theories of adsorption by Langmuir and BET [20–22], under external influence, namely, when surfaces with multimolecular boundary layers are compressed, which is characteristic of friction, all over monomolecular layers of adsorbed liquid molecules (the second, third, and so on layers) behave like a liquid. Only a monomolecular layer is capable of withstanding colossal compressive loads, since their modulus of elasticity is commensurate with the modulus of elasticity of the strongest structural materials. But under conditions of local rarefaction, all lubricating layers, including the monomolecular layer, in accordance with adsorption-desorption isotherms, can easily evaporate from surfaces - that is, desorb, which causes the conditions of quasi-dry friction and primary adhesion.

(6) The phenomenon of asymmetric wear observed and described by A. Sommerfeld on the bearings of wheel pairs of trains after their long-term operation [11] lies in the fact that the greatest destruction and wear of radial plain bearings in the vast majority of cases occurred in the area where the shaft came out of contact, that is in the divergent area. When examining the bearings of the axle boxes of locomotives in the Wittenburg repair shops after their long work, I visually observed some regularity in the wear of the plain bearing shells. In the work "On the theory of friction during lubrication" [11], Sommerfeld wrote: "Out of 20 bearings, 16 were worn more in front (in the direction of rotation, that is, in the divergent contact area), only two were worn more in the back (that is, in the convergent), while for the remaining two liners, the position of the place of greatest wear was unclear. In another series of cases, when examining 20 bearings, the results were as follows: 14 were worn more in front, 5 more in the back, and for one liner, the position of the point of greatest wear was indeterminate. A. Sommerfeld attributed this interesting fact to the confirmation of the hypothesis of a significant decrease in the lubricating layer in the divergent area of the plain bearing shells. The mechanism of this phenomenon and the reasons for its occurrence have not been disclosed to this day.

2.2.3 The main disadvantages of the Hydrodynamic friction model

(1)Denial of wear of the friction surfaces in the implementation of the hydrodynamic effect of the "oil wedge". The authors believe that adhesive wear occurs during fluid friction, as well as in other modes of friction during lubrication, only with a lower intensity.

(2)The minimum thickness of the lubricating layer $h_{\min}$, as the main criterion of the Hydrodynamic model, has not been reliably measured to this day, so the model itself remains more theoretical.

(3)Lack of connection between the elastic-deformation state of tribo-contact surfaces and hydrodynamic processes in lubricants adsorbed by mono- and multimolecular boundary layers on friction surfaces.

It will be shown below that all tribo-contacts are subjected to elastic deformation, and especially highly loaded ones, in which, at the slightest displacement in the boundary layers of the lubricant, extrusion immediately occurs in the narrowing and rarefaction in the expanding elastically deformed contact areas.

2.3 Elasto-hydrodynamic friction model without wear

The transition area of the Stribeck curve (Fig. 1) between the Boundary (left branch) and Hydrodynamic (right branch) modes of friction with lubrication is described from the standpoint of the Elasto-hydrodynamic

friction model [15-19], which is presented in the form of a scheme that has become classical (Fig. 6). This model arose as a result of an attempt to combine the Adhesion-Deformation and Hydrodynamic models into a certain generalized model and is very popular in modern tribology.

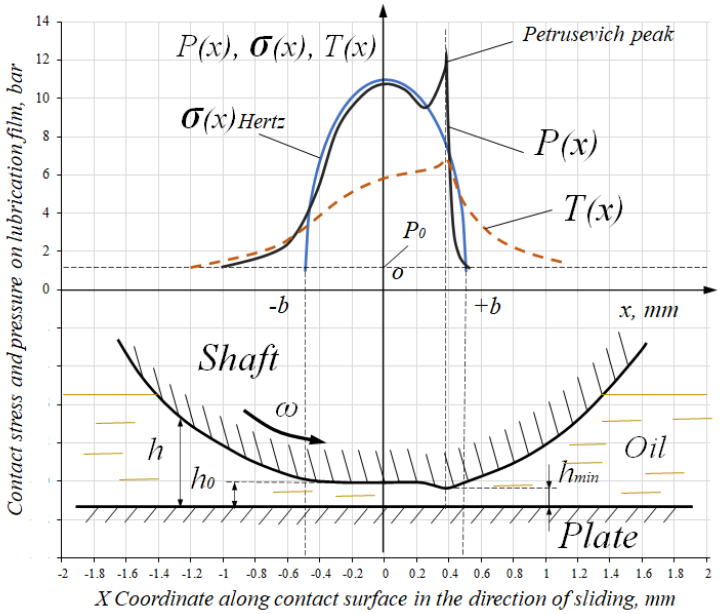

Fig. 6. Scheme of the Elasto-hydrodynamic friction model, where its main provisions are reflected: 1. The elastically deformed surfaces of the curvilinear contact are parallel; 2. The lubricating layers are strongly compressed from above and below by parallel compressing surfaces and have a constant thickness h_0 ; 3. The distribution of pressure in the lubricating film p(x) (EHL pressure) is everywhere greater than atmospheric p_0 and is identical to the contact stresses σ(x) according to G. Hertz, that is, p(x)=σ(x); 4. Contact stresses in the output region have a "Petrusevich peak", where the temperature T is maximum, and the thickness of the lubricating film is minimum $h_{\min}$, which should exceed the sum of surface roughness $\left(R_{a1}+R_{a2}\right)$; 5. Direct contact of the surfaces is not provided, therefore friction according to the Elasto-hydrodynamic model is theoretically wear-free.

The elasto-hydrodynamic friction model of Grubin, Ertel, Petrusevich and others [15-19] has become a classic and is presented in the form of a diagram (Fig. 6) in numerous textbooks on tribology for undergraduate and graduate students of higher technical educational institutions in the specialties "Tribology", "Tribo-technics", "Engineering".

2.3.1 The main points on which the Elasto-hydrodynamic model is built

(1) According to the scheme (Fig. 6), in curvilinear axisymmetric surfaces during their compression, the Hertzian contact stresses σ(x) are distributed axisymmetrically in the form of a semi-ellipse with respect to the vertical axis of symmetry OY. The half-width of the elastically deformed contact b, the distribution of contact stresses σ(x) of elastically deformed curved surfaces under the action of an external compressive force N within the contact width $\left[-b;+b\right]$, as well as the maximum contact stresses σ_{max} are calculated using the well-known formulas of G. Hertz. As applied to the Timken scheme "a model cylindrical shaft with radius R and length **l** – a flat surface", these formulas have the following form:

$$\sigma\left(x\right)=\sigma_{\max}\sqrt{1-\left(\frac{x}{b}\right)^2} \tag{4}$$

Where the maximum design contact stresses of elastically deformed curved surfaces σ_{max} under the action of an external compressive force σ_{max} within the contact width $\left[-b;+b\right]$ without taking into account roughness are calculated by the following formula:

$$\sigma_{\max}=0.418\sqrt{\frac{2E_{red}N}{lR}} \tag{5}$$

The half-width of a line contact is given by the following formula:

$$b = 2.15\sqrt{\frac{NR}{lE_{red}}} \tag{6}$$

where in Eq. (5) and Eq. (6) the reduced modulus of elasticity E_{red} is determined by the formula:

$$E_{red} = 2\frac{E_1 \cdot (1-\mu_1^2) \cdot E_2 \cdot (1-\mu_2^2)}{E_1 \cdot (1-\mu_1^2) + E_2 \cdot (1-\mu_2^2)} \tag{7}$$

where E_1 –the modulus of elasticity of the shaft material, E_2 - the modulus of elasticity of the material of the flat model bearing according to the Timken scheme, μ_1 and μ_2 – the Poisson's ratios of the shaft and flat bearing materials, respectively. Such formulas are of tremendous importance and are widely used in the strength departments of all design bureaus of modern aviation and other types of mechanical engineering.

According to Hertz, the main parameters of a stress-strain curvilinear contact are: contact half-width b, maximum contact stresses $\sigma_{\max}$ and their distribution $\sigma(x)$ in the form of a semi-ellipse. At the same time, it should be remembered that these parameters are calculated with a number of assumptions, such as: the surfaces are perfectly smooth, which is practically not achievable; contact is realized in absolute vacuum without any substances on them, which is also practically impossible.

Created on the basis of G. Hertz's formulas, modern software packages for calculating the stress-strain state of tribocontacts are practically not connected with any of the above-mentioned Adhesion-Deformation, Hydrodynamic and Elasto-hydrodynamic models due to the great inconsistency of their main provisions. In fact, calculation software packages, for example, for rolling bearings, are based on formulas obtained exclusively empirically, which include many coefficients that reflect both the influence of real roughness and the influence of the lubricating medium, temperature and other operational factors. Such software packages are of enormous value and are the subject of KNOW-HOW of well-known leading companies in the world of mechanical engineering. Therefore, these modern methods for calculating tribosystems are constantly being improved and still need to correctly reflect all the real processes in the lubricating film during friction of elastically deformed tribocontacts, which are not taken into account either in Adhesion-Deformation, or in Hydrodynamic, or in Elasto-hydrodynamic models of friction.

(2) The lubricating layer is limited by parallel elastically deformed surfaces and has a constant thickness h_0, and the pressure in the compressed lubricating layer p(x) in any contact area is constant and is always greater than atmospheric p_0;

(3) The lubricating film under the action of high (more than 400 MPa) contact stresses (according to Grubin) becomes a super viscous, “glass-like”, or “amorphous substance” [15-16], that is, not fluid, in which the pressure is identical to the contact stresses $p(x) \sim \sigma(x)$. Hydrodynamic processes in this so-called Elasto-hydrodynamic film are considered one-sidedly: only from the standpoint of pressure increases in the Elasto-hydrodynamic film, which determines its carrying capacity by balancing the load;

(4) Since, during friction, the gap h_0 of curved compressed surfaces is parallel to the plane, accordingly, the thickness of the compressed lubricating film is also practically unchanged with a slight thinning to $h_{\min}$ (Fig. 6) at the exit of the surfaces from the contact, which is explained by its heating during friction and a decrease in effective viscosity in this area.

(5) It is generally accepted that with increasing load, the area of the curvilinear contact with increasing contact width $[-b;+b]$ increases, the distributed contact stresses $\sigma(x)$ and their maximum values $\sigma_{\max}$ decrease, and therefore the bearing capacity of the lubricating layer in the Elasto-hydrodynamic film, increases.

(6) As in the Hydrodynamic model of friction, within the framework of the Elasto-hydrodynamic theory, it is assumed that the surfaces at different speeds never come into direct contact due to small surface roughness, the sum of which $(R_{a1} + R_{a2})$ is less than the minimum thickness of the Elasto-hydrodynamic film $h_{\min}$. In this case, the lubricating medium is considered as a Newtonian homogeneous fluid. Accordingly, the practically observed wear of the surfaces is associated only with the starting modes of friction when starting from rest, which is described by the Adhesion-Deformation model of friction and wear. At subsequent stages of friction with acceleration at ultra-small, low-medium sliding speeds up to operational friction speeds, wear of the surfaces theoretically does not occur.

2.3.1. Problematic issues of Elasto-hydrodynamic friction models

(1) The Elasto-hydrodynamic model, like the Hydrodynamic model, is a model of wear-free friction. The Elasto-hydrodynamic models take into account the stress state of surfaces in contact one-sidedly from the

standpoint of an increase in the contact area due to elastic deformation and an increase in pressure in the lubricating Elasto-hydrodynamic film, which is incorrectly identified with contact stresses. Other processes, such as rarefaction, reverse flows and end lateral overflows, are not considered.

(2) Identification of the pressure in the Elasto-hydrodynamic film and the contact stresses is a very doubtful statement, since, to date, physical scanning and measurement of local pressure in the elastically deformed region of the tribo-contact during friction in dynamics has not been performed by anyone, with the exception of [48].

(3) The minimum thickness of the lubricating layer $h_{\min}$, which is the main parameter of the tribocontact and a criterion in the Elasto-hydrodynamic model, as well as in the Hydrodynamic model, is not reliably measured today, but is speculatively postulated in a certain range from fractions to tens of micrometers.

(4) It is noteworthy that in the fluid friction mode, in accordance with the Elasto-hydrodynamic and Hydrodynamic models, the surfaces do not wear out, however, operating practice indicates the opposite: all friction surfaces wear out and it is not a fact that adhesive wear occurs only in starting modes, which is described within the Adhesion-Deformation model.

2.3.2. Critical analysis of the main provisions of the Elasto-hydrodynamic friction model

The Elasto-hydrodynamic model arose as a result of a search for a model that would cover the entire range of bearing operation from ultra-low to high speeds and loads in an elastically deformed contact area and under different lubrication conditions. In the course of the analysis of the main provisions of the Elasto-hydrodynamic model, contradictions are found with the fundamental physical laws of Hooke's deformation of solids, Pascal's hydrostatics, and the theories of adsorption by Langmuir and BET [20–22].

Thus, according to the Elasto-hydrodynamic model, in the region of maximum contact stresses (Fig. 7), the elastic deformation of the surfaces is the same as on the periphery of the contact, where the stresses are very small. This contradicts Hooke's law, according to which the amount of deformation is directly proportional to the applied force, in our case, contact stresses. Consequently, the curvilinear tribo-contact, in accordance with Hooke's law, is clearly inhomogeneous (in the center, where the greatest stresses are, the elastic deformation will be significantly higher than in the edge regions. Therefore, the gap profile will obviously be axisymmetric in the form of a fillet tapering towards the middle on the left and right (Fig. 7(a)).

When choosing the direction and the beginning of friction, it is also obvious that three elastically deformed characteristic regions will appear (Fig. 7(b)): a narrowing or confusing elastically deformed region, a transition elastically deformed region and an expanding or diffuse elastically deformed region. Since adhesive wear occurs only in elastically deformed regions (wear in non-contact regions with a gap is unlikely), it is these regions that require close attention to determine the causes and patterns of primary adhesion. Having answered the questions: in which of the three elastically deformed regions (confusing elastically deformed region, diffuse elastically deformed region or transition elastically deformed region) and why does primary microadhesion occur, we will be able to counteract it more consciously and effectively.

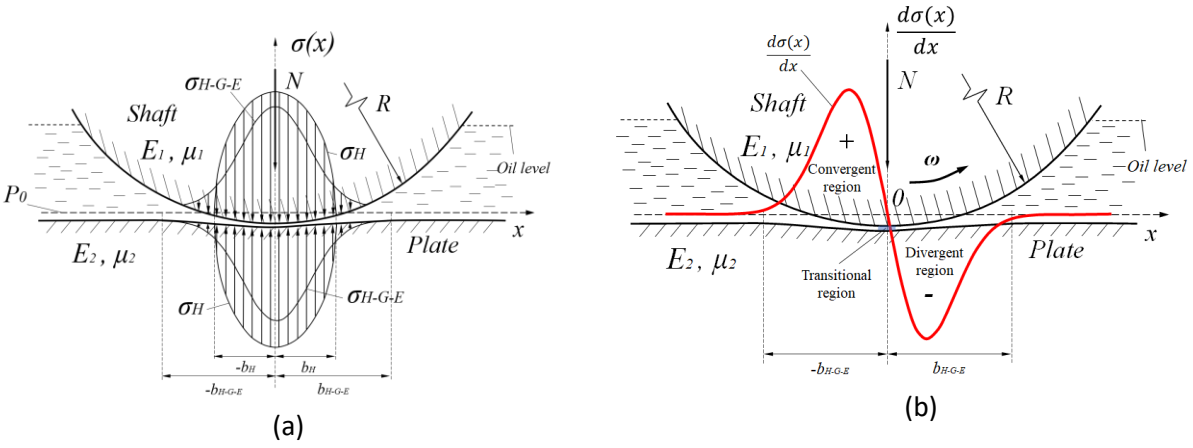

Fig. 7. Scheme of the formation of an elastically deformed linear contact of the shaft surface with a flat model bearing

Scheme of the formation of an elastically deformed linear contact of the shaft surface with a flat model bearing under static compression (without friction) with adsorbed layers of lubricant in the form of a fillet, as well as diagrams of contact stresses in the form of a semi-ellipse according to Hertz $\sigma^{H}(x)$ and in the proposed by the authors exponential distribution of Hertz-Gauss-Euler $\sigma^{H-G-E}(x)$ relative to the ambient pressure p_0 on the corresponding elastically deformed surfaces with the width of the curvilinear contact $[-b_H; +b_H]$ and

$\left[-b_{H-G-E};+b_{H-G-E}\right]$ (a). Gap profile in the form of a fillet and the appearance of three characteristic regions in an elastically deformed contact: convergent (confusing elastically deformed region), where $\frac{d\sigma(x)}{d(x)} > 0$ transitional (transition elastically deformed region), where $\frac{d\sigma(x)}{d(x)} \sim 0$ and divergent (diffuse elastically deformed region), where $\frac{d\sigma(x)}{d(x)} < 0$ at friction with shaft rotation frequency ω – (b).

Within the framework of the Elasto-hydrodynamic model, it is assumed that the thickness of the lubricating film in a curvilinear contact is constant and has the same value, which already contradicts the mono- and themselves as liquids. In accordance with this, even with static compression of surfaces with lubricating adsorbed layers, all supra-monomolecular layers will be squeezed out and flow into areas with lower pressure, and their microvolume pressure will tend to the oil pressure in the volume, in accordance with their main property - fluidity and Pascal's law. Therefore, in the case of a curvilinear contact, fragments of the boundary layers of the lubricant under the action of an external compression load in the convergent region realize extrusion. Looking ahead a little, we say that the extrusion of the lubricating layers will occur only in the narrowing convergent elastically deformed area of the tribocontact, where the lubrication fragments will be squeezed out in the opposite direction of friction and flow along the shortest path to the area where the oil pressure in the volume is minimal, which under normal conditions corresponds to atmospheric p_0.

In addition, within the framework of the Elasto-hydrodynamic model, a number of experimentally established effects were found that do not find their unambiguous explanation:

(1) Thermal effect of Murch and Wilson in the input area of the contact [19], which means that during friction of an elastically deformed curvilinear contact, the highest temperature occurs in front of the contact. The causes and mechanism of this effect have not been fully elucidated.

(2) Peak Petrusevich - the peak of the increase in contact stresses that occurs during friction in the output region of the elastically deformed contact, is associated with thinning of the lubricating layer in the "rear half of the contact", that is, in the output contact zone. This peak was observed at stresses of at least 200–300 MPa and is explained by its author [17-18] by the fact that the lubricating layers, passing through the contact zone, pass into a “quasi-plastic” or “amorphous” state with special properties of a certain “third body” according to Grubin [16]. In the input and central contact areas of the Elasto-hydrodynamic, the lubricant film heats up, its thickness decreases, and the contact stresses increase in the form of a peak, not exceeding the maximum values of the contact stresses determined by the formulas of G. Hertz (4-7) [17];

(3) The hydrodynamic effect of the “oil wedge” is also not fully disclosed, and such a main criterion for the bearing capacity of a lubricating Elasto-hydrodynamic film, such as its minimum thickness $h_{\min}$ has not been reliably measured for more than 100 years.

(4) Cavitation in lubricating layers of Elasto-hydrodynamic films, over the past 60 years, has become another effect in lubricating layers during friction, which has literally become a real trend in tribological research [23-46, 60-61]. During this time, the tribological literature on cavitation in lubricating layers during friction presents extensive results, most of which are aimed at determining the role and influence of cavitation bubbles on the bearing capacity of lubricating layers. Many researchers believe that frictional cavitation negatively affects the bearing capacity of lubricating Elasto-hydrodynamic films in accordance with the postulates of the Elasto-hydrodynamic model and can lead to adhesive wear. In widely known and popular works on this topic with extensive reviews and in-depth analysis of previous studies [60-61], as well as in reports from various research laboratories, friction cavitation is mostly explained from the standpoint of classical hydrodynamic cavitation at very high friction velocities. (700-15000 min^{-1}) [60-61]. A number of researchers associate the phenomenon of cavitation with dynamic oscillatory processes of surfaces in the radial direction due to the existing natural deviations of the shaft from the ideal geometric shape relative to the axis of rotation, which leads to oscillatory-pulsating radial loads per shaft revolution. The role of cavitation in tribological contacts has been discussed by many authors in relation to the bearing capacity of the lubricating film, namely its effect on the continuity and thickness of the Elasto-hydrodynamic lubricant film to determine the role of cavitation in frictional losses and wear of plain bearings [23-46].

2.4. The effect of cavitation during friction

The vast majority of works on cavitation during friction are in the nature of mathematical models and algorithms with different boundary conditions, by improving the Reynolds equations, to calculate the bearing capacity of the lubricating Elasto-hydrodynamic film in the gap of a radial plain bearing, taking into account cavitation phenomena. One of the very first works that led to the emergence of the cavitation direction in tribology was the work of Floberg [24, 60-61]. Many works devoted to the calculation of plain bearings and

optimization of their parameters were aimed at determining the field of hydrodynamic pressures under the Swift-Stieber boundary conditions by integrating the generalized Reynolds equation. However, the application of the Swift-Stieber boundary conditions led to an imbalance in the consumption of the lubricant entering the lubricant layer from the source and flowing into the bearing ends. Therefore, the Jacobson–Floberg–Olson (JFO) boundary conditions became more correct, and the first efficient algorithm that indirectly included the JFO boundary conditions was developed by Elrod and Adamson [27] in 1974.This algorithm is based on the finite difference method (FDM) and divides the solution region into two - the active region, where there is no cavitation and the lubricant completely fills the gap, and the cavitation region, where the lubricating layer breaks. The division into active area and cavitation area is done by using the original switching function. The flow in the cavitation region was considered as two-phase, consisting of liquid and gas (vapor) phases, with a uniform density, and the flow in the active region was considered as compressible with a constant modulus of elasticity.

Despite the fact that Elrod's algorithm is successfully applied in the theory of lubrication, the problems of convergence of calculation results remain unresolved [28]. Many researchers have worked and continue to work on improving the Elrod algorithm, applying it to different tribo-systems. So in 1986, Brewe [29] applied the Elrod algorithm to the study of dynamically loaded plain bearings. Brewe used an implicit alternating direction method, then, together with Woods [30], applied multigrid methods to increase the speed of convergence of the calculation results.

In modern mechanical engineering and, in particular, in engine building, in order to increase the resource, studies of the influence of deviations of the micro- and macro-geometry of friction surfaces from the ideal geometric shape are widely used. In addition to the structurally specified, macro-deviations are associated with natural errors in the processing of friction surfaces, load and thermal deformations, as well as friction and wear processes during the operation of tribocouples in the composition of the product. Therefore, Vijayaraghavan and Keith [31-32] modified the Elrod algorithm using different finite difference schemes for two flow regions, which improved its numerical stability, which was applied by Qiu and Khonsari [23] for textured thrust bearings. Qiu and Khonsari used a multi-grid method with Seidel's iterative scheme, and later they [33] applied the algorithm in conjunction with Patir and Cheng's method to investigate the effect of roughness within textures.

Also in 1991, Kumar and Booker [34-35] proposed an algorithm for transients optimized for the finite element method, which was applied by the authors of [36] to textured surfaces, taking into account roughness. Other FEM-based models have been developed by Shi and Paranjpe [37], Hajjam and Bonneau [38].Another approach by Gherca et al. [39] was implemented to study textured flat bearings under stationary and transient conditions. The cavitation algorithm was developed by Payvar and Salant [40] in 1992. Based on Elrod's theory, they developed a finite difference version of the algorithm with optimized numerical stability. Their model was adapted for mixed lubrication by Wang et al. in 2003 [41] using the method of Peter and Cheng as a rough surface contact model under real misalignment conditions in radial and thrust plain bearings. In [42], the authors used the Payvar and Salant algorithm to develop a universal Reynolds equation that allows one to simultaneously calculate macro- and micro-cavitation in plain bearings with rough surfaces. The Payvar and Salant algorithm is being applied to study lip seals with mixed lubrication [43], textured thrust bearings, and textured seals with rough surfaces [44-45]. Xiong and Wang [46] carried out a detailed analysis of the numerical implementation of this model by the finite volume method.

It should be noted that almost all of the above works [23-46,60-61] on cavitation in the lubricating layers of plain bearings are of a fundamental theoretical nature, and it is too early to talk about their applied use.

About the probable occurrence of cavitation in lubricating layers during rolling friction, in the well-known work of D. Klamman (1988) [62], on page 50, only a hypothesis was put forward that cavitation may occur in the rolling contact, which can lead to the destruction of surfaces with scaly petal look and pitting. These surface damage in the form of petals externally look like flakes raised in the rolling direction precisely in the areas where the surfaces of the rolling bodies roll out, which we also observed, that is, in the divergent areas. Then the scientific editor of the translation sharply criticized this hypothesis: "this statement is the personal opinion of the author (D.Klamman) and is not confirmed by official science (tribology)."

To a lesser extent, experimental works have been published with a detailed description of the methodology for conducting experiments and tangible results, which makes it difficult to reproduce them. Thus, a visible violation of the continuity of the lubricant flow when the shaft slides along a glass radial bearing in the zone of minimum clearance, that is, cavitation in the form of air gaps between oil streams, was observed as early as 1920 [63] by Hyde. A glass bearing and fluorescent lubricating oil were used by Cole and Hughes [64] in the study of the "negative pressure loop" of O. Reynolds in the area of the shaft exit from the contact, where the pressure reached 35...70 kPa (at atmospheric pressure approximately 102 kPa). A.Cameron (1962) [55] compared such pressure with real surface contact stresses, which usually amount to tens and hundreds of MPa and are two orders of magnitude greater than the pressure in the lubricating layer. Therefore, A. Cameron concluded that these negligibly small quantities can be neglected.

Cavitation in lubricating media during friction has also become the subject of many inventions and patents for methods and devices for its detection in the USSR, the USA, and China [65–67]. However, the main questions: where and why does cavitation occur during friction and how is it related to the primary adhesive wear today remain unanswered. The main drawback of the Elasto-hydrodynamic friction model is the absence of a relationship between the elastic-deformation processes between the contact surfaces and the hydrodynamic

processes in the mono-multimolecular boundary layers of the lubricant adsorbed on them during friction. The hypothesis about the Elasto-hydrodynamic film as some kind of amorphous substance is not valid, since it directly contradicts the BET theory and Pascal's law. It will be shown below that the elastic deformation of surfaces and especially highly loaded tribocontacts at the slightest displacement immediately leads to the appearance of extrusion in narrowing and rarefaction in expanding elastically deformed contact areas.

2.5 Adsorption

All three characteristic areas of the Stribeck curve (Fig. 1) for real highly loaded friction units have a common condition - the obligatory presence of lubricating layers on the friction surfaces. Therefore, the above analysis of the main friction of Adhesion-Deformation, Elasto-hydrodynamic and Hydrodynamic models should be supplemented with information about the surface adsorption of lubricants as the main process that ensures the very presence of boundary lubricant layers on friction surfaces.

Adsorption, as a process of concentration of a substance in the boundary layer at the contact boundary of different phases, as applied to tribology, covers two groups of phase separation - such as "solid - liquid" and "solid - gas". The last group is not considered within the framework of this article, due to the fact that we are talking about highly loaded friction units, which cannot work for quite a long time without a lubricant in real technology. At the same time, the friction surfaces are an adsorbent, and surfactants are an adsorbate, which are always present in a dissolved form in modern lubricants, which are adsorbents.

It is known that the adsorption of a lubricant boundary layer on friction surfaces, depending on the nature of the acting forces, proceeds through two main mechanisms, which are distinguished as physical adsorption and chemisorption. During physical adsorption between the molecules of the adsorbate and the active centers of the adsorbent, van der Waals forces act mainly, which have a dispersion, orientation, and induction character. The peculiarity is that these forces act between molecules or atoms that are in different phases. Physical adsorption, in contrast to chemisorption, is reversible and is most characteristic of lyophilic friction surfaces of real parts when they interact with modern lubricants, in which the most active adsorbate is surfactant molecules. At the same time, one cannot ignore the formation of secondary structures on friction surfaces in lubricating media as a result of chemisorption, which play an important role in the friction process and especially during long-term operation of tribo-systems.

The theory of adsorption of a monomolecular Langmuir layer [20–22] on a friction surface describes well the dependence of the adsorbate concentration on pressure using adsorption isotherms with increasing pressure. Obviously, as the pressure on the surface decreases, the adsorption isotherms become desorption isotherms. The BET multilayer theory of adsorption (Fig. 8) includes five main types of isotherms, which, depending on pressure, make it possible to predict the rate of adsorption-desorption and the thickness of adsorption layers, depending on the nature and properties of both the lubricating medium and the surface on which adsorption occurs. The modern literature contains tens of thousands of adsorption-desorption isotherms obtained for a wide variety of solids and liquids. However, most of the physical adsorption-desorption isotherms according to the IUPAC classification are based on the classical adsorption isotherms from I to V (BET), and according to the classification first proposed (1935-1940) by S. Brunauer, L. Deming , W. Deming and E. Teller (BDDT) already have them VI. These types of isotherms are shown in Fig. 9. Type I characterizes adsorption on surfaces with micropores, which are close to real rough friction surfaces. Type II and III isotherms are characteristic of macroporous materials often used in plain bearings. Isotherm types IV and V, which have a hysteresis loop, reflect capillary condensation in narrow gaps of near-contact elastically deformed sections of discrete protrusions of friction surfaces with adsorbed layers, that is, near actual contacts with a microrelief that is always present during compression of friction surfaces. The type VI isotherm describes the layer-by-layer filling of surfaces with adsorbate molecules and is extremely rare, for example, when nitrogen is adsorbed on the surfaces of some types of activated carbon. Common to all types of adsorption isotherms is that when the pressure is lowered, the opposite to the adsorption process occurs - the desorption process, when lowering the pressure to ultra-low values leads to the fact that the concentration of adsorbate molecules tends to zero (Fig. 9).

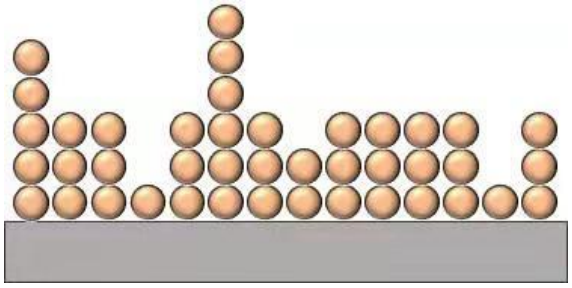

Fig. 8. BET multilayer adsorption model or random distribution of surfactant oil molecules (adsorbate) on the friction surface (adsorbent) in the form of circles included in one, two, three, and so on layers.

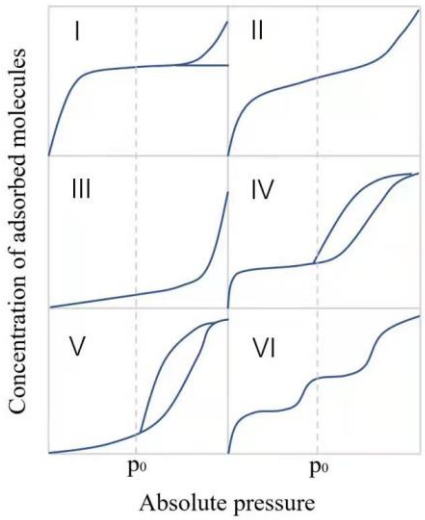

Fig. 9. Types of adsorption-desorption isotherms according to IUPAC and BDDT classification.

Another of the most important provisions of the BET theory for tribology is the conclusion that all supra-monomolecular adsorbed layers (second, third, etc.) under external force, including static compression, which is typical for all tribocontacts, lead themselves like liquid molecules. Thus, in the case of static compression of two surfaces with lubricating layers under the action of contact stresses, only the monomolecular layer is able to perceive and transmit uniaxial compression loads, and all other layers located above it (above the first monomolecular layer) will flow into areas of reduced pressure in accordance with the fundamental Pascal's hydrostatic law (Fig. 5).

However, in practice, during long-term operation of precision friction units, such as spool, plunger and other friction pairs with a roughness of Ra <0.02 μm, for example, fuel or hydraulic equipment with small contact stresses in contact of friction surfaces (6 ... 20 MPa), such tribosystems are often subject to adhesive micro-setting, seizing, jamming and wear. Therefore, naturally, the question arises why monomolecular layers on nano-rough surfaces, which under static conditions withstand high compression loads, are destroyed by friction. The mechanisms of desorption of monomolecular adsorbed lubricant layers on surfaces are experimentally little studied, not fully disclosed, and therefore this issue is an extremely urgent task for modern tribology. It should be emphasized that only in the BET theory there is information about the high sensitivity of multi- and monomolecular adsorbate layers to pressure reduction. So, all isotherms of the dependence of the adsorbate concentration on the adsorbent surface on pressure (Fig. 9) are also desorption isotherms, which indicate that with a local and rapid decrease in pressure at the adsorbent surface, the desorption of the adsorbate layers proceeds very intensively.

Thus, it is obvious that it is the desorption of multi- and monomolecular layers that is the key process that precedes the adhesive interaction of surfaces and adhesive wear. But the processes leading to the destruction of boundary layers and their desorption during friction are not fully understood.

2.6 General conclusions from a comprehensive analysis of the Adhesion-Deformation friction and wear model, Hydrodynamic and Elasto-hydrodynamic models of friction with lubrication and the elastic-deformation theory of solids by H. Hertz, the law of elastic deformation of solids by Robert Hooke and the law of hydrostatics by Blaise Pascal

Summing up the above analysis of Adhesion-Deformation, Hydrodynamic and Elasto-hydrodynamic friction models, the authors came to the conclusion that each of these models lacks some very important information about regular and objectively occurring processes in the elastically deformed regions of the tribocontact. These are the extrusion of the lubricating layers in the narrowing and their VACUUM in the expanding elastically deformed contact areas.

If each of the known Adhesion-Deformation, Hydrodynamic, and Elasto-hydrodynamic models is supplemented with regular and obvious processes of extrusion and rarefaction in combination with the adhesive interaction of working surfaces, then a generalized model will very likely arise, for example, the model of friction and wear proposed in [48].

Conclusions

1. The presented comprehensive analysis of the Adhesion-Deformation, Elasto-hydrodynamic and Hydrodynamic friction models, which describe different lubrication regimes during friction in different load-velocity ranges, in combination with the Langmuir-BET adsorption theory and the elastic-deformation theory of

curvilinear Hertz contacts made it possible to identify the following main contradictions: within the framework of the Adhesion-Deformation model of friction and wear, hydrodynamic processes in the boundary layers of the lubricant at low speeds and high loads are unlawfully denied; in the framework of the Hydrodynamic and Elasto-hydrodynamic friction models, the elastic-deformation state of the tribocontact is considered one-sidedly, only from the standpoint of a geometric increase in the contact area, which increases the bearing capacity of the Elasto-hydrodynamic lubricant film. At the same time, the wearlessness of friction surfaces is postulated unconvincingly and unjustifiably at low loads and at moderate to high friction velocities. At the same time, the minimum thickness of the lubricating film, which is the main criterion for non-contact and wear-free friction, is in fact not currently determined or measured by direct methods.

2. The revealed contradictions between Adhesion-Deformation, Hydrodynamic and Elasto-hydrodynamic models can be resolved if we take into account naturally occurring processes that have been hidden from direct observations for a long time - Extrusion of lubricating layers in convergent elastically deformed and Rarefaction in divergent elastically deformed regions of tribocontacts. Thus, a real opportunity arises to create a new, more complete model and theory of friction and wear, where extrusion and rarefaction of boundary layers play a dominant role in the occurrence of quasi-dry friction conditions that cause adhesive wear of various tribocontacts, including highly loaded tribosystems.

3. The Hydrodynamic and Elasto-hydrodynamic models of friction are mostly of a theoretical speculative nature, since they do not touch upon the topical issues of wear and service life of tribosystems. However, the practice of operation and the personal experience of the authors testify to the opposite: adhesive wear of surfaces of lightly and highly loaded tribosystems always occurs during friction: in all lubrication modes and in the entire range of loads and speeds, just the wear intensity will naturally be different.

Nomenclature

N axial load of the shaft on the plain bearing, N

h(x) respectively, the gap between the sliding friction surfaces of the shaft and the bearing in the current coordinate (x) in the direction of friction and its minimum value h_{min} or the minimum thickness of the lubricating layer according to Reynolds

O_1 the center of the axis of rotation of the plain bearing shaft

O_2 the center of the axis of the radial plain bearing

e the eccentricity between the central axes of symmetry of the rotating shaft O_1 and the cylindrical friction surface of the bearing O_2, which occurs during friction

p_0 ambient pressure: atmospheric pressure or pressure of the lubricating medium in the lubrication system

σ_{max} maximum contact stresses, determined by the formulas of G. Hertz

b the width of the linear contact, determined by the formula of G. Hertz

l length of the linear contact of the radial plain bearing

r radius of plain bearing shaft

R radius of plain bearing

υ Linear sliding speed

ν Kinematic viscosity of the lubricating medium

k_1, k_2 Rheological coefficients

x the coordinate of the contact points of the abscissa corresponding to the direction of sliding

CED convergent elastically deformed area of tribocontact

DED divergent elastically deformed area of tribocontact

Acknowledgements

This research did not receive any specific grant from funding agencies in the public, commercial, or not-for-profit sectors.

References

1. Kragelskiy I V, Dobychin M N, Kombalov V S. Basics of friction-wear calculations. Moscow: Mashinostroenie, 1977. (in Russian)
2. Demkin N B, Ryzhov E V. Surface quality and machine parts contact. Moscow: Mashinostroenie, 1981. (in Russian)
3. Bowden F P, Tabor D. Friction and Lubrication of Solids. Oxford (UK): Oxford University Press, 2001.
4. Kostetskiy B I. Wear resistance of machine parts. Moscow : MASHGIZ, 1950. (in Russian)
5. Khebdy M, Chichinadze A V. Handbook of Tribotechnics. Moscow: Mashinostroenie, 1989. (in Russian)
6. Kragelskiy I V, Alisin V V. Friction, Wear and Lubrication: A Handbook. Moscow: Mashinostroenie,

1978. (in Russian)
7. Garkunov D N. Tribotechnics. Moscow: Mashinostroenie, 1989. (in Russian)
8. Mashkov Y K. Tribology of Structural Materials: Tutorial. Omsk: OmSTU Press, 1996. (in Russian)
9. Luzhnov Y M, Aleksandrov V D. Basics of Tribotechnics: Tutorial. Moscow: MADI, 2013. (in Russian)
10. Akhmatov A S. Molecular Physics of Boundary Friction. Moscow: Fizmatgiz, 1963. (in Russian)
11. Leybenzon L V. Hydrodynamic theory of lubrication. Moscow: State Technical and Theoretical Publishing House, 1934. (in Russian)
12. Petrov N P. Friction in machines and the effect of lubricating fluid on it. Moscow: Trudy, 1883. (in Russian)
13. Reynolds O. On the theory of lubrication and its application to Beauchamp Tower's experiments including an experimental determination of the viscosity of olive oil Philos. London: London Ser, 1886.
14. Stribeck R. Die wesentlichen Eigenschaften der Gleitund Rollenlager. Berlin: Springer, 1902: 341. (in German)
15. Ertel A M. Hydrodynamic calculation of lubrication contact of curved surfaces. Moscow: CNIITMASH, 1945. (in Russian)
16. Grubin A N. Contact stresses in toothed and worm engagements // Fundamentals of the hydrodynamic theory of lubrication of heavily loaded cylindrical surfaces / Trudy CNIITMASH, book 30. Moscow: Mir, 1949. (in Russian)
17. Petrusevich A I. The main conclusions from the contact-hydrodynamic theory of lubrication. Izvestiya AN SSSR: OTN 2: 209-223 (1951). (in Russian)
18. Petrusevich A I. The main conclusions from the contact-hydrodynamic theory of lubrication. Izvestiya AN SSSR: OTN 2: 209-216 (1951). (in Russian)
19. Murch L E, Wilson R D. A thermal elastohydrodynamic inlet zone analysis. ASME J. Lubr Technol 97(2): 212-216 (1975).
20. Gregg S J, Sing K S W. Adsorption, Surface Area and Porosity: 2. Auflage. London: Academic Press, 1982. (in German)
21. Fenelonov V B. Introduction to the physical chemistry of the formation of supramolecular structure of adsorbents and catalysts. Novosibirsk: SO RAN, 2002. (in Russian)
22. Prodan V D. Tightness of detachable connections of equipment operated under the pressure of the working medium:tutorial. Tambov: FGBOU VPO 'TGTU' Press, 2012. (in Russian)
23. Qiu Y. On the prediction of cavitation in dimples using a mass- conservative algorithm. J Tribol 131(4): 1–11 (2009).
24. Jakobsson B, Floberg L. The finite journal bearing, considering vaporization. Sweden: Tran Chalmers University of Tech Gothenburg, 1957.
25. Olsson K O. Cavitation in dynamically loaded bearings. Sweden: Tran Chalmers University of Tech Gothenburg, 1965.
26. Elrod H G. A Cavitation Algorithm. Journal of Tribology 103(3): 350–354 (1981).
27. Elrod H G. A computer program for cavitation and starvation problems. Cavitation and related phenomena in lubrication: 37-41(1974).
28. Fesanghary M, Khonsari M M. A modification of the switch function in the Elrod cavitation algorithm. J Tribol 133(2) (2011).
29. Brewe D E. Theoretical modeling of the vapor cavitation in dynamically loaded journal bearings. J Tribol 108: 628–637 (1986).
30. Woods C M, Brewe D E. The solution of the Elrod algorithm for a dynamically loaded journal bearing using multigrid techniques. Tribology conference in Maryland : 302-308 (1989).
31. Vijayaraghavan D, Keith Jr T G. Development and evaluation of a cavitation algorithm. Tribol Trans 32(2): 225–233 (1989).
32. Vijayaraghavan D, Keith Jr T G. An efficient, robust, and time accurate numerical scheme applied to a cavitation algorithm. J Tribol 112: 44–51 (1990).
33. Qiu Y. Performance analysis of full-film textured surfaces with consideration of roughness effects. J Tribol 133(2): 021704 (2011).
34. Booker J F. A finite element cavitation algorithm. J Tribol 113(2-4): 276–284 (1991).
35. Kumar A, Booker J F. A finite element cavitation algorithm: application/validation. J Tribol 113(2): 255–260 (1991).
36. XIE Y. A mass - conservative average flow model based on finite element method for complex textured surfaces. Sci China Phys Mech Astron 56: 1909–1919 (2013).
37. Shi F. An implicit finite element cavitation algorithm. Comput Model EngSci 3(4): 507–515 (2002).
38. Hajjam M. A transient finite element cavitation algorithm with application to radial lip seals. Tribol Int 40(8): 1258–1269 (2007).
39. Gherca A. Effects of surface texturing in steady-state and transient flow conditions: Two-dimensional numerical simulation using a mass-conserving cavitation model. J Tribol 229(4): 505–522 (2014).
40. Payvar P. A computational method for cavitation in a wavy mechanical seal. J Tribol 114: 199–204 (1992).

41. Wang Y. Mixed lubrication of coupled journal-thrust-bearing systems including mass conserving cavitation. J Tribol 125(4): 747–755 (2003).
42. Harp S R. An average flow model of rough surface lubrication with interasperity cavitation. J Tribol 123(1): 134–143 (2000).
43. Shi F. A mixed soft elasto-hydrodynamic lubrication model with interasperity cavitation and surface shear deformation. J Tribol 122(1): 308–316 (1999).
44. Zhang J. Direct observation of cavitation phenomenon and hydro - dynamic lubrication analysis of textured surfaces. TribolLett 46(2): 147–158 (2012).
45. Brunetiere N. Numerical analysis of a surface-textured mechanical seal operating in mixed lubrication regime. TribolInt 49: 80–89 (2012).
46. Xiong S. Steady-state hydrodynamic lubrication modeled with the PayvarSalant mass conservation model. J Tribol 134(3): 1–16 (2012).
47. Koronatov V A. On the correct application of Coulomb's law when using experimental friction characteristics. Technology 3 (43): 35-43 (2019). (in Russian)
48. Stelmakh O U. Physical and technological bases of control of dynamic processes in lubricating layers to improve their performance of tribosystems. Khmelnitskiy (Ukraine): Khmelnitskiy National University, 2015. (in Russian)
49. Pinkus O. Thermal Aspects of Fluid Film Tribology. New York: ASME Press, 1990: 317-326.
50. Hardy W I. Collected Scientific Papers. London: Càmbridge, 1936.
51. Altoiz B A, Bondarev V N, Shatagina E A, Kiriyan S V. Model of organization of an epitropic liquid-crystal phase. Zh. Tekh. Fiz 84: 58-61 (2014). (in Russian)
52. Garkunov D N. Selective transfer in friction nodes. Moscow: Transport, 1969. (in Russian)
53. Garkunov D N, Kragelskiy I V. Wearlessness effect. USSR Patent 41: 12 Nov. 1956.
54. Dukhovskoy E A, Onischenko V S, Ponomarev A N, Silin A A, Talroze V L. The phenomenon of abnormally low friction in a vacuum. USSR Patent 121: 16 Sep. 1969.
55. Cameron A. Basic Lubrication Theory. Moscow: MASHGIZ, 1962. (in Russian)
56. Kravchuk A S, Kravchuk A I. Applied contact problems for a generalized rod model of coating. St. Petersburg: Naukoyemkie tekhnologii, 2019. (in Russian)
57. Johnson K. Mechanics of contact interaction. Moscow: Mir, 1989. (in Russian)
58. Kravchuk A S, Kravchuk A I. Mechanics of contact interaction of bodies with circular boundaries. Minsk: Tekhnoprint, 2000. (in Russian)
59. Zolotarevskiy V S. Mechanical properties of metals. Moscow: Metallurgiya, 1983. (in Russian)
60. Braun M J, Hannon W M. Cavitation formation and modelling for fluid film bearings: A review. J Eng Tribol 224(9): 839-863 (2010).
61. Information on https://oaktrust.library.tamu.edu/bitstream/handle/1969.1/93246/Notes06%20Liquid%20cavitation%20model.pdf?sequence=1&isAllowed=y.
62. Klamann D. Lubricant and related products. Moscow: Khimiya, 1988. (in Russian)
63. Donkin S B. Report of the Lubricants and Lubrication Inquiry Committee. London: Department of scientific and industrial research, 1920.
64. Cole J A, Hughes C J. Oil flow and film extent in complete journal bearings. Proceedings of the Institution of Mechanical Engineers 170(1): 499-510 (1956).

Олександр Стельмах, Хун'ю Фу, Іцяо Гуо, Сіньбо Ван, Хао Чжан, Павло Каплун. Екструзія та розрідження мастила в граничному шарі як ключьові процеси адгезійного зношування високонавантажених трибоконтактів.

Представлено комплексний аналіз адгезійно-деформаційної, пружно-гідродинамічної та гідродинамічної моделей тертя, які описують різні режими змащування відповідно до кривої Штрібека. Основні положення цих моделей розглядаються в поєднанні з теорією адсорбції Ленгмюра і пружно-деформаційною теорією криволінійних контактів Герца. Показано, що виявлені протиріччя потребують свого вирішення, а виявлені множинні ефекти потребують науково обґрунтованої інтерпретації. Пропонується розробити більш узагальнену модель тертя та зношування на основі природних процесів, які довгий час були приховані від прямих спостережень. Це: Екструзія змащувальних шарів у збіжних пружно деформованих і Розрідження у розбіжних пружно деформованих областях трибоконтактів. Розуміння цих процесів дає змогу передбачити місця локалізації та причини виникнення первинних наступних актів зчеплення поверхонь тертя та їх зношування за таким циклом: «розрідження та десорбція мастильних шарів, що призводить до деформаційного руйнування оксидних плівок та зрощення ювенільних ділянок поверхні, після чого до відриву осколкового матеріалу від підшипника та новоутворення виступу на валу – у розбіжних пружно деформованих ділянках контакту. Далі відбувається мікрорізання цим фрагментом опорної поверхні з виходом продукту зношування в конвергентну пружнодеформовану область, що відповідно призводить до зміни фактичної геометрії та натягу трибоконтакту. Крім того, в інших областях відновленого контакту адгезивна взаємодія відбувається в інших розбіжних областях відповідно до того самого механізму. Глибоке розуміння причин десорбції мастильних шарів дозволить розробити та застосувати нові високоефективні технологічні та матеріалознавчі методи з метою підвищення ресурсу високонавантажених трибосистем машин і механізмів.

Ключові слова: моделі макротертя; адгезійний знос; градієнт тиску; кавітація

Problems of Tribology, V. 27, No 3/105-2022, 27-33

Problems of Tribology
Website: http://tribology.khnu.km.ua/index.php/ProbTrib
E-mail: tribosenator@gmail.com

DOI: https://doi.org/10.31891/2079-1372-2022-105-3-27-33

Wear resistance of structural steels nitroded in cyclic-commuted discharge at limit modes of friction

M.S. Stechyshyn[1*], V.V. Lyukhovets[1], N.M. Stechyshyn[1], M. I. Tsepenyuk[2]

[1]Khmelnitsky National University, Ukraine
[2]Ternopil Ivan Pul'uj National Technical University, Ukraine

**E-mail: avmart@khmnu.edu.ua*

Received: 22 June 2022: Revised: 23 July 2022: Accept: 29 July 2022

Abstract

The article discusses the method of conducting tribological studies at the limit modes of friction of nitrided and non-nitrided steels 20 and 45 in order to achieve a comparison of the results of laboratory tests with operational data. The relationship of structural phases in time is significantly influenced by the initial state of the surface and its physical and mechanical characteristics, pressure on the contact surface, sliding speed, and all these parameters for the limit mode of friction are closely related. Carrying out tests on the wear resistance of samples made of different materials and with significantly different characteristics of the surface layer at the same parameters of the test regime is impossible in most cases, since the obtained results are problematic to compare.

Keywords: nitriding, limit friction, wear

Statement of the problem and analysis of the latest research.

One of the directions of development of tribology is the development of methods of objective tribological studies of nitriding characteristics of surface layers on structural steels, depending on the requirements of further operation of nitriding facilities. [1-3].

For the objectivity of research on the wear resistance of nitrided surfaces, attention should be paid to the fact that post-modification characteristics should be compared with similar parameters of geometrically similar surfaces that were not modified. At the same time, both for one and for the other, they should be determined according to the same type of methodology. Only if these requirements are met, the results of the modification can be assessed as real and having scientific and practical significance. Indeed, in the event of the impossibility of meeting these requirements, the problem of finding a transition function between the results of experiments will arise. Comparison of parameters obtained under different conditions of their fixation can lead to conclusions that are highly unlikely to be confirmed in practice. One of the essential points of establishing experimental results is to ensure the conditions of experiments, which would correspond to the maximum extent similar to the characteristics of real operation [4]. Indeed, there is almost always a certain inconsistency of the conclusions formed on the basis of experiments, if the test conditions differed significantly from the real operating conditions. Finally, the time factor is not the least important, since it is possible to apply such operating parameters of the experimental installation for the study of wear resistance, in which the wear process over time would approach the values recorded in the operating mode. Then the duration of experimental research, taking into account the need to ensure the necessary reliability of their results, will be such that the need for the research itself for practice will disappear by itself.

The purpose of the work is to develop a methodology and criteria for evaluating experimental studies of the wear resistance of samples after their surface modification by nitriding in a glow discharge to achieve the results of laboratory tests that correspond to the real conditions of operation of parts.

Methodology of conducting experimental studies.

Experimental studies were carried out on a universal machine for testing materials for friction, model 2168UMT with some modernization of the friction unit, which is described in detail in the work [5]. Working out the modes of experiments was carried out on samples, the method of preparation of which is given in the same place. To check the possibility of further comparison of wear processes, objects with significantly different surface characteristics were selected: soft surfaces are represented by samples from steel 20 without modification, modified - from steel 45 after nitriding in a glow discharge. The latter before nitriding had a surface hardness of HV0.1 215, after modification HV0.1 700...730. Since liquid lubricant was supplied to the friction zone, the friction coefficient was fixed in the range of 0.05...0.12, which corresponds to the limit mode of friction.

Presentation of the main material and received scientific research.

The initial series of experiments was carried out on steel 20 samples without their modification. The hardness of the counterbody made of hardened steel was HRC 60. The speed and pressure were chosen within such limits that the temperature of the surface of the samples in the friction zone did not exceed 40˚C, and in combination with the pressure value, the constant presence of lubricant on the friction area would be ensured. At the speed of the relative movement of the sample V=1.8 m/s and the pressure of 10 MPa (this value turned out to be optimal, since more or less heavy wear is observed with it and there are no sticking phenomena), uniform wear is observed, and the value of linear wear is on average 15, 3 μm/km of path. The coefficient of friction ranged from 0.05 to 0.12, which in the experimental conditions corresponded to a friction force of 29.5 to 64.6 N. The dependence of the linear wear averaged over several samples per one kilometer of the path on the path is shown in Fig. 1.

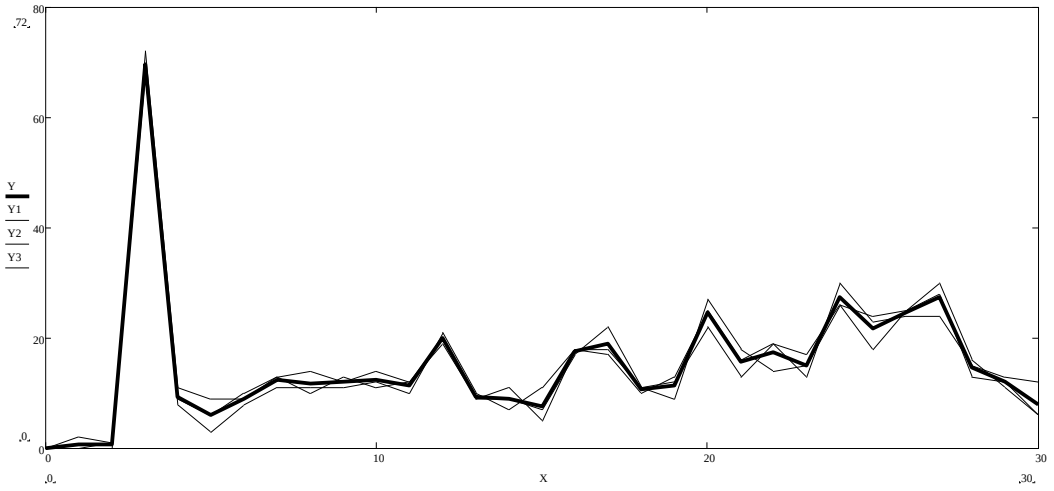

Fig. 1. Dependence of linear wear on the friction path of samples made of steel 20 non-nitrogenized at a pressure of 10 MPa, a speed of 1.8 m/s

In fig. 1, the friction path from 0 to 30 km is plotted on the horizontal axis, and the amount of wear in microns is plotted on the vertical axis (the main line is the amount of linear wear averaged over all samples, the thin lines are the average linear wear over groups of samples. From Fig. 1, it is clear the conclusion regarding the variable nature of the wear process itself is followed. In the first kilometers of the wear path, there is practically no wear, which can be explained by the fact that the samples were pre-loaded during the run-in process with a pressure of the order of 8 MPa. At the same time, a layer of compacted metal, a kind of slander, was formed on the future friction surface i.e., it strengthened on the surface. As this initial surface layer was removed, the process of intensive wear began. Further wear occurred according to the scheme of periodic surface compaction and destruction of this compacted layer. This explains the periodic fluctuations of both the coefficient of friction and the force of friction. Thus, from the above the first conclusion regarding the uneven character of wear follows formation of unmodified samples caused by constant structural transformations on the friction surface and the destruction of structures, the characteristics of which exceed the indicators of the surface hardness of the base of the samples. The same conclusion is confirmed in fig. 2 is a graph of the absolute wear of the samples depending on the traveled friction path (line markings are similar to Fig. 1).

The effect of surface compaction - slander when increasing the pressure is manifested in the increase of surface microhardness several times. For example, even for cast iron after treatment with a pressure of 1.2 MPa, the surface microhardness reached values of HV0.1 1000. It is not excluded that the constant presence of lubricant in the contact zone of the sample and the counterbody can contribute to the formation of metal-mineral structures, the processes of appearance and destruction of which also provoke unevenness wear [6].

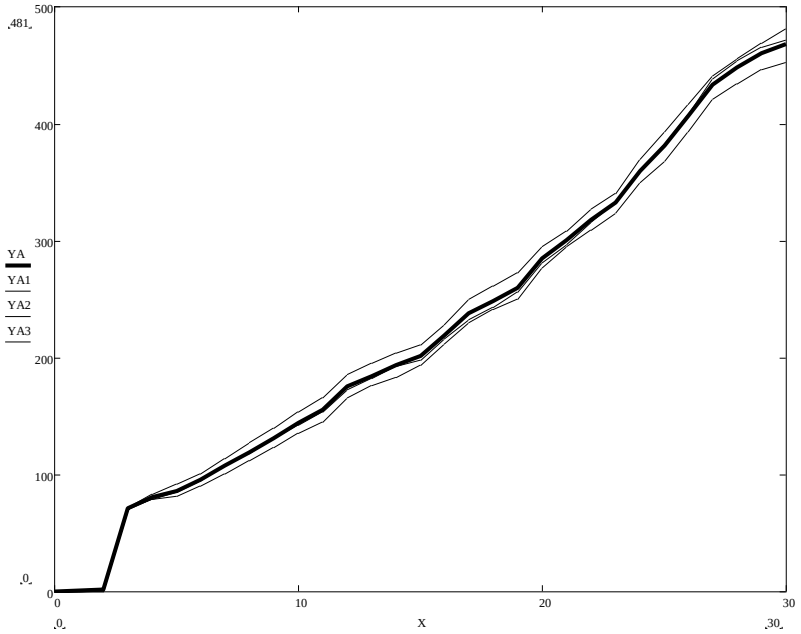

Fig. 2. Graph of the absolute value of linear wear of steel 20 samples

A change in the amount of pressure on the friction surface also significantly affects the wear process. The influence of the nature of the pressure change on the contact surface is confirmed by experiments with samples of unmodified steel 45. At an initial pressure of 10 MPa and a sliding speed of 1.8 m/s (that is, the parameters of the test regime completely coincided with those adopted for samples of steel 20) when reaching the path values 10 km of linear wear was practically not recorded. A stepwise increase in pressure by 2 MPa after each kilometer of the path up to 16 MPa also did not change the nature of the wear. At a pressure of 18 MPa, linear wear of 15-17 microns was observed in the next kilometer, but the wear stopped again in the next kilometer. After that (18 km of travel), the pressure was increased to 20 MPa, but no wear was observed. Thus, it follows from the foregoing that the surface of the sample is periodically compacted and strengthened, its destruction requires either a significant path of friction, or an increase in pressure to certain limits, which causes a frictional force sufficient for another change in the surface structure. In addition, it should be added that with the initial surface microhardness of HV0.1 215, after 20 km of the path and reaching a surface pressure of 20 MPa, the surface microhardness increased to the values of HV0.1 414. Subsequently, the pressure continued to be increased by 2 MPa for each new kilometer of the path, however linear wear was again not observed up to 26 MPa. At this pressure, at first wear increased intensively to values of 131-167 microns, and then the phenomena of seizing began. After the process began to be implemented at a pressure of 26 MPa, the surface microhardness increased to the values of HV0.1,856, i.e., in fact, the surface underwent mechanical modification. As for the nature of the pressure change on the surface, in the described experiment, the pressure increased according to a certain scheme (for example, by 2 MPa per kilometer of the path), its structural changes took place gradually. And in the next experiment with the participation of similar new samples and the counterbody, from the very beginning the pressure in the contact zone was set at the level of 24 MPa (at this pressure value, achieved by a stepwise increase in the previous experiment, linear wear was practically not fixed). Already in the first kilometer, the coefficient of friction increased rapidly to the values characteristic of adhesion, and the surface microhardness was HV0.1,892. In fact, at such a high pressure, the surface changed dramatically structurally, it is possible that these structural transformations led to the squeezing of the oil film from the contact zone and the nature of the friction process began to approach the regime of dry friction, which led to setting. The following experiment speaks about the role of the factor of the nature of the pressure change. On samples made of the same steel 45, the pressure from the very beginning changed according to the pattern of 2 MPa/km of the path and wear was practically absent, but already after 5 km the pressure was sharply increased to 20 MPa, which immediately led to the appearance of seizure phenomena, and the surface microhardness at the end of the experiment was HV0.1 838.

A parallel temperature control in the contact zone established that its value does not exceed 42°C immediately after stopping, and after 5-10 seconds after opening the contact, the surface temperature does not exceed 22°C. Thus, pressure was the decisive factor that influenced the nature of friction in these experiments, since the viscosity characteristics of the lubricant did not change significantly at the fixed temperature values.

The presence of a compacted layer on the surface as the main factor determining wear parameters was confirmed as follows. Without removing the sample from the stand, i.e. the basing conditions remained unchanged, a layer of 15-24 μm was removed with a fine sanding pad number 150 and number 500. Before that, at a pressure of 18 MPa, there was practically no linear wear on the 13 km path (only before grinding at different pressure values, the total path was 25 km). On the first kilometer after grinding, linear wear was recorded in the

range of 18-23 μm, on the next two kilometers it stopped again, then after similar grinding, the wear again amounted to about 10 μm with a gradual cessation, which once again confirms the above version of the influence on the nature of wear of the formation process compacted microstructures. It is interesting that the surface microhardness after grinding practically does not differ from the initial values.

The condition of the surface of the counterbody also significantly affects the course of the wear process. In the experiments described above, as already mentioned above, a hardened steel counterbody with a smooth surface (roughness parameter Ra 0.27) was used. The experiments described above were primarily time-consuming, for example even one series of steel 20 samples required, including time for temperature stabilization, measurements, etc., two full working days (15 hours). It is obvious that obtaining results that first of all meet the requirement of reliability of conclusions would require a time that cannot be considered real. This especially applies to those issues where obtaining operational data on the effectiveness of one or another method of modification and the technological parameters of its implementation is extremely necessary. Therefore, the next phase of the experiments were experiments in which the role of the mechanical component of wear was significantly increased. For this purpose, counterbodies were used, the surface roughness of which was artificially increased by sanding with a skin, a wheel, application of titanium and hard alloy on an electric spark unit, application of radial direction lines, etc. With the help of various methods of surface grinding, the roughness parameter Ra increased from a value of 0.2...0.3 μm to 0.5 μm when sanding with a leatherette by hand, to 0.37 μm when grinding with a circle on a grinding machine, and 1.15 μm when grinding with a circle on a grinding machine. After the application of titanium and hard alloy by the electric spark method, the roughness parameter exceeded 8 μm. The hardness of the surface after applying the coating by the electrospark method, depending on the polarity of the electrode, the brand of the implanted material, and the place of measurement (polished or fused surface) was HV0.1, 450...800, and higher values, as a rule, corresponded to the areas with subsequent grinding after implantation, which confirms the above-mentioned effect of surface sealing after grinding.

The graph of changes in linear wear of samples made of unmodified steel 45 (counterbody - modified by electrospark implantation, pressure 4 MPa, speed - 1.8 m/s) with observance of the curve designation system adopted in the previous figures is shown in fig. 3. As can be seen from this figure, at the beginning of the wear process, the mechanical wear component provides an incomparably greater intensity than in the previous experiments, and the pressure on the surface was significantly lower. The cutting ability of the counterbody leads to the destruction of surface structures, while preventing their compaction, but over time, as the microprotrusions on the surface of the counterbody become dull, the wear process becomes less and less intense, up to a complete cessation.

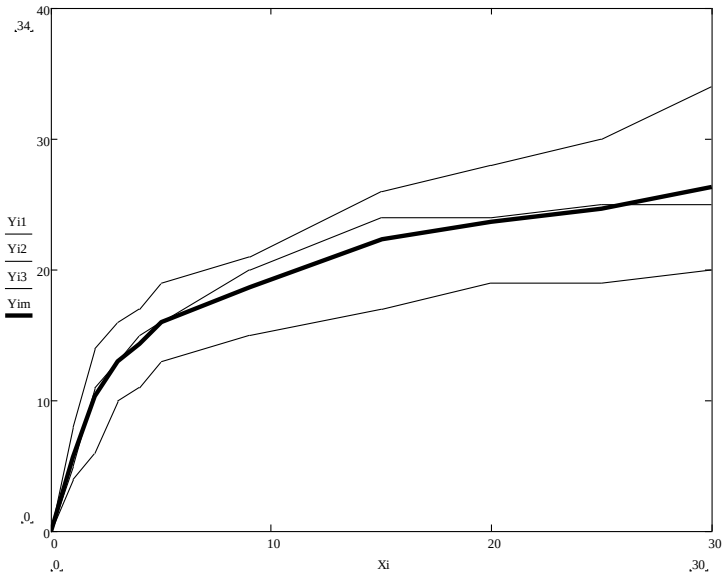

Fig. 3. Graph of changes in linear wear for a pair of samples made of unmodified steel 45; counterbody - implanted by the electrospark method

Results similar in content were obtained when using counterbodies, one of which was machined on a lathe with a VK8 cutter at a radial feed of 0.11 mm/rev, which provided a roughness parameter Ra of 2...3 μm. The intensity of wear on the first kilometer of the path at a pressure of 2 MPa was 8-10 microns for every 100 m of the path, but already at the beginning of the second kilometer this indicator decreased to the level of 1-2 microns per 100 m, and then to 1-2 microns/km.

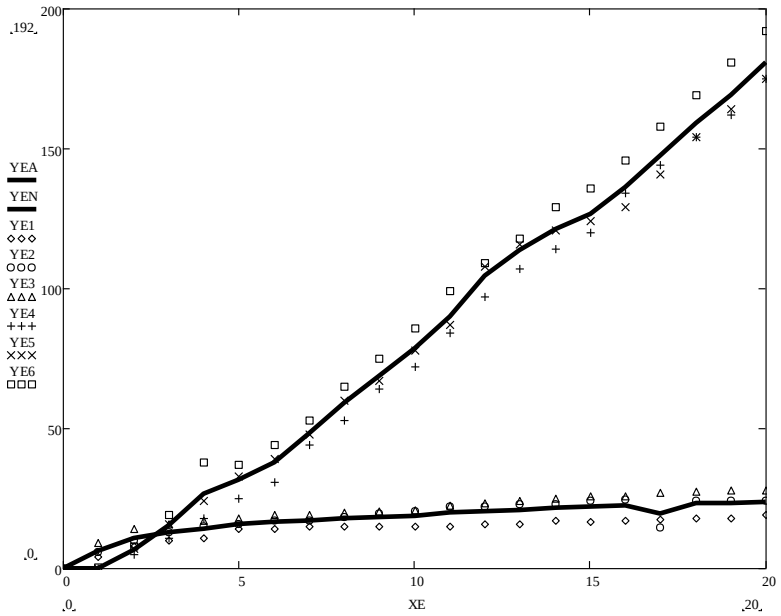

Fig. 4. Wear of nitrided (upper area) and non-nitrided samples (lower) due to the action of the mechanical component of friction (pressure 4 MPa, counterbody – VK8 hard alloy implanted by the electrospark method)

The nature of wear of nitrided samples in comparison with non-nitrided ones is shown in fig. 4. Nitrided samples (steel 45, surface microhardness HV0.1 466) were worn under the same conditions as those given above with the use of a machined counterbody, but the pressure was 4 MPa. As can be seen from the figure, the wear process for non-nitrogenized samples is traditional with the formation of compacted surface structures and practically stopping wear already after three kilometers of travel. Nitrided samples practically do not wear out in the first kilometer, since the strongest interlayer of the ε-phase comes into play. However, its thickness is insignificant, literally a few micrometers, so already in the next kilometers of the road, the process of wear begins with almost constant intensity. This is due to the fact that a really homogeneous interlayer of the γ′-phase and α-solid solution with sufficiently significant hardness indicators cannot be compacted and is removed due to the mechanical component of the wear process. Despite the fact that in the experiments, the results of which are shown in fig. 4, relatively little pressure was applied.

Further research developed in the direction of elucidating the influence of pressure on the wear process up to its large values. The results of this series of experiments are shown in fig. 5.

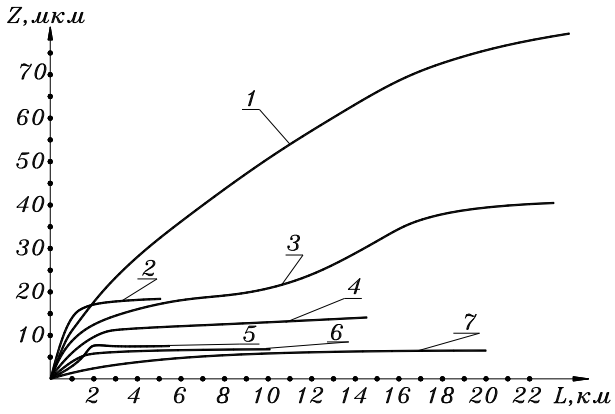

Fig. 5. Wear samples of nitrided steel 45 depending on the path at pressure in the contact zone and sliding speed: 1-65 MPa, 0.1 m/s; 2 – 50 MPa, 0.1 m/s; 3 – 120 MPa, 0.1 m/s; 4 – 80 MPa, 0.1 m/s; 5 – 40 MPa, 0.3 m/s; 6 – 65 MPa, 0.2 m/s; 7 – 20 MPa, 0.2 m/s

From fig. 5 follows the conclusion that at almost any pressure there comes a moment when the wear process practically stops, however, the way in which such stabilization is observed is different for different pressure values. The hypothesis that the wear process in conditions where the mechanical component of this process prevails is actually a combination of two competing processes - strengthening of the surface and destruction of this strengthened layer is confirmed by fig. 5. The harder the contact surface, the greater the

pressure threshold at which the compacted layer collapse phase occurs. However, the influence of pressure at its high values is extreme: in the demonstrated series of experiments, the wear process occurred most dynamically at a pressure of 65 MPa. At pressure values lower and higher than this value (at the same sliding speed), the intensity of wear was lower. An increase in the sliding speed leads to a decrease in the intensity of wear and an acceleration of the beginning of the stabilization phase, which can be explained by a decrease in the relaxation time of the surface layer compaction processes.

Conclusions

1. The wear process at extreme friction actually includes two competing processes: compaction of the surface layer with an increase in its microhardness and destruction of the surface layer with local adhesion of the surfaces.

2. The relationship of these phases in time is significantly influenced by the initial state of the surface and its physical and mechanical characteristics, pressure on the contact surface, sliding speed, and all these parameters for the limit mode of friction are closely related.

3. Carrying out tests on the wear resistance of samples made of different materials and with significantly different characteristics of the surface layer at the same parameters of the test regime is impossible in most cases, since the obtained results are problematic to compare.

4. Such test conditions should be considered promising, which can be applied to surfaces with different characteristics and provide results that are acceptable from the point of view of reliability, mutual comparison and time of their implementation

References

1.Kaplun V.H., Kaplun P.V. Yonnoeazotyrovanye v bezvodorodnыkh seredakh: monohrafyia / V.H. Kaplun, P.V. Kaplun. – Khmelnytskyi: KhNU, 2015.-315s.

2.Pastukh Y.M. Teoryia y praktyka azotyrovanyia v tleiushchem rozriade. Kharkov: NNTs KhFTY, 2006. – 364s.

3.Stechyshyna N.M., Stechyshyn M.S., Mashovets N.S. Koroziino-mekhanichna znosostiikist detalei obladnannia kharchovykh vyrobnytstv: monohrafiia / N.M., Stechyshyna, M.S.Stechyshyn, N.S. Mashovets. – Khmelnytskyi: KhNU, 2022.-181s.

4.Skyba M.Ie., Stechyshyna N.M. Koroziino-mekhanichna znosostiikist detalei obladnannia molokozavodiv / Kharchova promyslovist. Kyiv: NUKhT, 2019. №2. S97-106.

5.Stechyshyn M.S., Stechyshyna N.M., Martyniuk A.V. Kavitatsiino-eroziina znosostiikist detalei obladnannia molokozavodiv: monohrafiia. Khmelnytskyi: KhNU. 2018. 148s.

6.Zakalov O.V., Zakalov I.O. Osnovy tertia i znoshuvannia u mashynakh: navch. posib. Ternopil: TNTU im.. I.Puliuia, 2011. 322s.

Стечишин М.С., Люховець В.В., Стечишина Н.М., Лук'янюк М.В. Зносостійкість конструкційних сталей, азотованих в циклічно-комутованому розряді при граничних режимах тертя

У статті розглянута методика проведення трибологічнихдосліджень при граничних режимах тертя азотованих і не азотованих сталей 20 і 45 для досягнення порівняння результатів лабораторних випробувань з експлуатаційними даними. На взаємозв'язок структурних фаз у часі суттєвий вплив мають вихідний стан поверхні та її фізико-механічні характеристики, тиск на поверхню контакту, швидкість ковзання, причому всі ці параметри для граничного режиму тертя тісно пов'язані між собою. Проведення випробувань на зносостійкість зразків із різних матеріалів і зі суттєво різними характеристиками поверхневого шару при однакових параметрах режиму випробувань у більшості випадків неможливо, оскільки порівнювати отримані результати проблематично.

Ключові слова: азотування, граничне тертя ,знос

***Problems of Tribology**, V. 27, No 3/105-2022,34-40*

Problems of Tribology
Website: http://tribology.khnu.km.ua/index.php/ProbTrib
E-mail: tribosenator@gmail.com

DOI: https://doi.org/10.31891/2079-1372-2022-105-3-34-40

Comparison of two-body abrasive wear resistance of high chromium boron-containing Fe–C-B–13wt.%Cr-Ti alloy with incomplete replacement of Cr for Cu the Fe-C-B-4wt.%Cr-7wt.%Cu–Ti alloy

B. Trembach[1], V. Vynar[2], I. Trembach[3], S. Knyazev[4]

[1]PJSC «Novokramatorsky Mashinostroitelny Zavod»,Kiev, Ukraine
[2]Karpenko Physico-Mechanical Institute of NAS of Ukraine
[3]Donbass State Engineering Academy, Ukraine
[4]National Technical University «Kharkiv Polytechnic Institute», Kharkiv, Ukraine
E-mail: btrembach89@gmail.com

Received: 3 August 2022: Revised: 20 August 2022: Accept: 01 September 2022

Abstract

Hardfacing process commonly employed because of its low cost and high efficiency. The microstructure of an two sample of deposited metal by X-ray diffraction, scanning electron microscope (SEM). In this research, the mechanical and tribological properties of two deposited metal of Fe–C–Cr–B–Ti alloying systems, high chromium 140Cr13Si1MnBTi alloy, and low chromium and high copper 110Cr4Cu7TiVBAl alloy hradfecing by flux-cored arc welding process (FCAW) was studied. It provided a low content of chromium (4 wt.%) and a high content of copper (7 wt.% Cu). Results of the studies had showed that the introduction of exothermic addition (CuO–Al) to the core filler of the flux–cored wire electrode, change melting characteristic and provides the highest resistance of the deposited metal to abrasion wear due to additional alloying by copper and reduction in grain size.

Key words: hardfacing, two-body abrasive wear, Fe–C–Cr–B–Ti alloys, self-shielded flux–cored arc welding, exothermic addition.

Introduction

The competitiveness of machines operated at mining and processing plants and enterprises engaged in the processing of solid materials, in addition to price and energy consumption, is also determined by such indicators as productivity and reliability (technological breaks or emergency stops for scheduled and emergency repairs). The latter depends on the life of the parts, which are primarily short-lived which are parts subjected to intense wear [1]. The cost of worn parts in mining is approximately the same as the cost of maintenance [2]. In engineering abrasive wear is probably the most crucial type of wear, because it contributes to almost 63% of the wear costs [3]. The manufacture of tools from wear-resistant material is impractical both from an economic point of view and from a technological point of view. Since in most cases wear acts locally (on a certain area of the surface), the rest of the structure can be made from cheaper structural materials. Therefore, it is advisable to apply a reinforcing layer locally. Different technologies are used for coatings application. Hardfacing techniques are employed mainly to extend or improve the service life of engineering equipment components. In addition, hardfacing is also used to restore worn surfaces of parts, thereby extending the life of such parts. The flux-cored wires segment is the most significant by type segment in the global market, and is expected to be the first preference for new entrants due to their high deposition rate, efficiency in delivering work, high quality of the deposited metal and arc visibility [4].

During a long period the hypereutectic Fe-Cr-C hardfaced coating was used for strengthening and repair of parts and units subject to abrasive wearing. Its high wear resistance is due to availability of hard M_7C_3 carbides. However, these alloys are subject to cracking during hardfacing. According to explanation of Yılmaz [5] deposited metal cracking during hardening happens, because M_7C_3 carbide has a very high brittleness and

low fracture toughness. For this reason there is a great interest in alternative alloying systems implementation. To improve the toughness of hypereutectic overlay would inevitably sacrifice its wear resistance because reducing the amount of carbide hard phase is the solely effective way [6]. However, this will inevitably lead to a decrease epy abrasive wear resistance. Therefore, the use of alternative alloys is of interest, among which alloys with boron, which were first proposed by Lakeland, can be distinguished [7]. The matrix and wear-resistant phase here could be controlled by changing carbon and boron concentrations. Fe–C–B-Cr alloys has excellent wear resistance, good corrosion resistance, and oxidation resistance [8]. The more widespread by Fe-Cr-B-C and Fe-Cr-B-C-Ti system alloys, which have the best mechanical properties and wear resistance [10-13]. Available information suggests that the abrasive wear resistance of materials depends on factors like microstructure (their size and content), and mechanical properties of materials [14].

Abrasive wear can be classified according to the interaction conditions as two-body and three-body abrasive wear [15]. Two-body abrasion is caused by hard protuberances on the counterface or hard particles attached to it, while in three-body abrasion the hard particles are free to roll and slide between two, perhaps dissimilar, sliding surfaces.

The purpose of the work

The purpose of the work was to make a comparative researches of wear resistance of 110Cr4Cu5TiVBAl alloy having a low chromium content and high copper content with 140Cr15TiSi1MnVB alloy having a high chromium content in two-body abrasive wear conditions.

Hardfacing technology

The FCAW-S of 4 mm diameter was used for investigations. The hardfacing was carried out by three-layers on plates made from low carbon steel S 235 JRG2 EN 10025-2 with dimensions 10×100×200 mm on reverse polarity by A-874 automatic machine.

Weld deposition were realized as three-layered to minimize impact of mixing the layer with base material. Welding parameters where chosen to provide high deposition values (high deposition rate and low spattering factor) [16], as well as for low solution of the deposited metal with the base metal and providing welded bead optimal shape [17]. Thus, hardfacing was performed by FCAW-S were as follows: wire feed speed WFS=1.85 m/min, arc welding voltage U_a =28 V, travel speed TS=0.3 m/min, contact tip to work distance CTWD=45 mm, DCRP Polarity, temperature preheating T_p=250…300 °C. Average values of welding current when surfacing with flux-cored wire FCAW-S-140Cr15TiSi1MnVB was 410 A, while when surfacing with experimental flux-cored wire FCAW-S-110Cr4Cu5TiVBAl - 360 A.

The core powder of filler materials is composed of gas-slag-forming components (fluorite concentrate, rutile concentrate, calcium carbonate), deoxidizers components (ferrosilicon, ferromanganese), alloying components (metal chrome powder, boron carbide powder, graphite, ferrovanadium, titanium powder), exothermic addition component (oxide of copper GOST 16539 79, aluminium powder PA1 GOST 6058-73) and iron powder. The difference between filler materials was as follows: an equivalent amount of metal chrome powder was added to the flux-cored wire FCAW-S-140Cr15TiSi1MnVB instead of the exothermal addition (CuO-Al) components. The shell of the cored wire is made of steel H08A. H08A with 20 × 0.5 mm was filled with mixed powders and then compressed down to a diameter of 4 mm by rolling. The coefficient wire filling (filling factor) of the flux-cored wire electrode is 0.34-0.35.

There are 3 layers made during hardfacing. Each layer was formed by sequential deposition of weld bead with a partial overlap of the previous weld bead (1/3). Samples for microstructure analysis, mechanical properties investigation and two-body abrasive wear test where prepared by mechanical cutting from the deposited plates with subsequent surface preparation at cutting modes that do not lead to their overheating.

The methodology and parameters of the two-body abrasive wear test are given in Student et al [18]. The assumed reference sample is C45 (GOST 1050 88) in the annealed state having ε= 1.0. The tested material specific wear rate SWR is calculated using the Equation 1:

$$SWR = {WV}/{N \cdot L}, \tag{1}$$

WV – wear volume, mm^3;
N – normal load, N;
L – sliding distance, m.

Results of experimental studies

The analysis of the structure of coatings produced using electric arc and flame spraying revealed that the latter provides particle sizes which are 5-6 times smaller compared to traditional spraying. Consequently, the sizes and quantity of pores in EAS coatings decreased by 2-3 times.

Gas permeability is a structure-sensitive characteristic of coating, and there is a distinct enough dependence of it on open porosity [12 8]. Under optimal spraying conditions, the porosity of EAS coatings is

much lower than in the case of liquid metal spraying with cold air (2-4% and 9-11%, respectively), and the gas permeability is lower by approximately 30-40 times. This may be related to the essential decrease in the sizes of pore channels in coatings. Fig. 1 demonstrates the curves of pore size distribution for coatings obtained by electric arc and flame spraying.

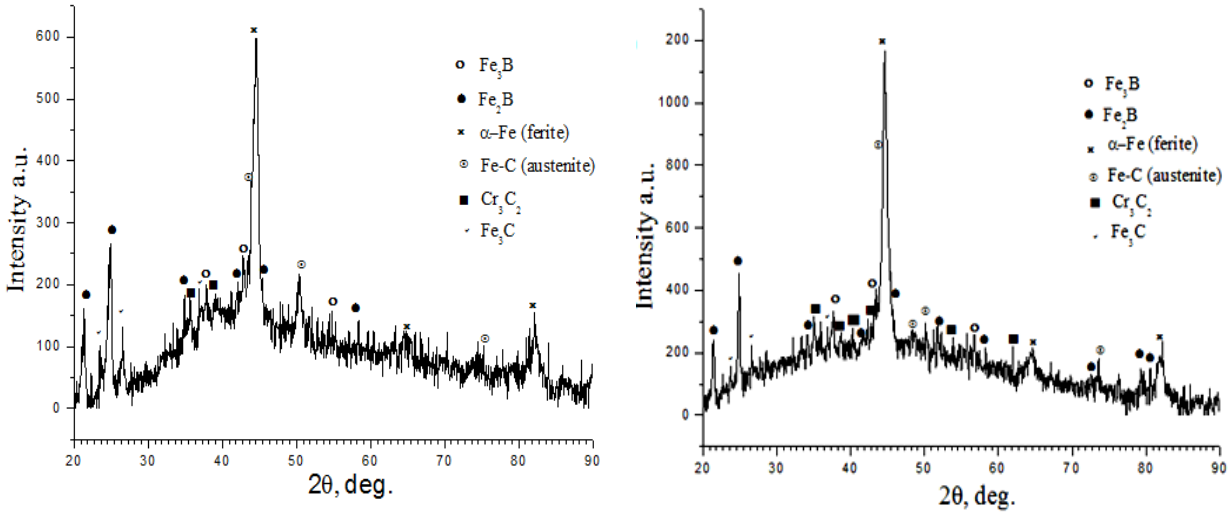

(a) (b)

Fig. 1. XRD pattern of deposited metal in 3 layers [1]: a) FCAW-S-140Cr15Si1MnBTi; b) FCAW-S-110Cr4Cu5TiVBAl with exothermic addition CuO - Al.

In weld metal deposited bt FCAW-S-140Cr15TiSi1MnVB and FCAW-S-110Cr4Cu5Ti1MnVB, apart from Fe_2B and $Fe_3(B,C)$ borides, the carbides Cr_2C_3 and TiC might be also present according to the reported results through X-ray diffraction analyses [4]. While the matrix is a eutectic of borides, α-Fe и γ-Fe. Whereas, in the high chromium alloy without copper, a large intensity of Cr_2C_3 carbide was observed. Whereas for the hardened layer FCAW-S-110Cr4Cu5Ti1MnVB, we observed a higher intensity for the Fe_2B boride, which indicated a larger proportion of this phase.

The microstructures of the deposited metal made using a scanning electron microscope (SEM) are shown in Fig. 2.

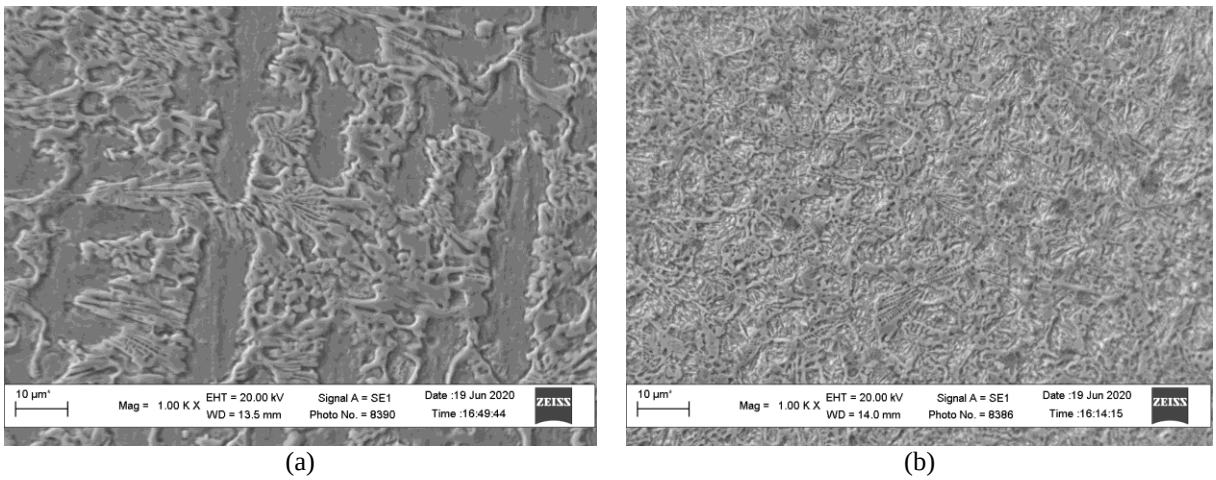

(a) (b)

Fig. 2. SEM images of the microstructures (×1000) deposited metal hardfacing by: (a) FCAW-S-140Cr15TiSi1MnVB and (b) FCAW-S-110Cr4Cu5Ti1VB with exothermic addition (CuO–Al).

The grain morphology parameters of the deposited metals were obtained according to the results of studies of the microstructure are presented in Table 1.

Table 1

The results of the analysis of grain length [1]

Sample	Number of analysed objects	Average value, µm	Minimum value, µm	Maximum value µm
140Cr15TiSi1MnVB	1488	15.3	2.6	719.8
110Cr4Cu5TiVBAl	1784	12.9	2.6	988.5

Data analysis showed that the introduction of an exothermic addition CuO-Al in the core filler of flux-cored wire electrode had a positive effect on the grain morphology. At that the average length of dendrites decreased from 15.3 μm to 12.9 μm. The introduction of exothermic additions into the core filler of flux-cored wire electrode has a positive effect on the grains morphology of the deposited metal. What could explain the formation of a large number of small non-metallic inclusions (NMI), which played the role of grain refiner/modifying agents.

Analysis and processing of the registered indentation curves allows to obtain mechanical properties of studied samples (Instrumented indentation hardness, modulus of elasticity, plasticity coefficient), calculated values are presented in Table 2.

Table 2

Mechanical properties determined by the depth-sensing indentation test

Flux-cored wire electrode	Instrumented hardness *HIT*, GPa	Elastic modulus *EIT*, GPa	Plasticity coefficient δ
FCAW-S-140Cr15TiSi1MnVB	9.938 ±3.054	176.987 ±13.697	0.766 ±0.045
FCAW-S-110Cr4Cu5TiVBAl	10.08 ±0.794	186.989 ±10.221	0.774 ±0.013

On Figure 3, a comparative diagram of tests on two-body abrasive wear of the studied alloys was shown.

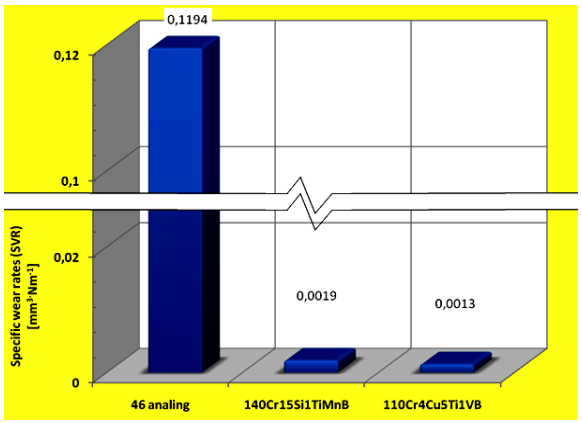

Figure 3. Two-body abrasive wear of deposited metals.

On Fig. 4, images of wear surfaces of welded metal samples were shown after two-body abrasive wear test was showing.

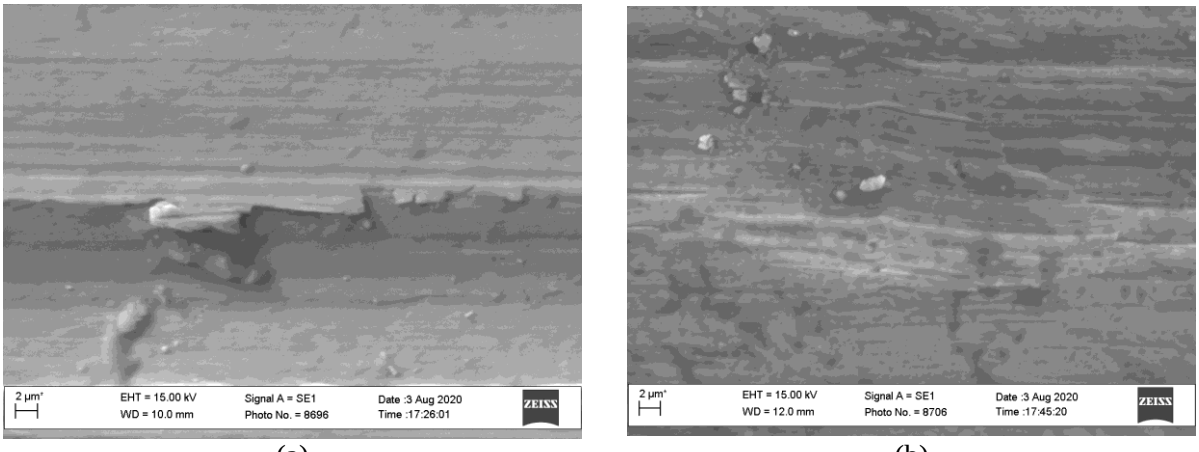

(a) (b)

Fig. 4. Worn surfaces of the hardfacings: (a) FCAW-S-140Cr15TiSi1MnVB; (b) FCAW-S-110Cr4Cu5Ti1VB with exothermic addition.

Combination of micro-cutting, microcracing and micro-ploughing wear mechanisms was observed in reinforced two deposited metals tested under the two-body abrasive wear. Dominant wear pattern of FCAW-S-140Cr15TiSi1MnVB hardfaced surfaces was micro-cutting and microcracing (Fig. 4 (a)). At that, micro-cutting is the main mechanism of deposited metal 140Cr15TiSi1MnVB wearing. Dendritic structure with

needle-like morphology led to such mechanism of metal wearing applied by FCAW-S-140Cr15TiSi1MnVB. Sharp tops of solid phase act as a stress concentrators, from which the deposited metal cracking with the further crumbling begins. For the reason that eutectic borides $(Fe, Cr)_2B$ and $Fe_3(B, C)$ were a barriers, resisting to wearing due to abrasive particles during contact of borides and abrasive, due to significant stresses after some time they were damaged and separated. Availability of cleavages at lines edges (Fig. 4 (a) indicates that the surface was damaged due to wearing by the fixed abrasive.

Samples wear pattern united two mechanisms: micro-cutting and micro-ploughing with predominant cutting (Fig. 4 (b)). Deposited metal received using proposed flux-cored wire FCAW-S-110Cr4Cu5TiVBAl had a higher wear-resistance to abrasive wearing. It is proved by the less specific wear rate SWR=0,0013 ($mm^3 \cdot N^{-1}$). Higher wear- resistance of the reinforcing layer applied by experimental flux-cored wire can be explained by the grain size reducing as well as an increasing of more damage-proof and plastic ferrite phase in the matrix. Due to the positive influence of the grain size reducing (first of all – borides needles size) the stress concentration in boride is reduced. It is not chipped during contact with abrasive particles. One of the factors for improving the resistance to impact load of the alloy may be its microstructure which included both the α-Fe phase and the γ-Fe phases. Increasing of ferrite phase in the matrix and eutectic allows to reduce the intensity of locations concentrations and due to this fact to reduce sensitivity of deposited metal to the stress accumulation.

Conclusions

1. Experimental studies comparing the effect of introduction of exothermic addition to the core filler of the flux-cored wire electrode on the structure, phase composition, mechanical properties of deposited metal and resistance to abrasive wear by two-body abrasive particles were performed.

2. The microstructure of the deposited metal (AW) was formed by a matrix of α'-Fe, M_2B borides, metal carboborides $M_3(B, C)$ and TiC, associated with the high concentration of alloying elements of the Fe–C–Cr–B–Ti system. The eutectic matrix consists of $M_3(C, B)$ carbides, together with ferrite and residual austenite.

3. Microhardness increasing was associated with the grain size decrease (dispersion structure) as per the Hall-Petch mechanism. The growth of the elasticity modulus was explained by a larger part of the ferrite phase in the matrix. The positive effect on the elastic modulus of the FCAW-S-110Cr4Cu7TiVBAl alloy, in which part of the chromium was replaced by copper, can be explained by an increase in the content of ferrite and austenite in the matrix.

4. Wear resistance of hardfacings tested under two-body wear conditions increased firmly introduction of exothermic addition CuO-Al to the core filler of the flux-cored wire electrode.

References

1. Ferguson S. A., Fielke J. M., Riley T. W. Wear of cultivator shares in abrasive South Australian soils. Journal of Agricultural and Engineering Research, vol. 69, no. 2, pp. 99–105, 1998.

2. Trembach B. O., Sukov M. G., Vynar V. A., Trembach I. O., Subbotina V. V., Rebrov O. Yu., Rebrova O. M., Zakiev V. I.. Effect of incomplete replacement of Cr for Cu in the deposited alloy of Fe–C–Cr–B–Ti alloying system with a medium boron content (0.5% wt.) on its corrosion resistance, Metallofiz. Noveishie Tekhnol., **44**, No. 4, pp. 493–515 (2022). DOI: 10.15407/mfint.44.04.0493 .

3. Davis JR. Surface engineering for corrosion and wear resistance. London: ASM International; 2001.

4. Trembach B., Grin A., Subbotina V., Vynar V., Knyazev S., Zakiev V., Trembach I., Kabatskyi O. Effect of exothermic addition (CuO-Al) on the structure, mechanical properties and abrasive wear resistance of the deposited metal during self-shielded flux-cored arc welding. Tribology in Industry. 43(3). pp. 452-. (2021) DOI: 10.24874/ti.1104.05.21.07 .

5. Yılmaz O. Abrasive wear of FeCr (M_7C_3–$M_{23}C_6$) reinforced iron based metal matrix composites. Mater. Sci. Technol, 17. pp. 1285–1292. (2001)

6. Jian, Y., Ning, H., Huang, Z., Wang, Y., & Xing, J. Three-body abrasive wear behaviors and mechanism analysis of Fe–B–C cast alloys with various Mn contents.Journal of Materials Research and Technology, 14, (2021). pp. 1301-1311. DOI: 10.1016/j.jmrt.2021.07.035.

7. Lakeland, K. D., Graham, E., & Heron, A. Mechanical properties and microstructures of a series of FCB alloys. The University of Queensland, Brisbane, Australia, 1-13. (1992).

8. Lentz, J., Röttger, A., & Theisen, W. Hardness and modulus of Fe_2B, $Fe_3(C, B)$, and $Fe_{23}(C, B)_6$ borides and carboborides in the Fe-CB system. Materials Characterization, 135, 192-202. (2018). DOI: 10.1016/j.matchar.2017.11.012 .

9. Tavakoli Shoushtari M. R., Goodarzi M., Sabet H. Investigation of microstructure, and dry sliding wear of hardfaced layers produced by FCAW using cored wire Fe-B-C-Ti alloy. Iranian Journal of Materials Science and Engineering, 15, 4, pp. 19-32. (2018).

10. Liu D., Wang J., Zhang Y., Kannan R., Long,W., Wu M., Li L. Effect of Mo on microstructure and wear resistance of slag-free self-shielded metal-cored welding overlay. Journal of Materials Processing Technology. 270, pp. 82-91. (2019). DOI: 10.1016/j.jmatprotec.2019.02.024 .

11. Prysyazhnyuk P., Shlapak L., Burda M., Ivanov O., Korniy S., Lutsak L., Yurkiv V. In situ formation of molybdenum borides at hardfacing by arc welding with flux-cored wires containing a reaction mixture of B4C/Mo. Eastern-European Journal of Enterprise Technologies. 4, 12-106. pp.46-51. (2020).

12. Öztürk, Z. T. Wear behavior and microstructure of Fe-C-Si-Cr-B-Ni hardfacing alloys. Materials Testing. 63, 3. pp. 231-234. (2021). DOI: 10.1515/mt-2020-0033 .

13. Yoo J. W., Lee S. H., Yoon C. S., Kim S. J. The effect of boron on the wear behavior of iron-based hardfacing alloys for nuclear power plants valves. Journal of nuclear materials. 352, 1-3. pp. 90-96. (2006). DOI: 10.1016/j.jnucmat.2006.02.071.

14. Efremenko V., Shimizu K., Pastukhova T., Chabak Y., Brykov M., Kusumoto K., Efremenko A. Three-body abrasive wear behaviour of metastable spheroidal carbide cast irons with different chromium contents, International Journal of Materials Research. 109, No. 2. pp. 147-156. (2018). DOI: 10.3139/146.111583.

15. Vingsbo O., Hogmark S., 1981. Wear of steels. In: Rigney D.A. (ed.), Fundamentals of Friction and Wear of Materials, ASME, Metals Park: 373–408.

16. Trembach B., Grin A., Zharikov S., Trembach I. Investigation of characteristic of powder wire with the CuO/Al exothermic mixture, Scientific Journal of TNTU 92, 4 (2018) 13-23. DOI: 10.33108/visnyk_tntu2018.04.013 .

17. Trembach B., Grin A., Turchanin M., Makarenko N., Markov O., Trembach I., Application of Taguchi method and ANOVA analysis for optimization of process parameters and exothermic addition (CuO-Al) introduction in the core filler during self-shielded flux-cored arc welding, The International Journal of Advanced Manufacturing Technology, 114 (2021) 1099–1118. DOI: 10.1007/s00170-021-06869-y .

18. Student M.M., Hvozdetskyi V.M., Dzhoba Y.V. Effect of high pressure air jet on the properties of electric arc coatings. Problems of Tribology, 89, 3. pp. 33-41. (2018).

Трембач Б.О., Винар В.А., Трембач І.О., Князєв С.А. Порівняння стійкості до зношування закріпленим абразивом високохромистого борвмісного сплаву Fe–C-B–13мас.%Cr-Ti з неповною заміною Cr на Cu сплав Fe-C-B-4мас.%Cr-7мас.%Cu–Ti.

Процес наплавлення широко використовується через низьку вартість та високу ефективність. Жлсдіджували мікроструктуру двох зразків наплавленого металу з використанням допомогою рентгенівської дифракції (XRD), скануючого електронного мікроскопа (SEM). У цьому дослідженні були визнасчені механічні властивості та трибологічні характеристики двох зразків наплавленого металу Fe–C–Cr–B–Ti системи легування, а саме сплаву з високим вмістом хрому 140Cr13Si1MnBTi та сплаву з низьким вмістом хрому та високим вмістом міді110Cr4Cu7TiVBAl, натоплені за допомогою процесу порошкових дротів (FCAW). Результати досліджень показали, що введення екзотермічної добавки (CuO–Al) до наповнювача серцевини електрода за рахунок еквивалентної кількості порошку металевого хрому у наповнювачі порошкового дроту змінює характеристику плавлення та забезпечує підвищення стійкісті наплавленого металу до абразивного зношування за рахунок додаткового легування міддю. і зменшення розміру зерна.

Ключові слова: наплавлення, зношування закріпленим абразивом, Fe–C–Cr–B–Ti сплав, зварювання самозахисним порошковим дротом, екзотермічне додавання.

***Problems of Tribology**, V. 27, No 3/105-2022,41-48*

Problems of Tribology
Website: http://tribology.khnu.km.ua/index.php/ProbTrib
E-mail: tribosenator@gmail.com

DOI: https://doi.org/10.31891/2079-1372-2022-105-3-41-48

Development of a technological process for the restoration of piston pins using deforming broaching

Ya.B. Nemyrovskyi, I.V. Shepelenko*, M.I. Chernovol, F.Y. Zlatopolskiy

Central Ukrainian National Technical University, Kropyvnytsky, Ukraine
**E-mail: kntucpfzk@gmail.com*

Received: 10 July 2022: Revised:05 August 2022: Accept:8 September 2022

Abstract

The article discusses the technological process of restoring the geometric dimensional accuracy of piston pins of internal combustion engines (ICE) due to the expansion of the internal hole by a deforming element. As part of conducting research taking into account the resource of the used plasticity of the processed material, the processing modes are determined, the deformation scheme is selected and the geometry of the deforming element is calculated. The selection of the necessary deformation of the part during processing of the piston pin was carried out under the condition of compensating for wear and ensuring an allowance for subsequent mechanical processing. This made it possible to ensure the necessary processing quality of the pin hole surface layer according to the resource parameter of the used plasticity. The deformation scheme was chosen from the condition of ensuring the geometric accuracy of the pin outer surface, which determines the size and uniformity of the allowance for subsequent processing. For these reasons, a scheme was chosen in which the deformation is carried out by two elements with a change of the support end after the first pass. The optimal geometry of the deforming tool was determined from the standpoint of minimizing errors and preserving the initial length of the pin. The results of the conducted experiments showed that using selected expansion schemes, tensions and geometry of the deforming tool, made it possible to ensure the necessary allowance for the next mechanical processing, as well as the invariance of the part length after processing.

Key words: piston pin, expansion of the inner hole, expansion modes, expansion scheme, geometry of the deforming tool, geometric dimensional accuracy

Introduction

An important and urgent task of machine-building production is the repair and restoration of parts that limit the service life of the ICE. The economic feasibility of restoring parts is due to the possibility of repeated use of worn parts. At the same time, the cost of restoration, as a rule, does not exceed the cost of manufacturing new ones, and the material consumption is 15 … 20 times lower than in the manufacture of new ones [1].

To the number of parts to be restored including piston pins, the manufacture of which requires high-precision machine equipment, tooling, control and measuring tools. The resource of these parts is small [2], the wear of the pins working surface over 0.01 mm leads to a deterioration in the conjugation operation. Therefore, the search for new and intensification of existing technologies for processing piston pins is an important and urgent problem.

Literature review

The main defect of the piston pins is wear on the outer surface in the contact areas with the sleeve of the upper connecting rod head and the holes in the piston. Existing methods of restoring the outer diameter of worn piston pins can be divided into the following groups:

- mechanical processing to repair size;
- applying an additional layer of material followed by mechanical processing to the nominal size;
- increasing the geometric dimensions of the part by heat treatment with various methods of heating and cooling.

It should be noted that in repair production, when restoring the outer size of a pin, technologies associated with heat treatment are most widely used [3].

As studies [4, 5] have shown, hydrothermal expansion in connection with the harsh conditions of 12HN3A steel cooling (water) can lead to the appearance of cracks in the cemented layer (Fig. 1).

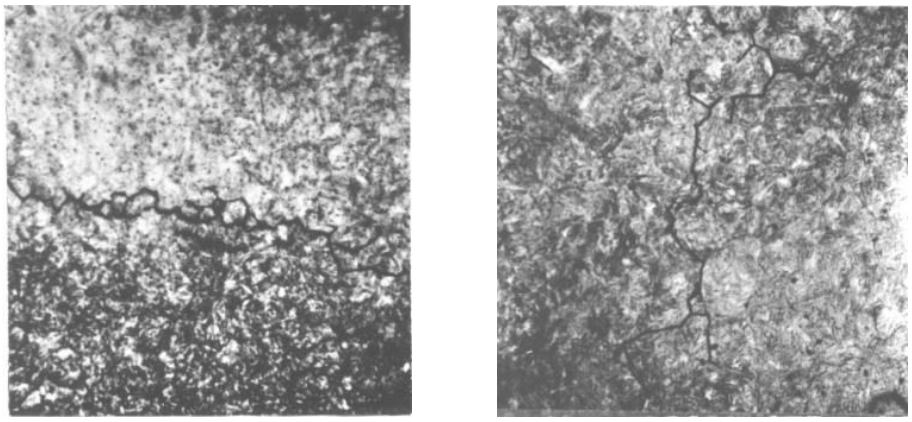

Fig. 1. Microstructure of a piston pin cemented layer made of 12HN3A steel, restored by thermoplastic expansion [5]

The cemented layer microstructure of the pin restored in this way consists of finely dispersed martensite, which is typical for the usual hardening of this steel in oil. After hydrothermal expansion, the core of the pin resembles pearlite in structure. Obviously, the heating for the core of the pin does not reach the point AC_3 (diagrams of iron – carbon) and hardening takes place in the interval AC_1 – AC_3. The AC_3 point for the carbon-saturated cemented zone is lower than for the low-carbon one. Therefore, heating is sufficient for complete hardening [5].

Despite the fact that the structure of the cemented layer of these pins is similar to the structure of pins processed by traditional technology, the thickness of the cemented layer is 0.5 mm, which does not meet the technical requirements for pins. In addition, the uncontrolled and uneven increase in the outer diameter along the length of the part leads to the need to remove significant allowances when grinding the outer surface of the pins. As a result, even within the same product, places with a small amount or complete absence of cemented layer can be observed.

The absence of a stabilizing release after hydrothermal expansion leads to the presence of thermal residual stresses in such pins. The latter can cause the appearance of cracks, or relax during the pin operation under the influence of alternating cyclic loads. This causes the loss of the pin working size.

More effective is the technology of piston pins restoration by the method of electric contact heating and combined spray cooling [6], which also has a number of disadvantages that are typical for methods of parts restoration based on the use of thermal deformations. The hardened cemented layer microstructure of restored pins represents martensite with the inclusion of cementite, residual austenite, and troostite. This indicates non-compliance with the basic requirements for the technological process of cemented steels heat treatment during heat treatment and leads to the appearance of defective signs in restored pins (presence of residual austenite).

At the V. Bakul Institute for Superhard Materials of the National Academy of Sciences of Ukraine developed a highly productive technology for restoring the outer surface of the piston pin using the deforming broaching operation [4]. The efficiency and, consequently, the feasibility of such a technology depends on a reasonable approach to choosing the modes of deforming broaching during expansion of ICE piston pins, taking into account the quality indicators of the treated surface layer. In this case, special attention should be paid to the choice of tool geometry for deforming broaching.

Purpose

The purpose of the work is to determine the modes, scheme, and geometry of the tool during the deforming broaching of ICE piston pins, taking into account the resource of the used plasticity of the processed material.

Research Methodology

Plastic deformation of a worn piston pin is practically impossible due to the presence of a brittle martensitic layer on its outer surface. Therefore, the worn pins are annealed, which restores the initial state of the material, and therefore creates the possibility of their plastic deformation [5].

The selection of the necessary pin deformation is carried out under the condition of pin wear compensation and provision of an allowance for the next mechanical processing. Experiments to determine the relationship between the pin hole deformation Σa and the required allowance of the pin outer surface made it possible to obtain the following dependence:

$$\frac{0.07AL}{d_0} = \frac{0.033}{d_0}\sum a, \tag{1}$$

where AL is the allowance of the processed part outer surface;

d_0 – the diameter of the processed part inner surface;

a – tension on the deforming element.

When choosing the amount of circumferential deformation of the pin hole (tension), the conditions affecting the quality of the pin material should be taken into account. One of these factors, according to the work [7], is the resource of used plasticity.

The technological process of restoring piston pins includes a heat treatment operation after a deforming broaching operation. As shown by studies [8], for parts exposed to the action of alternating loads during operation, the value of the resource degree of used plasticity in the operations preceding heat treatment should not exceed the following values:

$$\Psi = [\Psi] = 0.33, \tag{2}$$

where ψ – the resource of the used plasticity of the material.

When re-restoring the piston pins after the expansion operation, it is necessary to provide for additional cementation of the pin working surface. According to the data of works [9], the value of the preliminary plastic deformation Ψ is optimal from the point of minimizing the time for the cementation process, as well as for obtaining a fine-grained uniform martensitic structure after heat treatment of the cemented surface without the presence of residual austenite, which is within the limits of:

$$\Psi_{\max} \le [\Psi], \tag{3}$$

where $[\psi] = 0.2 \div 0.25$.

Therefore, the value of pin expansion, determined from the condition of ensuring the necessary technological allowance, must be checked based on condition (3).

As shown in works [10], on the outer surface of workpieces with a final wall thickness ($D/d_0 \le 2.5$), a rigid stress state scheme approaching the biaxial tension scheme is realized. Under such conditions, there is an intensive increase in the resource of the used plasticity even with small values of the accumulated circumferential deformation. For recoverable pins, the relation $D/d_0 = 1.7$, so it is necessary to check the quality of the recoverable pin according to the parameter Ψ for its outer surface.

The resource of used plasticity during two-cycle deformation of the pin on its outer surface, according to the data of work [7], is calculated by the formula:

$$\Psi = \frac{-1+\sqrt{1+4\left[n\bar{z}+(1+2\Theta)\left(n\bar{z}\right)^2\right]}}{2}, \tag{4}$$

where $\bar{z} = \dfrac{\bar{e}_0^{\,n}}{e_{ult}(2)}$ – experimental parameter;

e_0^n – deformation brought to the outer surface.

The magnitude of the ultimate deformation in case of uniform biaxial stretching:

$$e_{ult}(+2) = 0.0065\delta_p, \tag{5}$$

where δ_p – relative elongation of the sample in standard tensile tests. For the pins material – steel 12HN3A δ_p = 36%.

The main accumulation of damage to the processed material during deforming broaching occurs at the value of the stress state indicator η = +2, which is realized on the outer surface of the workpiece. Therefore, when calculating the ultimate deformation, it is sufficient to know the deformation of the workpiece material under conditions of uniform biaxial tension η = +2.

Determination of deformation during biaxial stretching was carried out according to the following method. Plates with a diameter of 100 mm and a thickness of 5 mm were cut from the studied material. One of the plate surfaces was ground and polished, and then marked with equidistant marks along two mutually perpendicular axes. Marks were applied with a diamond pyramid using a hardness tester head mounted on a BMI-1 universal microscope under a load of 50 N. The base of measurements, i.e. the distance between two adjacent marks, was 1 mm.

The sample prepared in this way was installed in a special device and loaded with a spherical punch (Fig. 2).

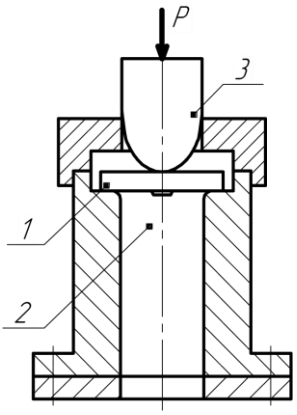

Fig. 2. Testing samples under biaxial uniform stretching: 1 – plastic sample; 2 – researched area; 3 – spherical punch

The punch polished surface and the sample were lubricated to reduce frictional forces. The load was applied until cracks appeared on the surface with marks. Destruction (the appearance of cracks) was observed in the immediate closeness of the punch top. At the same time, local thinning of the plate was not observed. According to the change in the distance between the marks, the deformation at the point of destruction e_x and e_y was determined.

The accumulated deformation was calculated according to dependence (5) given in work [10], based on the assumption that the deformation in the center of the plate is simple:

$$\bar{e}_0 = \sqrt{e_x^{\,2} + e_y^{\,2} + e_{x^i} + e_{y^i}} \,. \tag{6}$$

The value of the deformation at η = +2 made it possible to construct a plasticity diagram for the material of the piston pins – 12HN3A steel (Fig. 3).

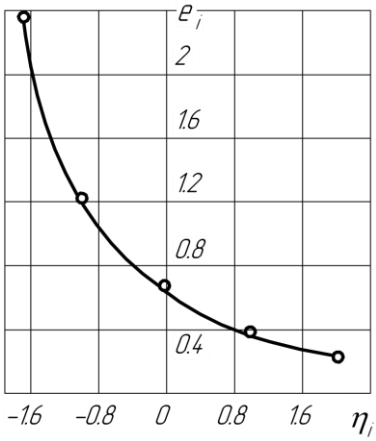

Fig. 3. Plasticity diagram of steel 12HN3A

The degree of the plasticity resource using on the inner surface of the pin, where intense local plastic deformation takes place, was performed according to the following dependence [8]:

$$\Psi = \frac{\Delta e_0^{\max}}{3e_{ult}(-1.73)}, \tag{7}$$

where $e_{ult}(-1.73)$ – plasticity under compression under conditions of plane deformation, i.e. at η = -1.73.

The dependence of the limit deformation during the processing cycle on the angle α was determined:

$$\Delta e_0^{\max} = 0.03\alpha + 0.1. \tag{8}$$

The deformation scheme was chosen from the condition of ensuring the geometric accuracy of the pin outer surface, which determines the size and uniformity of the allowance for subsequent processing.

The choice of the deforming tool geometry was carried out under the condition of preserving the pin initial length. At the same time, the case of part expansion in the absence of axial deformations is considered:

$$\alpha = \frac{0.35 + 34.8a / d_0}{t_0 / d_0}. \tag{9}$$

Results

The selection of the necessary part deformation during processing of the piston pin was carried out under the condition of compensating for wear and ensuring an allowance for subsequent mechanical processing.

Calculations performed according to expression (4) for real expansion conditions of pins A-01; D-37; 10D100, made of 12HN3A steel, showed that the resource of used plasticity on the pin outer surface during its expansion is within Ψ = 0.2 ÷ 0.21. This provides normal conditions for thermochemical treatment of deformed pins, which subsequently allows achieving the required quality of restored pins.

The degree of pin thickness D-37 is equal to: t = 2.05. Therefore, the stress-deformed state (SDS) of the pin hole surface layer approaches the SDS scheme of the workpiece with infinite wall thickness.

According to the recommendations of work [10], it is necessary to check the degree of the plasticity resource use on the pin inner surface, where intense local plastic deformation takes place.

According to the data of experiments on the samples compression, performed according to the method [11], e_{ult} (-1.73) for steel 12HN3A is equal to 2.34.

To calculate the plasticity resource according to dependence (7), it is necessary to know the value of the accumulated deformation $\Delta e_0^{\max}$ for 1 processing cycle in the considered inner surface of the pin.

In work [12] it was shown that when using a deforming element with an angle α = 5° for expansion, the value $\Delta e_0^{\max}$ = 0.25, and with an angle α = 10° – $\Delta e_0^{\max}$ = 0.39.

The conducted experiments showed that from the point of minimizing errors and ensuring the invariance of the pin length upon its expansion, the angle α = 2° is optimal. Using expression (8), we obtain the value of the accumulated deformation on the pin inner surface $\Delta e_0^{\max}$ = 0.16.

This value was used to calculate the resource of used plasticity for one cycle of deformation, according to expression (7). Then in one cycle of deformation $\Delta\Psi = \frac{0.16}{3 \cdot 2.34} = 0.024$.

Since the pins expansion is carried out in two cycles of deformation, we obtain that the full resource of the used plasticity in the surface layer of the hole processed in 2 cycles is Ψ = 2ΔΨ ≈ 0.05. This value does not exceed the limit value Ψ. Therefore, the processing quality of the pin hole surface layer according to the resource parameter of the used plasticity is ensured.

After determining the required deformation, the deformation scheme was selected. Taking into account the shape and design features of the pin, the presence of chamfers up to 3 mm long in the A-01 pin and 14 mm – 10D100 pin, a scheme was chosen according to which the deformation is carried out by two elements with a change of the support end after the first pass. A necessary condition when using this scheme is the constancy of the axial force Q at each pass. The general deformation ε is carried out by two deforming elements with tensions a_1 and a_2:

$$\varepsilon = a_1 + a_2, \tag{10}$$

where a_1 – tension on the first deforming element, $a_1 = \frac{\beta}{1+\beta}\varepsilon$;

a_2 – tension on the second deforming element, $a_2 = \frac{\varepsilon}{1+\beta}$.

The calculation of tensions values a_1 and a_2, their total value ε, as well as the values of the deforming tool angles α for different brands of pins, calculated according to dependence (9), are given in Table 1.

Table 1

Values of tension *a*, total deformation and angles of the tool α, necessary for the restoration of different brands of pins

No.	The brand of ICE restoring pin	a_1, mm	a_2, mm	ε, mm	α, degree
1	D37	0.42	0.40	0.82	$2°30^{I}$
2	D240	0.44	0.42	0.86	$2°30^{I}$
3	A01	0.47	0.43	0.9	$2°30^{I}$
4	10D100	0.75	0.7	1.45	$2°30^{I}$

The results of the experiments given in the Table 2 and Fig. 4 show that the use of the selected expansion schemes, tensions and geometry of the tools, made it possible to ensure the necessary allowance for the next mechanical processing, as well as the invariance of the part length after expansion.

Table 2

The value of allowances for the pin length for the next mechanical processing and the pin length after its expansion

No.	The brand of ICE restoring pin	Allowance Δ, mm			L, mm
		I end	middle	II end	
1	D37	0.19	0.2	0.19	$89_{-0.1}$
2	D240	0.2	0.21	0.2	$102_{-0.1}$
3	A01	0.21	0.22	0.21	$110_{-0.1}$
4	10D100	0.24	0.26	0.24	$182_{-0.1}$

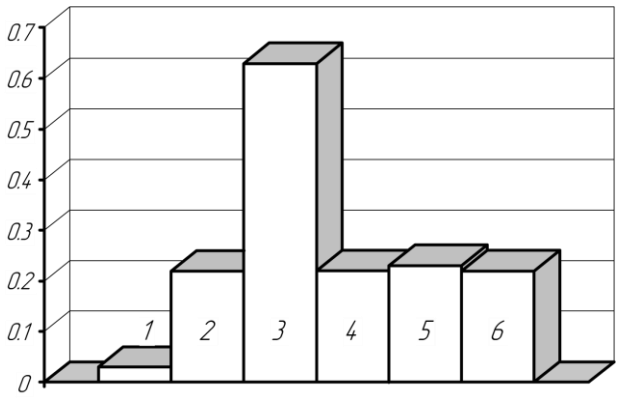

Fig. 4. Histogram of the allowance change for the pin A01 length when processing a batch of pins in production conditions in the amount of 100 pcs.: 1, 3, 4, 6 – allowance value on the edge areas of the processed pin; 2, 5 – allowance value in the middle of the processed pin; 1, 2, 3 – pin processing according to the compression scheme; 4, 5, 6 – pin processing according to the scheme with a change of the support end

The conducted research made it possible to determine the deforming broaching modes and the geometry of the tool during the expansion of ICE piston pin. Thus, the developed technological process of processing ICE piston pins, which includes their deformation and subsequent heat treatment, ensures the obtaining of piston pins, the quality of which meets the requirements for new pins.

Conclusions

1. Carrying out theoretical and experimental studies of ICE piston pins deforming broaching made it possible to make a choice:

- necessary deformation under the condition of wear compensation and provision of allowance for mechanical processing.
- scheme of the pin deformation from the conditions of ensuring the geometric accuracy of the part.
- geometry of the tool from the condition of ensuring the invariance of the part length.

2. The relationship between the total deformation of the hole and the amount of the required allowance on the pin outer surface has been established.

3. It has been proven that processing according to the scheme with a change of the support end ensures geometric accuracy of the pin outer surface.

4. It has been proven that the selected broaching modes and the geometry of the tool ensure a zero change in the pin length during its processing.

References

1. Chernovol M.I., Poedinok S.E., Stepanov N.E.. (1989) Povyshenie kachestva vosstanovleniya detalej mashin. Kiev, Tekhnika, 168 s.

2. Nemirovs'kij Ya.B., Shepelenko I.V., Krasota M.V. (2022) Ocinka micnosti porshnevih pal'civ, vidnovlenih za rahunok rozdachi vnutrishn'ogo otvoru [Zbirnik naukovih prac'. Naukovij visnik. Tekhnichni nauki. - Vip.5 (36) _I] – S.14-22. https://doi.org/10.32515/2664-262X.2022.5(36).1.14-22.

3. Kapelyushnij F.M. (2001) Vpliv ekspluatacijnih faktoriv na znoshuvannya pal'civ dizel'nih dviguniv [Praci Tavrijs'koï derzhavnoï agrotekhnichnoï akademiï. Vip.2, T.17] – S.113-117.

4. Posviatenko E.K., Nemyrovskyi Ya.B., Sheikin S.E., Shepelenko I.V., Cherniavskyi O.V. (2021) Inzheneriia detalei, obroblenykh protiahuvanniam. Kropyvnytskyi, Vydavets Lysenko V.F., 466 s.

5. Nemirovs'kij Ya.B. (2018) Naukovi osnovi zabezpechennya tochnosti pri deformuyuchomu protyaguvanni [Avtoreferat dysertatsii doktora tekhnichnykh nauk] 40 s.

6. Kapelyushnij F.M. Udoskonalennya tekhnologiï termichnoï obrobki porshnevih pal'civ dizel'nih dviguniv pri ïh vidnovlenni [Avtoreferat disertaciï kandidata tekhnichnih nauk] 18 s.

7. Nemyrovskyi, Y., Shepelenko, I., Solovykh, E., Bevz, O., Leshchenko, S. (2022). Studying the Mechanics of Low-Plastic Materials Surface Layer Processed by Deforming Broaching. In: Karabegović, I., Kovačević, A., Mandžuka, S. (eds) New Technologies, Development and Application V. NT 2022. Lecture Notes in Networks and Systems, vol 472. Springer, Cham. pp. 128-134. https://doi.org/10.1007/978-3-031-05230-9_15.

8. Smelyanskij V.M. (2002) Mekhanika uprochneniya detalej poverhnostnym plasticheskim deformirovaniem. Moskva, Mashinostroenie, 300 s.

9. Levitas V.I. (1987) Bol'shie uprugo-plasticheskie deformacii materialov pri vysokom davlenii. Kiev, Naukova dumka, 231 s.

10. Cekhanov Yu.A., Shejkin S.E. (2001) Mekhanika formoobrazovaniya zagotovok pri deformiruyushchem protyagivanii. Voronezh, Izdatel'stvo Voronezhskogo universiteta, 200 s.

11. Hvan D.V. (1992) Tekhnologicheskie ispytaniya metallov. Voronezh, Izdatel'stvo Voronezhskogo universiteta, 152 s.

12. Balaganskaya E.A., Golodenko B.A., Nemirovskij Ya.B., Cekhanov Ya.A. (2001) Matematicheskoe modelirovanie processa deformiruyushchego protyagivaniya. Voronezh, Izdatel'stvo Voronezhskogo universiteta, 194 s.

Немировський Я.Б., Шепеленко І.В., Черновол М.І., Златопольський Ф.Й. Розробка технологічного процесу відновлення поршневих пальців з використанням деформуючого протягування

В статті розглянуто технологічний процес відновлення геометричної розмірної точності поршневих пальців двигунів внутрішнього згорання за рахунок роздачі внутрішнього отвору деформуючим елементом. З врахуванням ресурсу використаної пластичності оброблюваного матеріалу визначено режими обробки, обрано схему деформування та розраховано геометрію деформуючого елементу. Вибір необхідної деформації деталі при обробки поршневого пальця виконували з умов компенсації зношування та забезпечення припуску під наступну механічну обробку. З метою забезпечення геометричної точності зовнішньої поверхні пальця, що визначає величину й рівномірність припуску під наступну обробку, обрано схему деформування, при якій деформація здійснюється двома елементами зі зміною опорного торця після першого проходу. З позицій мінімізації похибок, збереження вихідної довжини пальця визначена отптимальна геометрія деформуючого інструменту. Результати проведених експериментів показали, що використання запропонованих схем роздачі, натягів та геометрії деформуючого інструменту дозволило забезпечити необхідний припуск під наступну механічну обробку, а також незмінність довжини деталі після обробки.

Ключові слова: поршневий палець, роздача внутрішнього отвору, режими роздачі, схема роздачі, геометрія деформуючого інструменту, геометрична розмірна точність.

Problems of Tribology, V. 27, No 3/105-2022,49-54

Problems of Tribology
Website: http://tribology.khnu.km.ua/index.php/ProbTrib
E-mail: tribosenator@gmail.com

DOI: https://doi.org/10.31891/2079-1372-2022-105-3-49-54

Adhesion-Deformation-Hydrodynamic model of friction and wear

Oleksandr Stelmakh[1], Hongyu Fu[1], Yiqiao Guo[1], Xinbo Wang[1], Hao Zhang[1*], Oleksandr Dykha[2]

[1]School of Mechanical Engineering, Beijing institute of technology, Beijing 100081, China
[2]Khmelnitskyi National University, Ukraine
**E-mail: hao_zhang@bit.edu.cn*

Received: 12 July 2022: Revised:09 August 2022: Accept:12 September 2022

Abstract

The proposed Adhesion-Deformation-Hydrodynamic model of friction and wear is based on the relationship of elastic-deformation processes in the surfaces of curvilinear contacts with hydrodynamic regular processes of extrusion and rarefaction in lubricating layers in tribocontacts, as well as with the processes of primary adhesion of friction surfaces and subsequent acts of adhesive wear. The proposed Adhesion-Deformation-Hydrodynamic model of friction and wear and its main provisions on the relationship between extrusion, rarefaction in lubricating layers and primary adhesion of friction surfaces of curvilinear contacts cover the entire load-speed range and all modes of lubrication of friction surfaces.

Keywords: model of friction, lubricating layers, contact pressure, adhesion

1. The main provisions of the Adhesion-Deformation-Hydrodynamic model

Wear of friction surfaces always occurs in elastically deformed areas of tribocontacts. It is clear that in areas, for example, in the gap of a radial plain bearing, where the surfaces are not elastically deformed and there is a gap, the surfaces do not wear out, since they do not contact.

Under static conditions, when the surfaces are compressed, all supramolecular layers flow into areas with lower pressure, that is, they are extruded in all directions from elastically deformed contact with mono- and multimolecular lubricant layers, as noted by O. Reynolds at the beginning of his well-known work [11]. Contact stresses are distributed axisymmetrically in the form of a semi-ellipse according to G. Hertz (Fig. 10(a)).

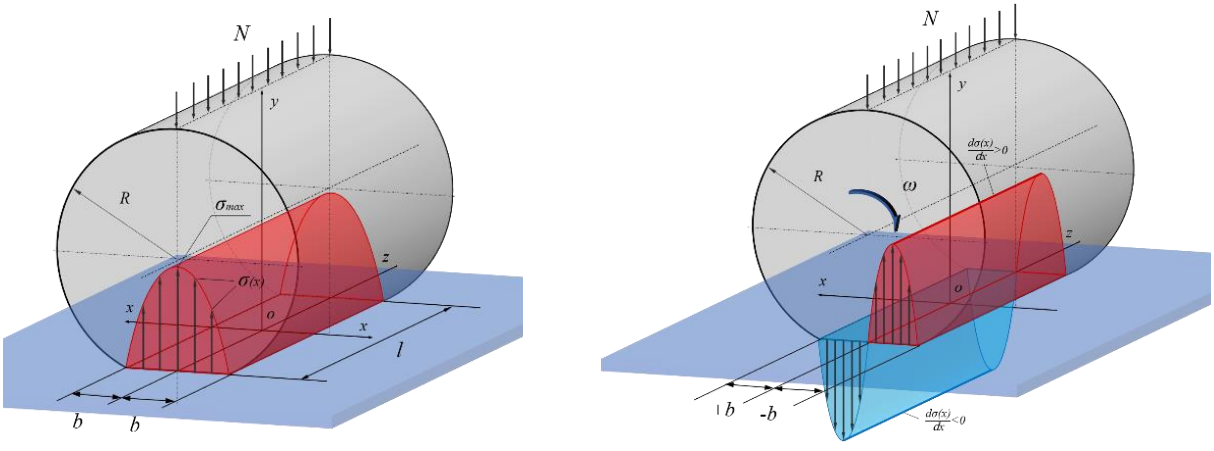

Fig. 1. Axisymmetric distribution of contact stresses.

Axisymmetric distribution of contact stresses *σ(x)* from the applied load *N* under static compression in contact *2b* of a shaft with radius *R* and length *l* with maximum values of σ_{max} in the *ZOY* plane in the form of a semi-ellipse according to G. Hertz (Fig 1, a) and a centrally symmetric distribution of the contact gradient stresses $\frac{d\sigma(x)}{d(x)}$ when choosing the friction direction along the *OX* axis (Fig1,b).

When one or two surfaces break off, in the direction of friction, in the entire elastically deformed area of the tribo-contact, characteristic areas immediately appear in the direction of friction of the shaft along the radial bearing (Fig. 1(b)): 1. First - Convergent elastically deformed area - with a positive gradient of contact stresses, which leads to the extrusion of lubricating layers in which the overpressure rapidly increases relative to the ambient pressure; 2. The second is the transition region, where the contact stress gradient is approximately equal to zero, and the pressure in the lubricating layer changes extreme from the maximum excess to the minimum rarefaction, passing through the pressure area equal to the ambient pressure (in laboratory conditions, this is atmospheric pressure P_0); 3. The third one is an elastically deformed divergent area with a negative contact stress gradient, which leads to a rarefaction of the lubricating layers, in which the pressure is less than the ambient pressure.

When friction in a given direction with a shaft rotation frequency ω in the convergent elastically deformed area of the tribocontact, the lubricating layers are compressed, which squeeze out all supra-monomolecular layers of the lubricant into the volume in accordance with the Hertz theory (Fig. 1(a)) and the Langmuir and BET adsorption theories, in an area with lower pressure (in laboratory conditions, this is the ambient pressure P_0) in accordance with Pascal's law along the shortest path, that is, the boundary layers are extrusion.

In the convergent elastically deformed region, the lubricating layers, under the action of a positive gradient of contact stresses (Fig. 1(b)), contracting, realize Extrusion and return flow in the region with lower pressure (since the pressure is even greater in front) along the shortest path (at the contact ends, the squeezed out fragments of the lubricant flow immediately outward, and in the middle of the contact, the most compressed fragments flow strictly in the direction opposite to friction), which is schematically shown in Fig. 2 (a)).

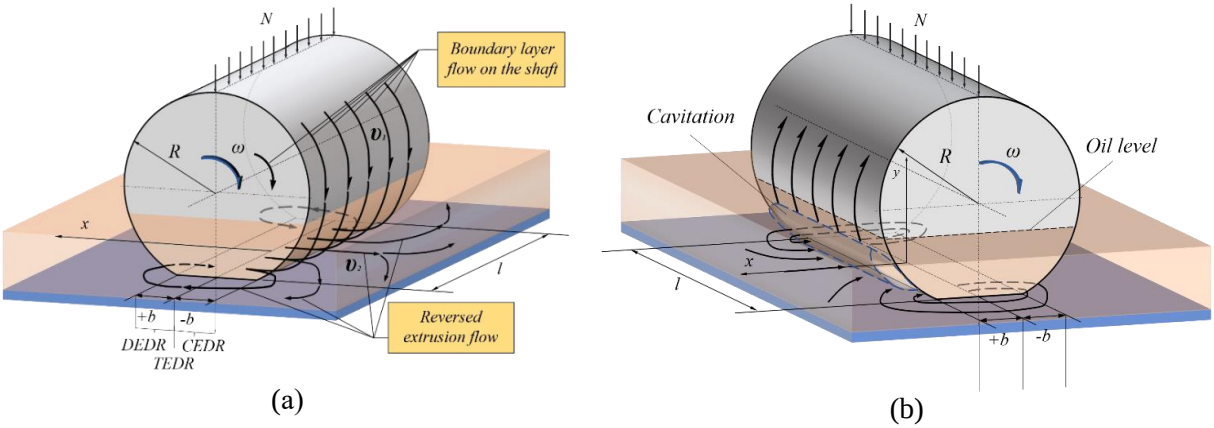

Fig. 2. Scheme of the occurrence of extrusion and reverse flows in the convergent non-contact and elastically deformed regions (a) as well as rarefaction in the divergent non-contact and elastically deformed regions (b) of the tribocontact according to the Timken scheme

Here, in the convergent area of contact, the incoming boundary layers of the lubricant together with the shaft and the extrusion flows in front of and in the elastically deformed convergent area are directed towards each other, which, when colliding and braking, lead to the emergence of the so-called "oil wedge" (Fig. 2(a)).

In the transition region, the contact stresses reach their maximum values, and between the surfaces there is a minimum amount of lubricant remaining after extrusion in the convergent elastically deformed contact region. This very short region is characterized by an almost zero contact stress gradient (Fig. 1(a)), and the pressure in the residual lubricating layer is equal to the ambient pressure. Obviously, only in this region is the classical Newtonian viscous flow of mono- or multimolecular boundary layers of lubricant with a rectangular velocity diagram realized.

Then, from the transitional elastically deformed region, a part of the remaining small amount of lubricant, together with the shaft, enters the divergent elastically deformed contact region and enters the conditions of bilateral tension.

In the divergent elastically deformed region of the friction surface, from the maximum compressed state, relative bilateral stretching of the remaining fragments of the boundary layers is realized, which leads to their rapid rarefaction and a rapid decrease in pressure in them.

Under these conditions, rarefaction, evaporation and DESORPTION of residual adsorbed substances occur, then: nucleation of the vapor-gas phase: first in the form of cavitation nuclei, then to their merger and the formation of a cavitation cavity attached to the moving surface, which is schematically shown in Fig. 2(b)). Such an idea of the process of rarefaction of lubricating layers is in good agreement with the mechanism of desorption of mono- and multimolecular near-surface boundary layers of lubrication in accordance with the Langmuir and BET theories.

Mechanism of adhesive wear within the framework of the proposed Adhesion-Deformation-Hydrodynamic model.

In the divergent elastically deformed region of the tribo-contact, the residual boundary layers are under conditions of rapid rarefaction. They are desorbed, evaporate, and the areas of contacting oxide layers of the surfaces are under conditions of quasi-dry friction. Under these conditions, oxide films are easily removed by cracking, which leads to adhesion of juvenile areas of elastically deformed surfaces in the divergent contact area, i.e. to micro- and submicro-seizure of the surfaces, followed by tearing of the material from the friction surface of the bearing and neoplasm on the shaft.

Thus, during friction of surfaces with adsorbed layers of lubricant active substances, primary adhesion occurs precisely in divergent elastically deformed regions of curvilinear micro- and macrocontacts. The photographs of the worn friction tracks of the flat surface of the model bearing shown in Fig. 3 after friction on it with the model shaft confirm the correctness of the assumed adhesive wear mechanism and the Adhesion-Deformation-Hydrodynamic model of friction and wear.

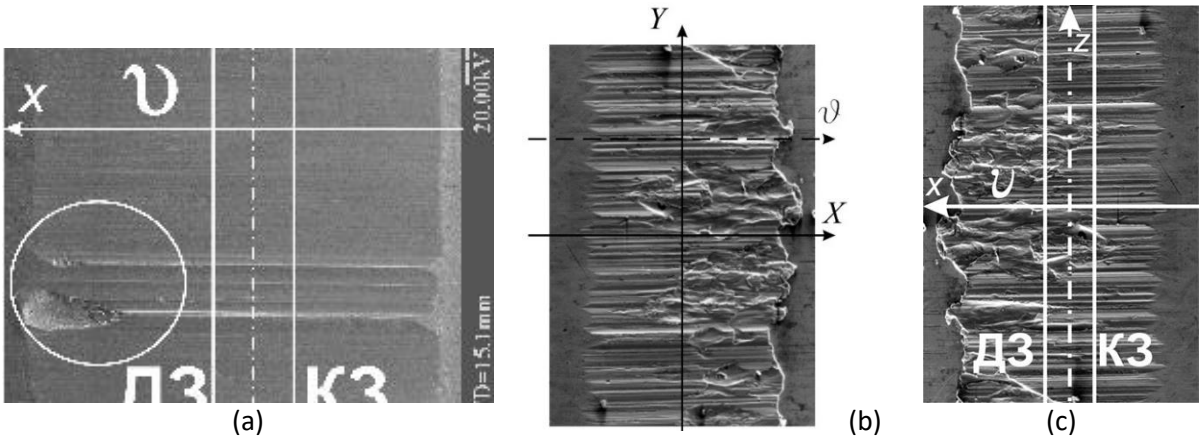

Fig. 3. Primary adhesion in the divergent area of contact with a characteristic pull-out of a fragment of the bearing material (a) and the regular appearance of friction tracks (wear traces): in the direction of friction: at the exit from the shaft contact (in the divergent elastically deformed area) - characteristic pull-outs of the material of a model plain bearing (b, c), and at the contact entry (in the convergent elastically deformed area) there are characteristic risks of deformation microcutting. Friction conditions: steel ШХ-15 with HRC=59~62, Ra<0.02mkm, initial, design, maximum contact stresses 2000MPa, linear velocity 0.3m/s, friction device ПТИ ТРИБО-04

The above model of the occurrence of extrusion and rarefaction in an elastically deformed curvilinear contact is experimentally confirmed by the following regularities (Fig. 13), when with an increase in friction speed and load, the pressure in the lubricating layer in the convergent elastically deformed area of the tribo-contact always increases, and in the divergent area it decreases. In the convergent elastically deformed region, this is explained by the fact that with an increase in only the friction velocity at a constant load, the speed of the incident flows and return extrusion flows simultaneously increases, and with an increase in only the load and contact stresses, only the velocity of the return extrusion flows increases correspondingly to meet the boundary layers incident with the shaft. In the divergent region, a similar but reverse picture occurs: with an increase in the friction velocity and contact stresses, the extension rate and the gradient of negative stresses increase, which leads to an increase in the degree of rarefaction.

The lower part of Fig. 4 shows the schematic appearance of return flows as a result of extrusion in the convergent region of the elastically deformed contact and cavitation nucleation as a result of rarefaction in the divergent elastically deformed region of the contact. This scheme is fully consistent with the measured distribution of local pressure in the lubricating layers during sliding friction of a model shaft over a plain bearing in dynamics, which will be described in more detail in the following reports of the authors.

In this case, as can be seen in Fig. 4, the degree of rarefaction in the divergent region also increases with an increase in both the sliding speed and contact stresses. It is noteworthy that with an increase in the degree of rarefaction in the divergent region of the elastically deformed contact, in addition to an increase in the rate of desorption of the lubricating layers, the actual contact stresses in the microcontacts of the elastically deformed vertices will also increase, which will experience an additional load due to the suction effect. This further exacerbates the situation of the contacting quasi-dry tops of the surfaces and contributes to their more intense adhesive interaction and wear.

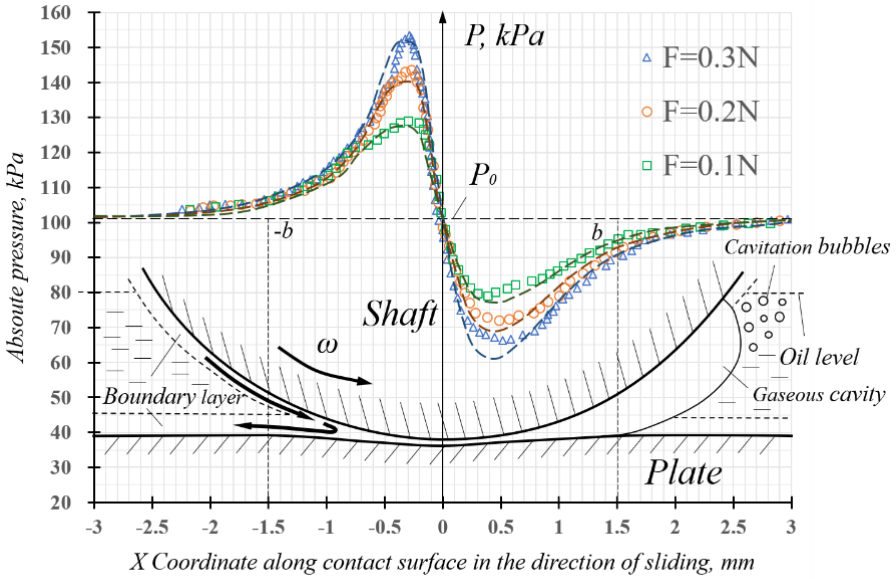

Fig. 4. Experimentally measured (solid lines) and calculated (dashed lines) values of local pressure in the lubricating layer during friction of a model shaft on a model flat bearing according to the Timken scheme within the width of the elastically deformed contact [-b;+b] at different axial loads (0.1N, 0.2N, 0.3N) and one stabilized speed of 0.251m/s.

2. Summary of the Adhesion-Deformation-Hydrodynamic model of friction and wear

The main provisions presented above find their experimental confirmation (Fig. 3, 4) and will be detailed in the following. Adhesion-Deformation-Hydrodynamic model of friction and wear in relation to a radial plain bearing. Previously, the main assumptions of the Adhesion-Deformation-Hydrodynamic model were given on the example of a plain bearing with the Timken scheme. With regard to the radial plain bearing Adhesive wear in conjunction with the hydrodynamic processes of extrusion and rarefaction in the boundary layers in the elastically deformed region of the Adhesion-Deformation-Hydrodynamic model of friction and the wear process is presented as follows (Fig. 5).

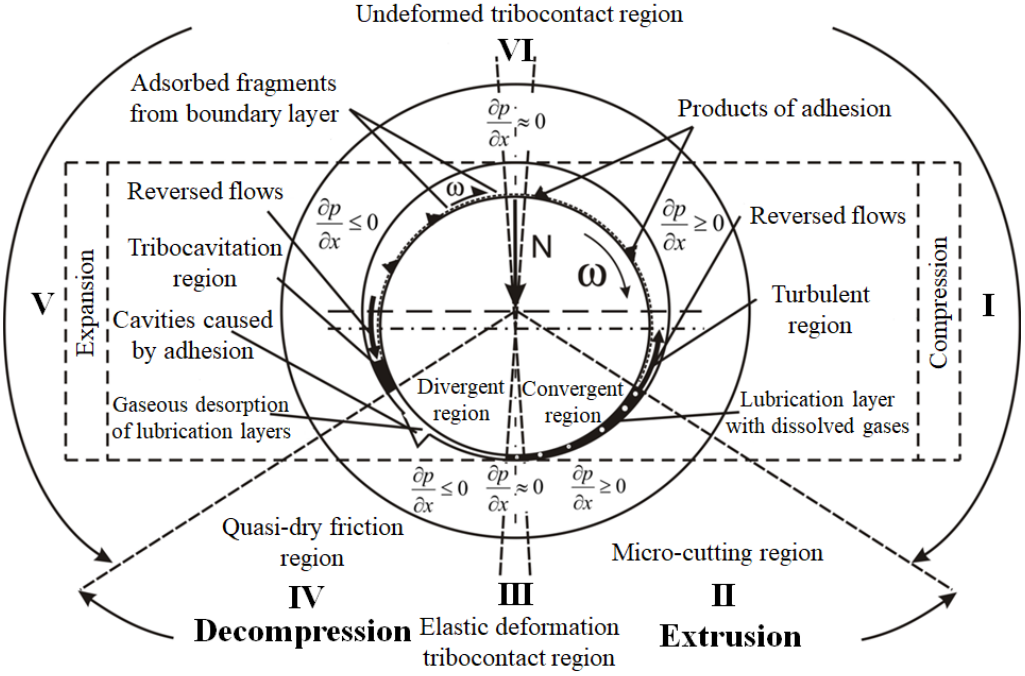

Fig. 5. Schematic representation of the physical friction model of a radial plain bearing with characteristic convergent, transition and divergent non-contact and elastically deformed areas, taking into account extrusion and rarefaction processes.

In the elastically deformed divergent region of the tribo-contact, rarefaction occurs in the boundary layers of the lubricant and their desorption. Desorption of lubricating layers leads to the appearance of conditions of

quasi-dry friction and primary adhesion of friction surfaces (Fig. 5). Such local adhesion leads to tearing of a fragment of material from the bearing surface and neoplasm on the friction surface of the shaft. This neoplasm, in the case of a radial plain bearing, enters the convergent region, where, due to the increased radial dimensions of the initial shaft surface, it implements microcutting as follows: part of it is cut and carried out into the lubricant volume in the form of a wear product, and the rest implements microcutting, which is shown in the diagram (Fig. 5). This leads to a rapid change in the micro- and macro-geometry of the contact, which immediately leads to a redistribution of contact stresses and a change in all parameters of the initial contact both along and in the radial direction. After that, friction occurs, in fact, already in other newly formed elastically deformed - convergent and divergent areas. Then, new areas appear in elastically deformed contact with quasi-dry friction conditions in other new divergent contact areas, where adhesive micro- and submicro-seizure occurs. Then, pull-out in the divergent area, micro-cutting in the convergent area, and so on (Fig. 5).

Conclusions

1. The development of a new Adhesion-Deformation-Hydrodynamic model of friction and wear should be based on experimental and theoretical studies of hydrodynamic processes of extrusion and rarefaction of lubricating layers in characteristic elastically deformed areas of tribocontact in the entire range of loads and friction velocities. For this, it is necessary to establish the relationship 1 - the stressed state in the contact of elastically deformed surfaces, 2 - the structural-phase state of the boundary layers of the lubricant adsorbed on them, and 3 - the adhesion of friction surfaces.

2. The proposed Adhesion-Deformation-Hydrodynamic model of friction and wear and its main provisions on the relationship between extrusion, rarefaction in lubricating layers and primary adhesion of friction surfaces of curvilinear contacts cover the entire load-speed range and all modes of lubrication of friction surfaces.

3. To create a new Adhesion-Deformation-Hydrodynamic model of friction and wear, it is necessary to establish experimental patterns that directly or indirectly confirm the objectively occurring processes of extrusion and rarefaction in boundary layers in elastically deformed curvilinear contacts of highly elastic real and materials such as bearing steel ШХ-15 during friction, when the elastically deformed area is several tens of microns, in conjunction with the adhesive interaction of surfaces. In addition, it is required to develop and use new laboratory instruments and techniques, for example [2-4], which will allow observing Extrusion and Vacuum in lubricating layers, as well as scanning and metrologically measuring the local pressure in them as accurately as possible and other parameters of lubricating layers and tribo-contacts of model low-elastic and optically transparent materials during friction in dynamics.

References

1. Leybenzon L V. Hydrodynamic theory of lubrication. Moscow: State Technical and Theoretical Publishing House, 1934. (in Russian)

2. Stelmakh O U. A teaching aid for demonstrating friction cavitation and jet phenomenon in line contact friction. China Patent ZL202022922297.0, Sep. 2021.

3. Stelmakh O U. Line contact friction testing machine for observing friction jet streamline and friction cavitation. China Patent ZL202022922298.5, Sep. 2021.

4. Stelmakh O U. Line contact friction testing machine with pressure scanning function. China Patent ZL202022922275.4, Sep. 2021.

Олександр Стельмах, Хун'ю Фу, Іцяо Гуо, Сіньбо Ван, Хао Чжан, Олександр Диха. Адгезійно-деформаційно-гідродинамічна модель тертя та зношування

Запропонована адгезійно-деформаційно-гідродинамічна модель тертя та зношування базується на зв'язку пружно-деформаційних процесів на поверхнях криволінійних контактів з гідродинамічними закономірними процесами видавлювання та розрідження в мастильних шарах у трибоконтактах, а також з процесами первинного зчеплення поверхонь тертя і подальші акти адгезійного зношування. Запропонована адгезійно-деформаційно-гідродинамічна модель тертя і зношування та її основні положення про взаємозв'язок між видавлюванням, розрідженням у мастильних шарах і первинним зчепленням поверхонь тертя криволінійних контактів охоплюють весь діапазон навантажень-швидкісність і всі режими змащування поверхонь тертя.

Ключові слова: модель тертя, мастильні шари, контактний тиск, адгезія

***Problems of Tribology**, V. 27, No 3/105-2022,55-60*

Problems of Tribology
Website: http://tribology.khnu.km.ua/index.php/ProbTrib
E-mail: tribosenator@gmail.com

DOI: https://doi.org/10.31891/2079-1372-2022-105-3-55-60

Increasing the durability of cold volume stamping equipment

Y.V. Savytskyi*, V.V. Mylko, S.S. Bys

Khmelnitskyi National University, Ukraine
**E-mail: yra.savisky@gmail.com*

Received: 15 July 2022: Revised:22 August 2022: Accept:11 September 2022

Abstract

The work examines the process of cold three-dimensional stamping, which is a very effective method of manufacturing blanks for machine parts. When using cold extrusion, high-cost stamping equipment wears out quickly and defects appear on the finished products. The development of rational technological processes of stamping helps to solve the tasks of expanding the possibilities of cold extrusion by reducing the specific force perceived by the punches, finding the optimal shape of the punch, and testing different grades of steel in order to select them according to the best operational properties. The process of radial extrusion was theoretically investigated and its mathematical model was built based on the energy method, which allows for the analysis of the force mode of extrusion and the kinematics of metal flow, to determine the relative specific force of deformation, to construct the velocity fields for different metal flow zones, and already from these data to calculate the total force deformations The resolution of the model made it possible to formulate recommendations for reducing production defects and increasing the durability of die equipment.

Key words: metal flow, deformations, extrusion, matrix, punch.

Introduction

Cold three-dimensional stamping is a highly efficient process of manufacturing parts and is widely used in the world engineering industry. Extrusion occupies a special place among volume stamping operations. In the conditions of the free economic zone with the EU, the main criteria of product competitiveness are its price and quality, which is achieved by introducing new and improving existing technologies.

Analysis of the latest research

One of the highly productive and economical processes for the production of parts is cold extrusion (CE) from alloys of non-ferrous metals and various grades of steel [1]. The economic feasibility of using cold extrusion is determined by improving the quality of parts, reducing metal consumption, reducing labor intensity, and reducing cost. The highest efficiency of cold extrusion processes is achieved in the production of axisymmetric parts and a complex shape with large differences in the intersections of cavities of different configurations [2].

Highlighting the previously unsolved part of the general problem

In fig. 1 shows a drawing of an extruded M42x2 nut blank. This nut is used to complete the high-pressure hose (Dy=25-4SH, R=320 Bar.), which ensures the operation of the power hydraulic system of grain harvesters. However, during the manufacture of this part, some problems arise, namely:

- surface defects appear (cracks, depressions, burrs, and other defects (Fig. 2);
- low stability of expensive stamping tools (matrices and punches), which reduces work productivity and increases its cost.

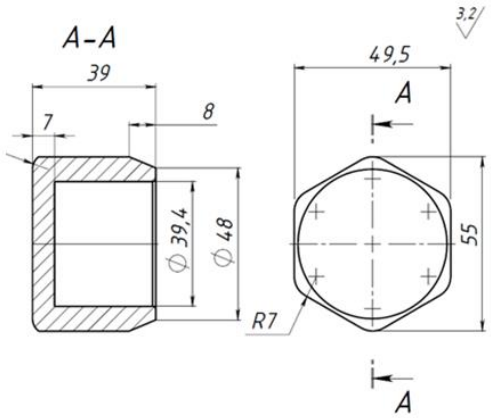

Fig. 1. Workpiece of nut S50(M42x2)

Presenting main material

The choice of one or another method in the production of products by extrusion requires the development of scientifically based technology [3], which allows predicting the mechanical characteristics of the resulting parts at the stage of designing the technological process. In addition, the development of rational technological processes contributes to the solution of the tasks of expanding the possibilities of cold extrusion by reducing the specific force perceived by punches, finding the optimal shape of the punch, and testing different grades of steel in order to select them according to the most optimal operational properties.

a) b) c)

Fig. 2. Surface defects of the nut blank obtained by cold extrusion: a – surges, weights; b – cracks, roughness, c – longitudinal lines.

It has been theoretically proven [4] that the processes of extrusion of parts with variable wall thickness along the perimeter are characterized by a specific three-dimensional flow of metal. This flow is not axisymmetric, which has not been taken into account in theoretical solutions until now. It has been proven that extrusion takes place in two stages: the first, which occurs as a radial flow of metal, during which the festoon is formed on the upper end of the part (Fig. 3); the second is three-dimensional (vortical), i.e. all three velocity components are different from zero: $v_r \neq 0$; $v_\theta \neq 0$; $v_z \neq 0$) (Fig. 4). The initial parameters are the dimensions of the punch r_n, the matrix A, and the workpiece $h_з$. For the first stage of deformation, we assume that radial flow takes place in zones 1, 2, zone 3 can be plastic (due to shear), and zone 4 has no deformation, therefore it is a rigid zone. Velocity fields in zones 1, 2, 3 in the cylindrical coordinate system have the following form (Fig. 3):

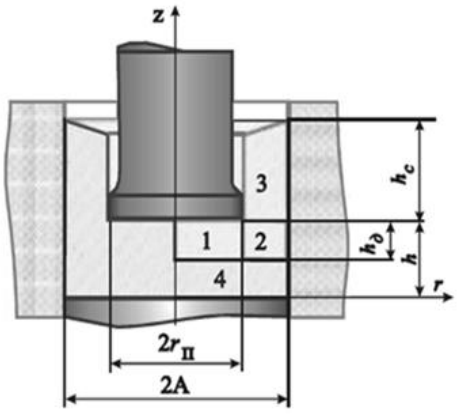

Fig. 3. Diagram of the process of radial extrusion at v_θ=0

For zones 2 and 3, the components *vr*1, *vz*2 and *vr*2 are obtained on the basis of the law of constancy of volume. Dependencies for metal flow rates, deformation rates, and intensity of deformation rates make it possible to describe the deformed state in the entire volume of the workpiece and proceed to the construction of a mathematical model of the process.

Zone 1: $h - h_\partial \le z \le h,\ 0 \le r \le r_n;\ v_{z1} = -\frac{v_n}{h} z - h_\partial - h;\ v_{r1} = \frac{v_n}{2h_\partial} \cdot r;\ v_{\theta 1} = 0;$

Zone 2: $h - h_\partial \le z \le h,\ r_n \le r \le A/\cos\theta;\ v_{z2} = -\frac{v_n}{h} - h_\partial - h \cdot f\theta;\ v_{r2} = \frac{v_n}{2h_\partial} \cdot \frac{A^2 - r^2\cos^2\theta}{r} \cdot f\theta;$

where $f\theta = \frac{r_n^2 \cos^2\theta}{A^2 - r^2\cos^2\theta};\ v_{\theta 2} = 0;$

Zone 3: $h \le z \le h + h_c,\ r_n \le r \le A/\cos\theta;\ v_{z3} = v_n \cdot f\theta;\ v_{r3} = 0;\ v_{\theta 3} = 0;$

Zone 4: $0 \le z \le h - h_\partial,\ r_n \le r \le A/\cos\theta;\ v_{z4} = 0;\ v_{r4} = 0;\ v_{\theta 4} = 0,$

where $v_п$ – punch speed

h – is the depth of propagation of the center of plastic deformation;

h_c – the height of the part wall;

h – bottom thickness;

r, z, θ – coordinates of the cylindrical coordinate system.

To build a mathematical model of the process, we use the first basic equation of the energy method [5]:

$$F_\partial = \frac{1}{v_п}\left[\sum_{j=1}^{J}\left(\iiint \sigma_s(\varepsilon_i)\xi_i dV\right)_j + \sum_{m=1}^{M}\left(\iint \tau_k \sqrt{v_k{}^2 + v_l{}^2}\, dA\right)_m + \sum_{n=0}^{N}\left(\iint \tau_s \Delta v dG\right)_n\right] \quad (1)$$

where F − the variable active force in the process of deformation, H;

vп − punch speed, m/c;

$\sigma(\varepsilon_i)$ – flow stress as a function of strain intensity εi, Pa;

V − volume of the zone in the center of deformation, m^3;

κ − friction stress on the contact surfaces, Pa;

A − surface area of this element of the deformed workpiece, m^2;

v_k, v_l – speed along the generalized coordinate axes k and l, m/c;

S − shear stress on the surfaces of the speed gap, Pa;

Δv – gap of shear rates, m/c;

G − surface area of the speed gap, m^2;

J − the number of zones into which the deformation center is divided;

M – the number of contact friction surfaces;

N − the number of velocity discontinuity surfaces.

The power of the external deforming force applied to the punch:

$$N_{12} = F_\partial \cdot v_п = \pi r_п^2 \cdot p\, v_n \sigma_s, \quad (2)$$

where p – the relative specific deformation force as a function of the dimensionless depth of the distribution of the plastic deformation cell.

Based on (1), we can write:

$$\pi r_п^2 \cdot p v_n \sigma_s = \sum_{i=1}^{11} N_i \quad (3)$$

By substituting into the ratio (3) the value of the calculated power of the internal forces of resistance to deformation, contact friction and shear, which are calculated for each of the zones of the part - Ni, dividing the right and left parts by $vn\ \sigma s$ and the area of the working face of the punch πr_n^2 , after conversion to the criterion form, we find p

$$p = A_0 + A_1 h_\partial + A_2 / h_\partial \quad (4)$$

Values A0, A1, A2 are calculated constants. Ratio (4) is a mathematical model of the radial extrusion process (under the conditions $v_\theta = 0$). (4) can be considered as a function of the properties of the deforming material (σ_s), the dimensions of the workpiece and the tool (shown in Fig. 2), the friction conditions on the contact surfaces of the matrix and the punch (μ_1 and μ_2), as well as the varied parameter h_∂ - depth spread of plastic deformation center.

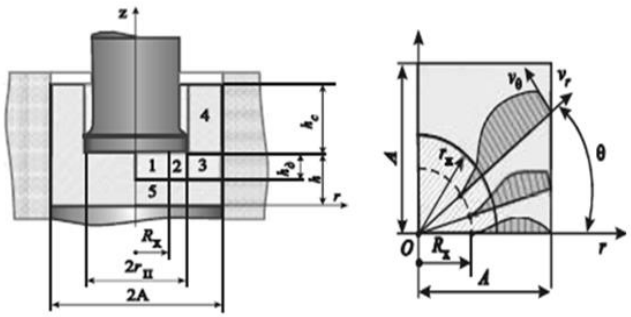

a) **b)**

Fig. 4. The diagram of the division of the part into zones (a) and the diagram of the three-dimensional flow in zones 2 and 3 (b) at the second stage of extrusion

Dependence (4) makes it possible to analyze the force mode of extrusion and the kinematics of the metal flow, determine the relative specific deformation force *p*, construct the velocity fields for zones 1 - 4, and use this data to calculate the total deformation force F∂.

It is shown that the theoretical analysis of three-dimensional flow processes when $v_x \neq 0;\ v_y \neq 0;\ v_z \neq 0$ (or in the cylindrical coordinate system $v_r \neq 0;\ v_\theta \neq 0;\ v_z \neq 0$) (which is conventionally called "vortex", as recommended by A. G. Ovchinnikov [4]), can be carried out in full. The analysis performed the second stage, in which the wall formed by the overhang h_c with the festoon Φ acts as a rigid end and equalizes the velocity v_z along the angle θ. At this stage, the dimensions of the formed festoon no longer change (which is confirmed by experiments), and since the thickness of the wall along θ is variable, then this leads to a significant change in the character of the flow - the formation of a three-dimensional flow, in which we have $v_\theta \neq 0$ in zones 2 and 3 (Fig. 4, b). For a three-dimensional flow (when all components *vr*, *vθ* and *vz* are different from zero) the condition of constancy volume has a more complex form than with radial:

$$\frac{\partial v_r}{\partial_r} + \frac{\partial v_z}{\partial_z} + \frac{1}{r}\left(\frac{\partial v_\theta}{\partial_\theta} + v_r\right) = 0. \qquad (5)$$

Equation (5) contains three unknown functions v_r , v_θ and v_z. If two functions v_θ and v_z are specified, then the function v_r can also be determined from the condition of constant volume. For this, you can use suitable functions that describe the flow of metal in zones 1, 2 and 3 (see Fig. 4, a). Zones 4 and 5 are hard, because in them all components of strain rates, except v_{z4}, are equal to zero. In addition, v_{z4} = const. Suitable functions must satisfy the boundary conditions. Zone 1 ($0 \le r \le R_x$) is characterized by a radial flow of metal, which is described by functions linear with respect to the independent variables *r* and *z*:

$$v_{z1} = -\frac{v_n}{h_\partial}[z - (h - h_\partial)];\quad v_{r1} = \frac{r v_n}{2h_\partial};\qquad v_{\theta 1} = 0; \qquad (6)$$

where *Rx* – the unknown radius separating the regions of radial and three-dimensional flow.

Zones 2 and 3 ($R_x \le r \le r_п$, as well as $r_п \le r \le A/\cos(\theta)$ are characterized by an eddy flow that can be described by complex suitable functions. The velocities v_{z2} and v_{z3} are easily determined from the conditions of constancy of volume, and the function for the velocity $v_{\theta 2}$ can be given as a fit with five parameters (a_0, a_1, a_2 , a_3 and λ) that must be varied to obtain min (F_∂):

$$v_{z2} = -\frac{v_n}{h_\partial}[z - (h - h_\partial)];\qquad v_{z3} = \frac{v_n}{h_\partial}[z - (h - h_\partial)]\frac{\pi r_n^2}{4A^2 - \pi r_n^2}; \qquad (7)$$

$$v_{\theta 2} = [a_0 + a_1 r + a_2 r^2 + a_3 r^3](\sin 4\theta + \lambda \sin 8\theta)\cdot v_n;\quad v_{\theta 3} = v_{\theta 2}; \qquad (8)$$

where *r, θ* and *z* – independent variables; a_0 , a_1, a_2 , a_3 and λ – variable parameters.

It was established from previous experimental studies that $0 < \lambda < 0.55$. The functions v_{r2} and v_{r3} for zones 2 and 3 can be found from the condition of constant volume:

$$v_{r2} = -\frac{1}{r}\left[\int\left(\frac{\partial v_{z2}}{\partial_z} + \frac{1}{r}\frac{\partial v_{\theta 2}}{\partial_\theta}\right)\cdot dr + C_2\right];\qquad v_{r3} = -\frac{1}{r}\left[\int\left(\frac{\partial v_{z3}}{\partial_z} + \frac{1}{r}\frac{\partial v_{\theta 3}}{\partial_\theta}\right)\cdot dr + C_3\right]; \qquad (9)$$

Integrating (9) taking into account boundary conditions by zones leads to obtaining complex functions of the general form:

$$v_{r2} = f_r(a_0, a_1, a_2, a_3, h_\partial, \theta, \lambda, R_x);\qquad v_{r3} = f_r(a_0, a_1, a_2, a_3, h_\partial, \theta, \lambda, R_x), \qquad (10)$$

where R_x – variable, which allows to determine the border of zones 1 and 2, based on boundary conditions $0 \le R \le r_x$.

The velocity functions v_θ and v_r have the following properties: 1) the eddy current (when $v_\theta \neq 0$) starts from some coordinate $r = R_x$; 2) at the point $r = R_x$ function v_θ is continuous; 3) the metal of the workpiece does not penetrate through the wall of the matrix.

From these properties, we obtain additional information about the behavior of the corresponding functions v_θ, v_r and additional conditions: 1) at $r = R_x$ $v_\theta = 0$; 2) at $r = R_x$ we have $dv_\theta / d_r = 0$, as well as $d_2v_\theta / d_r^2 = 0$; 3) at $r=A/\cos(\theta)$ $v_{r3} / v_{\theta 3} = tg(\theta)$.

From these additional conditions follows the possibility to reduce the number of varied parameters by connecting them through 2 generalized parameters. This simplifies the process of minimizing function (4) depending on the depth of propagation of the plastic deformation center (Fig. 4), makes it possible to follow the transition of the deformation process from the initial stage (purely radial flow) to the second stage - three-dimensional flow, when $v_\theta \neq 0$ as an energetically more advantageous option with a sufficient height of the rigid end (extruded wall).

The accepted assumptions for determining the parameters of the functions v_θ and v_r, which minimize the function p (4), made it possible to perform calculations and describe the nature of the metal flow at all stages of extrusion with sufficient accuracy.

The strain rate intensity ξ_i is determined by the well-known formula, which contains the components of the strain rate tensor determined according to the Cauchy equations.

The obtained dependences for flow rates, deformation rates, intensity of deformation rates in each zone made it possible to describe the deformed state in the entire volume of the workpiece and proceed to the construction of a mathematical model of the process.

The power of the external deforming force applied to the punch:

$$N_{14}=F_\partial v_n = \pi r_n^2 \cdot p\, v_n\sigma_s \tag{11}$$

Based on (1), we can write:

$$\pi r_n^2 \cdot p\, v_n\sigma_s = \sum_{i=1}^{13} N_i \tag{12}$$

By substituting the values of the calculated capacities into expression (12), dividing its right and left parts by $v_n\sigma_s$ and the area of the working face of the punch πr_n^2, converting the obtained complex function to the criterion form, we find the relative specific deformation force p for extrusion in three-dimensional flow conditions [5].

The considered process is a process in which the radial and "eddy" currents flow sequentially. The MathCAD software package was used for the analysis and research of the process of metal pressure processing - a practical and effective tool that allows you to predict the nature of formation during metal pressure processing operations without the expense of experimental research.

The work analyzes the technological process of manufacturing a part of the "thin-walled glass" type with a variable wall thickness along the perimeter by cold reverse extrusion, as well as the influence of the CE parameters on the mechanical characteristics of this type of parts.

Conclusions and prospects for the development of the direction

1. The use of active forces of contact friction will reduce the specific force on the punch by 20-30%.

2. When choosing the optimal taper angle of the punch end, it is possible to reduce the specific force on the punch by 7 - 13%.

3. When choosing the optimal dimensions of the outline on the end of the workpiece, it is possible to reduce the specific force on the punch by 4 - 15%. Under the action of active frictional forces, the influence of the technological outline decreases.

All of the above factors increase the stability of the cold-drop tool (matrices and punches) by 40-45%. The stability of technological equipment directly affects the cost of production of blanks due to the significant costs of its production. Currently, in order to reduce the deforming force, various lubrication materials, tool shapes, methods of processing the surface of the workpieces are used, which allow to reduce the forces of contact friction, and extrusion with active frictional forces is also carried out. In addition, due to a significant improvement in the condition of the surface of the workpieces, the number of rejected products is reduced from 15% to 5%.

References

1. Vorontsov A.L. Theory of extrusion stamping / AL // M. Vorontsov: Mechanical Engineering 1, 2004. – 721p.

2. Cold forging / Ed. G.A. Navrotskogo. //M.:Mashinostroenie - 1987 – 384 p.

3. The theory of plastic deformation of metals / ed. E.P. Unksova, A.G. Ovchinnikov. - M .: Mashinostroenie, 1983 - 598 p.

4. Forging and Stamping: A Handbook. B-4 T .; m. 3. The cold forging / Ed. G.A. Nawrocki - M .: Engineering, 1989. – 368 p.

5. Analysis of extrusion processes under conditions of three-dimensional metal flow. / Krotenko G.A. NTU "KhPI" // Kharkiv, 2011 – 20 p.

Савицький Ю.В., Милько В.В., Бись С.С. Підвищення довговічності обладнання для холодного об'ємного штампування

В роботі вивчено процес холодного об'ємного штампування, який є дуже ефективним методом виготовлення заготовок деталей машин. При застосування холодного видавлювання відбувається швидке зношування високовартістної штампової оснастки та з'являються дефекти на готових виробах. Розробка раціональних технологічних процесів штампування сприяє вирішенню завдань по розширенню можливостей холодного видавлювання за рахунок зниження питомої сили, яка сприймається пуансонами, знаходження оптимальної форми пуансона, апробація різних марок сталей з метою їх підбору по найкращим експлуатаційним властивостям. Теоретично досліджено процес радіального видавлювання та побудовано його математичну модель на основі енергетичного методу, яка дозволяє провести аналіз силового режиму видавлювання і кінематики плину металу, визначити відносне питоме зусилля деформації , побудувати поля швидкостей для різних зон течії металу, а вже за цими даними розрахувати повне зусилля деформації. Розв'язок моделі дозволив сформулювати рекомендації по зменшенню виробничого браку та підвищенню довговічності штампового оснащення.

Ключові слова: течія металу, деформації, видавлювання, матриця, пуансон.

***Problems of Tribology**, V. 27, No 3/105-2022,61-69*

Problems of Tribology
Website: http://tribology.khnu.km.ua/index.php/ProbTrib
E-mail: tribosenator@gmail.com

DOI: https://doi.org/10.31891/2079-1372-2022-105-3-61-69

Investigation of corrosion and wear resistance of steels nitrided in a glow discharge in distilled water

O. Yu. Rudyk*, P.V. Kaplun, K.E. Golenko, V.A. Honchar, M.M.Poberezhnyi

Khmelnitskyi National University, Ukraine
**E-mail: yukhymovych@gmail.com*

Received: 20 July 2022: Revised:28 August 2022: Accept:15 September 2022

Abstract

The article is devoted to the study of corrosion resistance and wear resistance (sliding friction) of unhardened and glow discharge nitrided (ion or ion-plasma nitriding) structural steels 20, 45, 45X and 38X2MЮA in distilled water. The influence of temperature (T = 793 – 873 K), the composition of the saturating mixture (nitrogen N_2, argon Ar and propane C3H8) and its pressure (P = 80 – 450 Pa), the duration of the process on the structure and phase composition of the nitrided layers was studied (carried out using metallographic and X-ray structural analyses). A comparison of the physical and mechanical characteristics of the surface layer of unhardened and nitrided steels before and after the tests was carried out and it was concluded that nitrided steels have an increased service life due to greater hardness, corrosion resistance and wear resistance. It is recommended to increase the corrosion resistance of the studied steels in distilled water, to carry out their ionic nitriding in a nitrogen-containing atmosphere, and to increase wear resistance - in a carbon-containing atmosphere (carbonitriding).

Key words: structural steels, physical and mechanical properties, ionic nitriding, carbonitriding, distilled water. corrosion, wear.

Objective

The influence of ionic nitriding (IN) and carbonitriding on the corrosion resistance and wear resistance of structural steels 20, 45, 45X, 38X2MЮA in distilled water.

Introduction and formulation of research objectives.

Iron and alloys and its bases are the most widespread metal structural materials. Therefore, the specific features of their corrosion and wear are of primary importance for mechanical engineering.

Description of the research methodology. Materials

For the researched materials (steels 20, 45, 45X and 38X2MЮA), the following heat treatment was applied [1]: normalization (steels 20 and 45), improvement (steels 45X and 38X2MЮA). Samples for testing were made from bars of one melt. The chemical composition was analyzed on a DFS-51 quantometer. The application of selected structural steels can be made more efficient by glow discharge nitriding (IN). But the mechanism of its influence on corrosion resistance and wear resistance in distilled water has not been studied yet. This leads to conflicting results of evaluating this method of chemical-thermal treatment (CTT) on the performance of friction units operating in this environment.

Analysis of recent research and publications. Corrosion of steels in water

It is known that the corrosion of steel in water is mainly controlled by the cathodic reaction, that is, by the delivery of oxygen. The pH of water and its ability to form protective sediments are also important [2]. Small additives in low-alloy steels do not noticeably affect the rate of general corrosion in water [3]. Thus, according to [4], the corrosion rate of steel in distilled water is 0.256 g/m2*h. And, according to [5], the corrosion rate of carbon steel when mixing chemically desalinated water at a speed of 0.5 - 1.0 m/s is (0.17 - 0.24) g/m2*h.

Distilled water (according to DEST 6709-72) still contains salts that provide low electrical conductivity. But this value is enough for water to become a weak electrolyte and provide the possibility of electrochemical corrosion. Another cause of corrosion is gas corrosion, that is, the combination of oxygen atoms dissolved in water with iron atoms. Distilled water is devoid of salts, but it contains all atmospheric gases, of which oxygen is of primary importance [5]. And according to [6], metals of increased thermodynamic instability (Fe, etc.) can corrode even in a neutral water environment in the absence of dissolved oxygen.

Dissolved oxygen in water affects steel corrosion because oxygen reduction is the predominant cathodic reaction that controls the anodic reaction. Thus, all factors that change the content of dissolved oxygen affect metal corrosion. Mixing the solution intensifies the transport of dissolved oxygen, increasing the rate of corrosion [7].

The influence of the speed of movement of the neutral electrolyte on the electrochemical corrosion of metals is complex [8]: it facilitates the diffusion of oxygen.

To date, a large number of methods of protecting metal from corrosion have been developed, which include the use of coatings, HTO, plasma treatment, rational selection of the composition and structural state of alloys, etc.

Wear of steels in water

According to [9], corrosion of low-alloy steels in the presence of moisture is accompanied by the formation of iron oxides. These deposits can play a negative role as an abrasive, increasing wear. The authors of [10] investigated the wear resistance of steel 45 (normalization and hardening) and steel 45X (electrolytic nitriding) when rubbing on foam padding in distilled water. It was established that the wear resistance of normalized steel 45 is determined by the adhesive strength of the films formed on its pearlitic and ferritic components. And hardened steel 45 has a uniform martensitic structure and increased anti-corrosion properties. During friction, oxide films softer than the base are formed on it, which flow over the friction surface without the formation of cracks.

Regarding studies of corrosion resistance and wear resistance of non-strengthened and nitrided test steels in distilled water, they were not found.

Nitriding in a glowing discharge

Experimental studies were carried out on the UATR-63 glow discharge nitriding unit, designed and manufactured at the Podilskyi Scientific Physics and Technology Center of the Khmelnytskyi National University.

The nitrogenized layer is characterized by the following main parameters: thickness, surface and depth hardness, phase composition, structure, etc. They depend on the grade of steel and the technological parameters of the process: temperature (T), the composition of the medium in % (nitrogen N_2, argon Ar and propane C_3H_8), the pressure of the gas medium (P) and the duration (D) of diffusion saturation (in all studies, the duration of ionic nitriding (IN) or carbonitriding was □ = 4 hours). These factors under the conditions of ionic nitriding are practically independent [11].

Thus, as a result of IN, a high complex of properties of the strengthened layer (hardness, plasticity, etc.) is ensured, which affects the strength characteristics and operational characteristics of structural elements.

Structure

The study of structural strength properties of nitrided layers was carried out with the help of metallographic and X-ray structural analysis, which made it possible to establish correlations between the studied properties and the observed macro-submicrostructure of the hardened layer.

The sub-microscopic structure of the nitride zone (size, number and nature of discharges) was studied on a SEM-200 scanning electron microscope. X-ray structural phase analysis of the surface layers of the samples was carried out on a DR0N-3 X-ray diffractometer using chromium α-radiation. A semi-quantitative analysis was performed based on the ratio of the intensities of the (101) ε-phase, (111) γ'-phase, and (110) α-phase lines. The calculation of the periods a and c of the ε-phase was carried out by the position of the maxima (110) and (101), the content of the introduced element was determined by the ratio c/a.

The cross-sectional structure of the diffusion layer and the distribution of microhardness over the thickness of the layer were studied on etched sections using an MIM-10 optical microscope. The microhardness of the surface was measured separately and the fragility of the strengthened layer was assessed according to the VINM four-point scale. To measure the microhardness of all studied materials (performed on a microhardness

tester PMT-3 in accordance with DEST 2999-75; a Vickers diamond tip was used) in order to obtain comparable data, a load of 0.98 N was adopted, which provides the smallest relative measurement error. The value of microhardness was recorded both on the surface and at a certain distance from it deep into the sample. The thickness of the nitride zone was measured at ten different locations. The uniformity of indicators was judged by the scatter area.

Corrosion research

Corrosion and electrochemical properties of materials were studied by gravimetric and potentiostatic methods by taking polarization curves, as well as changes in potential over time. Samples for testing (Fig. 2.4; working surface area 1 cm^2) were made on a lathe from one unit from one rod, subjected to heat treatment, polished on a flat grinding machine and refined on an M20 sandpaper. After grinding, the side surface of the samples was insulated with 88NP glue, and the end surface was cleaned with benzene, degreased with acetone, and dried with filter paper. The samples were placed in a desiccator and kept for at least a day.

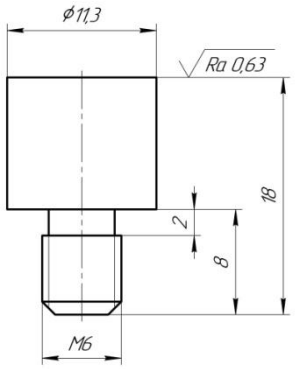

Fig. 1. Sample for studying the electrochemical properties of materials

The kinetics of electrochemical processes that took place in the sample (working electrode) - electrolyte system were studied using a P-5827M potentiostat in a YASE-2 three-electrode cell. The solutions in these experiments were mixed with a magnetic stirrer. Before taking the polarization curves, the samples were kept in the test environment for a time sufficient to establish the rate of change of the potential of the working electrode by no more than 10 mV in 30 min before the start of measurements. Potentials were recorded: immediately after immersion, after 0.5, 1, 2, 3, 4, 5, 30, 60, 90, 120 min. The last measurement was carried out after 96 hours.

Polarization curves were recorded in potentiodynamic mode. The speed of the sweep (change in the potential of the working electrode over time) in all experiments was constant (with a multiplier of the potential speed equal to one). A silver chloride electrode of the EVL-1M1 type, immersed in the electrolyte by 10...20 mm, served as a standard. The auxiliary platinum electrode was placed until the contact was completely immersed in the working solution. The current between the working and auxiliary electrodes was measured with a M2020 millivolt ampmeter.

Corrosion current was determined by extrapolation of rectilinear (Tafel) sections of polarization curves in the region of small overvoltages. According to the corrosion current, taking into account the fact that iron passes into the solution in the form of divalent ions, according to Faraday's law, the corrosion loss of the mass of the samples was determined.

For a deeper study of the dissolution process of materials, the corrosion products in the solution were studied. Qualitative determination of divalent iron ions was carried out using a solution of potassium hexacyanoferrate, trivalent - using a solution of potassium rhodate.

The influence of temperature on the rate of corrosion processes was studied. The temperature of the electrolyte was measured directly near the sample.

To compare the data of electrochemical measurements, the corrosion resistance was studied by means of an open glass with the samples fully immersed in the solution, the amount of which was 4*106 g mm3 per 100 mm^2 of the sample surface. Tests were conducted at room temperature and natural aeration for 720...1100 hours. Corrosion products were removed with a strong stream of water while wiping the sample with a glass stick with a rubber tip. Corrosion losses were determined by weighing the samples on analytical scales VLR-200g before and after the tests, the mass index of corrosion was determined by the formula:

$$K = (m_0 - m)/S\tau$$

where $(m_0 - m)$ – loss or gain of mass, g;
S – sample area, m^2;
τ– duration of tests, hours.

Corrosion-mechanical wear (CMW)

For a comprehensive study of the CMW of materials in a wide range of external loads and working environments of different chemical composition and properties, a laboratory installation of end friction has been designed, which makes it possible to study the change in electrode potential, frictional and wear characteristics, temperature on the friction surface of the sample, friction characteristics depending on the electrode potential system, take polarization cathode and anode curves [11].

The installation (Fig. 2, a) consists of a rigid bed on the basis of a 2M112 machine, a working chamber, a spindle assembly with a drive and a loading device, measuring and recording equipment for measuring and recording electrode potentials, friction characteristics and temperature on the friction surface of the sample (Fig. 2, b).

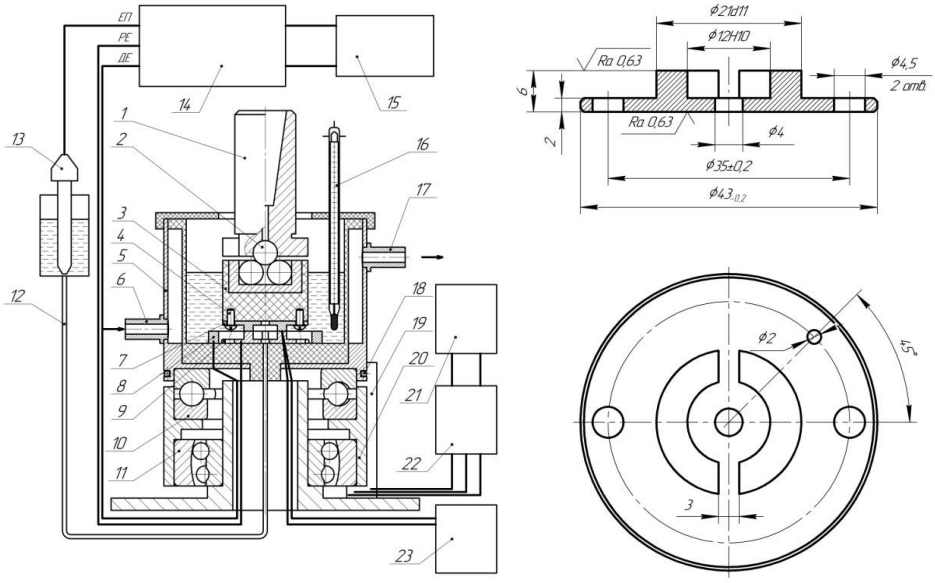

a b

Fig. 2. Scheme of the installation (a) and sample (b) for the study of CMW materials

The rotational movement and vertical force from the conical shank I (Fig. 2.2, a) is transmitted through four balls 2 to the body 3, to which the upper sample 7 is attached with the help of two screws 4. The lower sample 9 is attached with two screws to the electrochemical cell 5 - a three-electrode system , in which the working electrode (WE) is a friction pair, and the auxiliary electrode (AE) is a ring electrode 8 made of 12Х1Ш9Т steel, which forms a polarization chain with WE.

The cell is installed on the thrust bearing 10 and, together with the housing 20, on the double-row spherical bearing 11. The angular fixation of the cell is ensured by the cable 18 attached to the finger 19. To isolate the samples from the installation, the cell 5 and the housing 4 are made of kaprolon, and the non-working surfaces of the samples together with the fastening screws are covered with 88NP glue.

During the friction of metals in electrolytes, the flow of adsorption, diffusion and other processes on their surfaces is determined by the electrode potential of the system. Being a fundamental energy characteristic of the double layer, the electrode potential shows in which stage – active or passive dissolution – the steel is and can affect its friction and wear in electrically conductive environments. The kinetics of electrochemical processes of materials in static conditions, during mixing and friction were studied by the potentiodynamic method using the P-5827M potentiostat (14), and the polarization curves were recorded with a self-writing potentiometer PDP4-002 (13 - Fig. 2, a). Static and stirring tests were performed with a distance between the working surfaces of the samples of 3 mm. The electrode potentials were measured relative to the silver chloride reference electrode EVL-1M1 (13) in a saturated solution of KCl, which is fed into the friction zone using a polymer tube 12 through an axial hole in the lower sample. Thoroughly cleaned, degreased and aged for at least a day in a desiccator, the samples were immersed in a solution with a specified pH value. The volume of the solution was 2 * 105 mm^3, and its temperature was controlled by an electric contact thermometer 16 and maintained by a thermostat. Through the fittings 6 and 17 (Fig. 2, a), thermostated water was supplied and discharged. The average surface temperature of the sample during the tests was measured using a self-recording electronic potentiometer KSP-2 (23) at a distance of 1 mm from the friction surface (Fig. 2, a). To obtain reliable results, an artificial thermocouple with a hot permanent junction (round head) of chromel-alumel thermoelectrodes with a diameter of 0.5 mm was used. The wear resistance of the friction pair was evaluated by friction force (friction moment) and linear wear of the samples. The force of friction was measured by the tensometric method. The signal generated by the deformation of the 19 strain gauges glued to the finger was transmitted through the strain amplifier 8АНЧ-7М (22) to the KSP-2 potentiometer (21). The established coefficient of friction was calculated

on the basis of the diagram of the moment of friction, which is recorded by a self-recording device; linear wear of the samples was determined by an indicator of the hour type MKM with a division price of I μm.

The lower sample made of U8A steel, hardened to (61 – 63) HRCe, had two grooves 3 mm wide on the working surface, which ensured free access of the medium to the friction surface. The upper one was a sample from the researched material. The initial roughness of the working surfaces of the samples was Ra = 0.63. The heating of the samples at the point of contact did not exceed 393 K, which excluded the possibility of significant structural changes in the material. Experiments were conducted at sliding speeds of 0.05, 0.6, and 1 m/s in the pressure range of 1–48 MPa.

Presentation of the main material and obtained scientific results

It was established (Table 1) that the corrosion rate of unreinforced steels is approximately the same. Since the anodes and cathodes are located close to each other in the low-conductivity medium under investigation, the OH- ions formed at the cathode are always close to the Fe^{2}+ ions formed at the anode. As a result, a film of $Fe(OH)_2$ appears, which is adjacent to the metal surface and is an effective diffusion barrier. Increasing the speed of movement of distilled water improves the access of oxygen to the surface and contributes to the removal of corrosion products, thereby increasing the corrosion rate (Table 1 - the obtained data coincide with those given in [5].

Table 1

Electrode potentials and corrosion rate of the investigated materials in static conditions (numerator) and when stirring at a circular speed of 0.05 m/s (denominator)

Steel	Electrode potential, mV						Corrosion rate, g/m²*h	
	After 24 hours exposure			After 96 hours exposure				
	Without hardening	Nitriding*	Nitriding**	Without hardening	Nitriding*	Nitriding**	Without hardening	Nitriding*
20	-578 -386	+42 +37	+37 +35	-584 -390	+78 +77	+48 +44	0.218 0.35	0.0003 0.0005
45	-572 -378	+76 +50	+60 +56	-582 -390	+86 +85	+65 +60	0.210 0.35	0.0003 0.0005
45X	-525 -362	+102 +102	+80 +78	-538 -374	+118 +118	+84 +84	0.151 0.28	0.0003 0.0005
38Kh2MYuA	-520 -355	+122 +122	+85 +82	-535 -363	+131 +130	+88 +88	0.112 0.28	0.0002 0.0004

*one-stage (793 K; 75% N2 + 25% Ar; 265 Pa);

**combined (793 K; 75% N_2 + 25% Ar – 3 hours and 90% N_2 + 10% C_3H_8 – 1 hour, 265 Pa) – carbonitriding.

IN of the studied steels significantly increases their corrosion resistance (Fig. 3), which, in particular, is indicated by a significant improvement of the electrode potential of the surface (Table 1, Fig. 4).

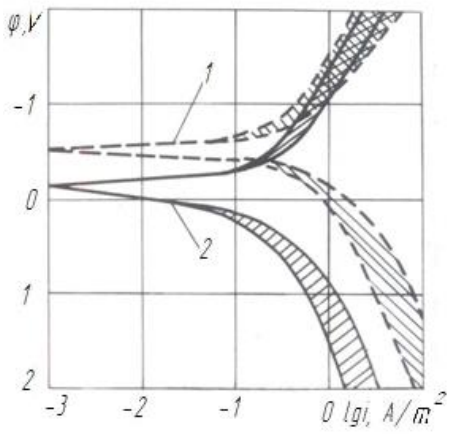

Fig. 3. Polarization curves of unhardened (1) and nitrided (2) at temperature T = 793 K in the single-stage mode of the studied steels

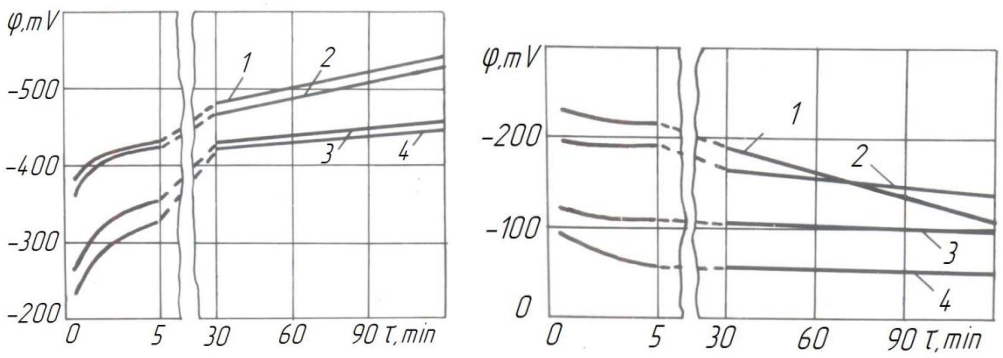

a b

Fig. 4. Curves change over timeτelectrode potentialφunhardened (a) and nitrided (b) at T = 793 K in the one-stage regime of steels 20 (1), 45 (2), 45X (3), 38Kh2MYuA (4)

X-ray structural analysis established that regardless of the composition of the gas atmosphere (table PP.2), ε-$Fe_{2-3}N$, γ′-Fe_4N and α-phases are formed in the surface layer. At the same time, the phase composition and ratio of phase structures in the nitrided layer can be adjusted by changing the nitriding parameters [1].

From Fig. 5, as well as given in table. 1 and 2 of the data shows that with an increase in the content of the ε-phase in the surface layer of materials, their corrosion resistance increases. Therefore, to reduce the corrosion rate of materials in distilled water, a nitrogen-containing atmosphere is better than a carbon-containing one.

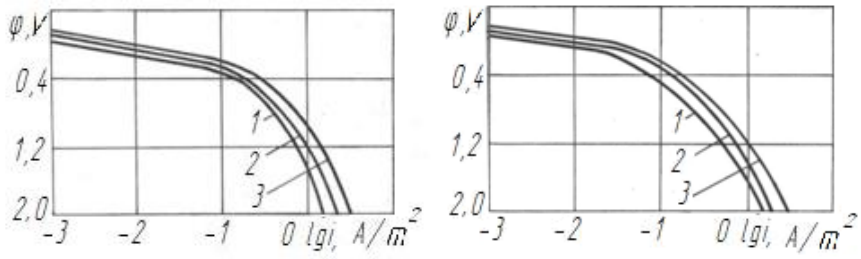

a b

Fig. 5. Anodic polarization curves in distilled water in static conditions: a) nitrided steel 45X at temperatures of 793 (I), 833 (2) and 873 (3) K, pressure 265 Pa, in an atmosphere of 100% N_2; b) nitrided steels 38Kh2MYuA (I), 45X (2), 45 and 20 (3) at parameters of 843 K, 75% N_2 + 25% Ar, 265 Pa

Table 2

Crystal lattice parameters (a and c), nitrogen concentration in the surface layer (Ka) and phase composition of nitrided (843 K; 75% N_2 + 25% Ar; 265 Pa) steels

Indicators	Steel 20	Steel 45	Steel 45X	Steel 45X*	Steel 38Kh2MYuA
a, кX	2.775	2.757	2.761	2.762	2.764
c, кX	4.443	4.441	4.439	4.447	4.436
c/a	1.613	1.611	1.608	1.611	1.605
K_a, %	7.3	7.6	8.3	7.6	8.7
ε - $Fe_{2-3}N$, %	19	21	31	20	45
γ'– Fe_4N, %	56	62	55	9	55
α - Fe, %	25	17	14	71	–

*843 K; 75% N_2 + 25% Ar – 3 hours and 90% N_2 + 10% C_3H_8– 1 hour; 265 Pa

The established regularities indicate that with a decrease in the nitriding temperature, the corrosion resistance of materials in distilled water increases due to an increase in the nitrogen content in the diffusion layer. At the same time, the fragility of the surface area increases, which reduces wear resistance. Therefore, in order to increase the wear resistance of the studied steels in distilled water, their nitriding was carried out at T = 793 K, which helps to increase the saturation of the diffusion layer with nitrogen (Table 3), according to the combined mode of saturation (75% N_2 + 25% argon, 3 hours and 90 % N_2 and 10% C_3H_8, 1 hour; 265 Pa), which increases the plasticity of the surface zones.

Table 3

Dependence of crystal lattice parameters (a and c), nitrogen concentration in the surface layer (Ka) and phase composition of the diffusion layer of steel 45X on IN regimes for 4 h.

Indicators	Temperature, K*			N_2 content, %**					Pressure, Pa***		
	793	833	873	45	60	75	90	100	80	265	450
a, κX	2.775	2.768	2.757	2.759	2.761	2.762	2.765	2.768	2.762	2.762	2.763
c, κX	4.413	4.428	4,447	4.441	4.440	4.439	4.433	4.428	4.440	4.439	4.438
c/a	1.590	1.600	1.613	1.610	1.608	1.607	1.603	1.600	1.608	1.607	1.606
K_a, %	10.8	9.0	7.3	7,6	8.1	8.4	8.8	9.0	8.4	8.4	8.5
ε - $Fe_{2-3}N$, %	63	42	20	22	27	32	38	42	29	32	35
γ'– Fe_4N, %	30	46	59	66	61	56	50	46	59	56	53
α - Fe, %	7	12	21	12	12	12	12	12	12	12	12

*100% N_2; 265 Pa;

**833 K; 265 Pa;

***833 K;75%N_2+ 25% Ar

When wearing materials in distilled water, it is characteristic that it is both a corrosive agent and a friction lubricant. The presence of a low-viscosity aggressive medium causes the appearance of boundary and semi-fluid friction. However, for the accepted test conditions (V = 1 m/s, P = 4 MPa), the surfaces of unreinforced materials seize (Fig. 6). At the same time, the friction coefficient reaches a value of 0.19. Analyzing presented in the table. 4 data, it can be seen that when rubbing in distilled water, the use of unhardened alloyed steels does not give a significant advantage over unalloyed ones.

Table 4

Wear intensity (μm/km) of steels (V = I m/s, P = 4 MPa)

Steel 20	Steel 45	Steel 45X	Steel 38Kh2MYuA
14 1.7	13 1.5	12 1.2	12 1.0

Numerator – without hardening, denominator – combined nitriding (carbonitriding)

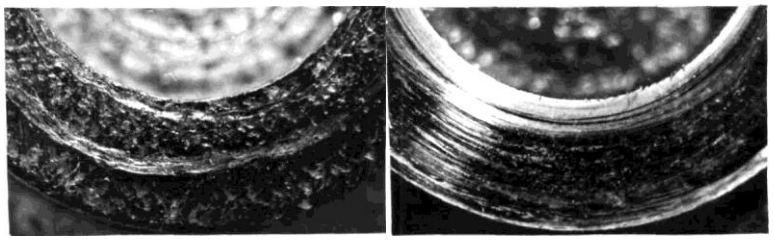

a b

Fig. 6. Friction surfaces of non-hardened (a) and nitrided according to the combined mode (b) 45X steel after CMW (x7.5)

Research has also shown (Table 4) that nitrided steels are characterized by significantly higher wear resistance compared to normalized and improved steels. There is no sticking of nitrided friction surfaces, the friction coefficient is within 0.15. Obviously, this is explained by the increased corrosion resistance of the nitrided layer, the presence of compressive stresses in it [1], as well as the intermetallic structure of Fe_3N nitride, which has a low tendency to cold welding and good antifriction properties. Steel 38Kh2MYuA, which has the highest hardness, has the maximum wear resistance. For unhardened steels, the intensity of wear is directly proportional to the friction path, and for nitrided steels 45X and 38Kh2MYuA, it increases as the diffusion layer wears. Wear of the nitride layer of nitrided steels 20, 45 exposes a zone with reduced hardness (Fig. 7), which leads to an increase in the intensity of wear.

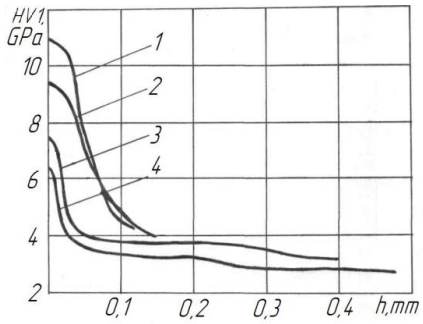

Fig. 7. Distribution curves of microhardness HV1 along the thickness h of the diffusion layer of nitrided steels 38Kh2MYuA (1), 45X (2), 45 (3), 20 (4)

Conclusion

1. X-ray structural analysis established that the phase composition and the ratio of structural components of the strengthened layer can be adjusted by changing the parameters of the IN.

2. With an increase in the content of the ε-phase in the surface layer of the studied steels, their corrosion resistance in distilled water increases. Therefore, from this point of view, a nitrogen-containing atmosphere is better than a carbon-containing one.

3. When rubbing in distilled water, the use of unhardened alloyed steels does not give a significant advantage over unalloyed ones.

4. To increase the wear resistance of nitrided test steels in distilled water, a carbon-containing atmosphere is better than a nitrogen-containing one.

5. In order to determine the maximum wear resistance of steels, further research should be aimed at clarifying the propane content at IN.

Reference

1. O. Yu. Rudyk. Ionic nitriding: regulation of physical and mechanical properties / Bulletin of the KhPI National Technical University. Collection of scientific works. Series: Mechanical and technological systems and complexes. - Kh.: NTU "KhPI" - 2017 - pp. 22-29.

2. Corrosion of steel in fresh and sea water [Electronic resource]. - Access mode:https://mash-xxl.info/info/604830/

3. Steel: corrosion rate in different waters [Electronic resource]. - Access mode:https://mash-xxl.info/info/148717/

4. Corrosion rate of cast iron, steel, stainless steel [Electronic resource]. - Access mode:https://dpva.xyz/Guide/GuideMatherials/Metalls/CastIron/CastIronCorrosionProperties/

5. What is the corrosion rate in distilled water? [Electronic resource]. - Access mode:https://www.warme-rus.ru/help/korroziya-v-sisteme-otopleniya.php

6. Avdeenko A.P. Corrosion and protection of metals: A short course of lectures / A.P. Avdeenko, A.E. Polyakov. - Kramatorsk: DSMA, 2003. - 104 p.

7. Brykov M.N. Wear resistance of steels and cast irons under abrasive wear: Scientific publication / M.N. Brykov, V.G. Efremenko, A.V. Efremenko. - Kherson: Grin D.S., 2014. - 364 p.

8. Electrolyte movement speed [Electronic resource]. - Access mode:https://mash-xxl.info/info/211426/

9. Corrosion — low-alloy steel[Electronic resource]. - Access mode:http://techtrend.com.ua/index.php?newsid=26002922

10. Wear resistance of metal alloys and coatings in packing seals of sugar factories pumps [Electronic resource]. - Access mode: http://lib.osau.edu.ua/jspui/bitstream/123456789/377/1/7.pdf

11. Kaplun V.G. Ionic nitriding in hydrogen-free media: Monograph / V.G. Kaplun, P.V. Kaplun. - Khmelnitsky: KhNU. - 2015. - 315 p.

Рудик О.Ю., Каплун П.В., Голенко К.Е., Гончар В.А., ПобережниЙ М.М. Дослідження корозійної та зносостійкості азотованих у тліючому розряді сталей у дистильованій воді

Стаття присвячена дослідженню корозійної стійкості та зносостійкості (тертя ковзання) незагартованих і тліючим розрядом азотованих (іонним або іонно-плазмовим азотуванням) конструкційних сталей 20, 45, 45Х і 38Х2МЮА в дистильованій воді. Вплив температури (Т = 793 – 873 К), складу насиченої суміші (азот N2, аргон Ar і пропан C3H8) та її тиску (Р = 80 – 450 Па), тривалості процесу на структуру та досліджено фазовий склад азотованих шарів (здійснено методами металографічного та рентгеноструктурного аналізів). Проведено порівняння фізико-механічних характеристик поверхневого шару незагартованої та азотованої сталі до та після випробувань і зроблено висновок, що азотована сталь має підвищений термін служби за рахунок більшої твердості, корозійної стійкості та зносостійкості. Рекомендується для підвищення корозійної стійкості досліджуваних сталей у дистильованій воді проводити їх іонне азотування в азотовмісній атмосфері, а для підвищення зносостійкості – у вуглецевмісній атмосфері (карбонітрування).

Ключові слова: конструкційні сталі, фізико-механічні властивості, іонне азотування, карбонітрування, дистильована вода. корозія, знос.

***Problems of Tribology**, V. 27, No 3/105-2022,70-75*

Problems of Tribology
Website: http://tribology.khnu.km.ua/index.php/ProbTrib
E-mail: tribosenator@gmail.com

DOI: https://doi.org/10.31891/2079-1372-2022-105-3-70-75

Dynamics of wear and tear of garbage trucks in Khmelnytskyi region

O.V. Bereziuk[1], V.I. Savulyak[1], V.O. Kharzhevskyi[2]

[1]Vinnitsa National Technical University, Ukraine
[2]Khmelnytskyi National University, Ukraine
E-mail: berezyukoleg@i.ua

Abstract

The article is dedicated to determining the regularity that describes the dynamics of wear and tear of garbage trucks at the regional level, using the example of the Khmelnytskyi region. During 2015-2020, wear and tear of the fleet of garbage trucks of municipal enterprises of Khmelnytskyi region decreased from 63% to 59%. Using the method of regression analysis, an adequate power law was determined that describes the dynamics of wear and tear of garbage trucks in the region in 2015-2020. To perform the study, the method of regression analysis of the results of one-factor experiments and other paired laws was used by choosing a more adequate type of function from the 16 most common options according to the criterion maximum correlation coefficient. The regression was carried out on the basis of linearizing transformations, which allow reducing the non-linear regularity to a linear one. A graphical dependence describing the dynamics of wear and tear of garbage trucks was constructed, and the sufficient convergence of the obtained regularity was confirmed. According to forecasts the wear and tear of garbage trucks in the Khmelnytskyi region by 2030, at the current rate of decline, will decrease to 51.9%. The expediency of conducting further studies to determine the influence of factors on the dynamics of wear and tear of garbage trucks has been revealed.

Key words: dynamics, garbage truck, wear and tear, municipal solid waste, regression analysis.

Introduction

Among the important tasks of utility engineering, increasing the wear resistance and reliability of parts and machines in general are mentioned in the following works [1, 2]. For the collection and transportation of municipal solid waste (MSW) to landfills and incineration sites in Ukraine, body-mounted garbage trucks in the amount of more than 4,100 units are used, which are capable of compacting solid waste, reducing transportation costs and the required area of landfills. The decrease in the rate of growth of land plots for solid waste disposal is facilitated by their primary treatment during loading into the garbage truck by compaction, dehydration and grinding. At the same time, during technological operations, the surfaces of the working bodies of garbage trucks are subjected to intensive wear. This is caused by the presence of small metal products, glass, ceramics, stones, bones, dust, polymer materials in the waste that have abrasive properties. In addition, the moisture present in MSW, which is an average of 39-92% by mass, creates an aggressive corrosive environment. Despite the taken measures, wear and tear of the fleet of garbage trucks of municipal enterprises of the Khmelnytskyi region during 2015-2020 almost did not change; it decreased only from 63% to 59% [3, 4]. According to Cabinet Resolution No. 265 [5], it is important to ensure the use of modern highly efficient garbage trucks in the country's communal economy, as the main link in the structure of machines for collection and primary processing of solid waste. This allows not only to solve a number of environmental problems, but also to increase the reliability of the work of utility companies. The planning of renewal, maintenance and repair of garbage trucks is facilitated by the determination of the regression law, which describes the dynamics of wear and tear of garbage trucks at regional levels, in particular, using the example of Khmelnytskyi region. An urgent task is to combine the solution of the problem of wear and tear with the improvement of the drives of the working bodies of machines for handling municipal solid waste.

Analysis of recent research and publications

The article [6] proposed a mathematical model for calculating the rate of wear of triboelements in the tribosystem under conditions of corrosive-abrasive wear. At the same time, the following factors were considered by the authors: active acidity, abrasiveness, roughness, load and sliding speed. The degree of influence of the above factors on the rate of wear has been determined theoretically. It was established that abrasiveness is the most important factor, followed by the level of active acidity and load in descending order of influence.

When the authors of the work [7] evaluated the data of observations of garbage trucks, it was found that the largest number of failures occurs due to wear and corrosion of the working surfaces of the working equipment parts. Failures of hydraulic cylinders due to wear of the working surfaces of couplings, deformation of the rod and cylinder during operation make up 32% of all failures of hydraulic drive elements, which is associated with uneven loading of the body and abrasive wear of the working surfaces in difficult working conditions of the garbage truck. During the investigation of the causes of failures, it was found that the predominant cause is the wear of the working surfaces of the main parts in the structure of the hydraulic drive, namely spools and housings of hydraulic distributors, hydraulic cylinder rods, etc. The main cause of wear was hydroabrasive damage due to untimely replacement of the working hydraulic fluid and the use of poor-quality or worn sealing parts (for example, seals of hydraulic cylinders), which causes dust particles and wear products to enter the sliding zone, which accelerate the process of wear of the working surfaces of the parts. One of the promising ways of restoring worn parts is chrome plating in a cold self-regulating electrolyte, which makes it possible to obtain high-performance chrome coatings with high deposit quality.

The analysis [8] of developments in the field of municipal engineering showed that in most garbage trucks, technological operations are carried out with the help of a hydraulic drive of working bodies. According to studies [9], the hydraulic system has the shortest durability (mileage to failure) among the main components of garbage trucks with a side-loading method of solid waste, which makes the most significant contribution to increasing the wear and tear of garbage trucks. According to the results of observations [10], the structure and most frequent causes of failures of the hydraulic equipment of garbage trucks were determined: hydraulic cylinders - 34.92% (wear of cuffs, seals, rod; rupture of the nut attaching the piston to the rod; bending of the rod; mechanical damage), hydraulic pump - 16.40% (casing failure, wear of gears, extrusion of oil seals, cracks in the casing), pipelines, hoses - 15.34% (breakage of hoses, wear of pipelines), hydraulic distributor - 13.23%, (wear of seals, spools; cracks in the casing). Significant loads on drive elements caused by transients during start-up are the most dangerous. Taking into account the considerable mass of solid waste containers (up to 0.5 tons), dynamic overloads can reach significant values. This poses a particular danger for the hydraulic cylinder-lever, hydraulic cylinder-body connection units, as well as for high-pressure flexible pipelines that supply the working fluid to the hydraulic cylinder. Such pressure jumps in the mode of transient processes can cause the rupture of high-pressure pipelines, the exit of the equipment from the operating state. Therefore, the stability of the operation of the hydraulic drive and the quality of transient processes during start-up and acquisition were investigated depending on such indicators of the quality of transient processes as regulation time and relative overregulation, from the main parameters of the working bodies of garbage trucks during loading and unloading of solid waste [8], respectively, which began to be calculated rational parameters of the working bodies of garbage trucks, which ensure high-quality transient processes during the start-up of hydraulic drives, and, therefore, a decrease in the intensity of their wear.

In the work [11], it was established that electronic telemetric navigation and control systems of the machine during operation on the route allow automatic control of the machine and ensure a smoother movement of the levers, reduce their jerks and vibrations during the unloading of solid waste containers. These jerks and vibrations have a negative effect on the car. As a result of reducing the negative impact, the service life of the body and chassis increases, and their wear and tear decreases.

A system analysis showed that a complex of machines is needed to solve the problems of MSW [12], a promising way to minimize the amount and harmfulness of solid waste is their dehydration and subsequent vibration compaction with a press plate with a hydraulic drive and vibration excitation using a pressure pulse generator. On the basis of the studied interaction of the working body – MSW with the executive bodies of the machines, the structure of machines for collecting and primary processing of solid waste was formed [13]. It was established that the design of the garbage truck should take into account the strategy of handling solid waste and the technology of their collection. Thus, for the collection of mixed solid waste with subsequent burial at a landfill or pyrolysis waste incineration, garbage trucks with maximum dehydration and compaction of waste should be used, and in the case of a dual system of collection of "dry" and "wet" waste or their separate (fractional) collection with further processing and repeated using secondary resources, container garbage trucks should be used. Therefore, the production of new constructions of garbage trucks with enhanced functionality will also contribute to reducing the rate of wear and tear of the fleet of garbage trucks of municipal enterprises.

In the article [14], it was established that the tires of cars for collecting and transporting solid waste, which are installed on the front axle, have less wear than on the rear axle. This is due to the fact that in the process of transporting solid waste, the load on the rear axle is greater than on the front. Accordingly, it is possible to compare the actual mileage of the tires with the standards of the enterprise.

The works [3, 4] provide statistical data on wear and tear of garbage trucks in the Khmelnytskyi region in 2015-2020. However, as a result of the analysis of known publications, the authors did not find specific mathematical regularities that describe the dynamics of wear and tear of garbage trucks and can be used for planning the infrastructure of communal enterprises.

The aim of the article

Determining the regularity that describes the dynamics of wear and tear of garbage trucks at the regional level (on the example of Khmelnytskyi region) to solve the problem of forecasting and planning the infrastructure of communal enterprises (warehouse and renewal of garbage trucks, production base for maintenance and repair).

Methods

The determination of the paired regularity describing the dynamics of wear and tear of garbage trucks in the Khmelnytskyi region was carried out by the method of regression analysis [15]. Regressions were determined on the basis of linearizing transformations, which allow reducing the non-linear regularity to a linear one. The coefficients of the regression equations were determined by the method of least squares using the developed computer program "RegAnalyz", which is protected by a certificate of copyright registration for the work.

Results

In the table 1 the statistical data on the dynamics of wear and tear of garbage trucks in the Khmelnytskyi region in 2015-2020 is shown [3, 4].

Table 1

Statistical data for 2015-2020 on the dynamics of wear and tear of garbage trucks in the Khmelnytskyi region [3, 4]

Year	2015	2017	2018	2019	2020
Wear and tear of garbage trucks in the Khmelnytskyi region, %	63	61,52	60,29	60,2	59

Based on the data in the table 1, it was planned to obtain a mathematical model in the form of a pairwise regression regularity of wear and tear of garbage trucks in the Khmelnytskyi region. Since the argument of the regression regularity is the year, the order of values of which is three orders of magnitude greater than the order of the width of the range of its change, in order to increase the accuracy of the regression regularity, it is proposed to take the year preceding the beginning of the studied range ($x = t - 2014$) as the origin of the coordinates.

The results of the regression analysis are shown in the table 2 where the cells with the type of regression with the maximum value of the correlation coefficient R are marked in gray.

Table 2

The results of the regression analysis of the dynamics of wear and tear of garbage trucks in the Khmelnytskyi region

№	Type of regression	Correlation coefficient R	№	Type of regression	Correlation coefficient R
1	$y = a + bx$	0,98609	9	$y = ax^b$	0,95645
2	$y = 1 / (a + bx)$	0,98541	10	$y = a + b \cdot \lg x$	0,95914
3	$y = a + b / x$	0,89699	11	$y = a + b \cdot \ln x$	0,95914
4	$y = x / (a + bx)$	0,97975	12	$y = a / (b + x)$	0,98541
5	$y = ab^x$	0,98581	13	$y = ax / (b + x)$	0,88818
6	$y = ae^{bx}$	0,98581	14	$y = ae^{b / x}$	0,89263
7	$y = a \cdot 10^{bx}$	0,98581	15	$y = a \cdot 10^{b / x}$	0,89263
8	$y = 1 / (a + be^{-x})$	0,85706	16	$y = a + bx^n$	0,98620

So, according to the results of the regression analysis based on the data in the table 1, the following regression model was finally accepted as the most adequate

$$W_{GKhm} = 63,89 - 0,8874\left(t - 2014\right)^{0,9396} \text{ [\%]},$$

where W_{GKhm} – wear and tear of garbage trucks in the Khmelnytskyi region, %; t – year.

Fig. 1 shows a graphical dependence describing the dynamics of wear and tear of garbage trucks in the Khmelnytskyi region, it was built using the regression equation (1), which confirms the previously determined sufficient convergence of the obtained theoretical dependence compared to the data given in the works [3, 4].

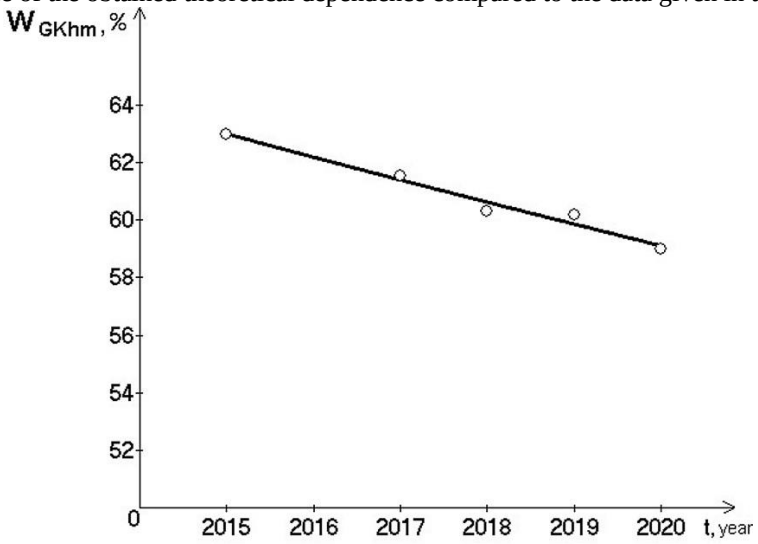

Fig. 1. The dependence describing the actual (○) and theoretical (—) dynamics of wear and tear of garbage trucks in the Khmelnytskyi region in 2015-2020.

The analysis of the graphic dependence in fig. 1 showed that the wear and tear of garbage trucks in the Khmelnytskyi region in 2015-2020 decreased exponentially.

Using pattern (1), it is possible to forecast that by 2030, the wear and tear of garbage trucks in the Khmelnytskyi region will decrease to 51.9% at the current rate of decline.

Determining the influence of factors on the dynamics of wear and tear of garbage trucks in the Khmelnytskyi region requires further research.

Conclusions

A regression regularity has been determined that describes the dynamics of the wear and tear of garbage trucks in the Khmelnytskyi region and allows it to be forecasted and planned for the infrastructure of municipal enterprises (warehouse and renewal of garbage trucks, production base for maintenance and repair), which is necessary to solve the problem of municipal solid waste management. A graphical dependence was built that describes the dynamics of wear and tear of garbage trucks in the Khmelnytskyi region and allows to visually illustrate this dynamic, to show a sufficient convergence of theoretical and actual results. It was established that the wear and tear of garbage trucks in the Khmelnytskyi region in 2015-2020 decreased according to a power law. It is foreseen that by 2030, the wear and tear of garbage trucks in the Khmelnytskyi region will decrease to 51.9% at the current rate of decline. Therefore, determining the influence of factors on the dynamics of wear and tear of garbage trucks in Khmelnytskyi region requires further research.

Reference

1. Kutsova V.Z., Kindrachuk M.V., Kovzel M.A., Tisov O.V., Grebeneva A.V., Shvets P.Yu. (2016) Vplyv struktury, fazovogo skladu ta vlastyvostej na abrazyvnu znosostijkist' hromomargancevyh chavuniv u lytomu stani [The impact of the structure, phase structure and power on the abrasive wear resistance of chromium-manganese chavuns at the cast steel]. Problem of Friction and Wear, 2, 78-85.

2. Dykha O.V .(2018) Rozrahunkovo-eksperymental'ni metody keruvannja procesamy granychnogo zmashhuvannja tehnichnyh trybosystem [Computational and experimental methods of controlling processes of boundary lubrication of technical tribosystems]: monograph. Khmelnytskyi: KhNU.

3. Ministry of Regions. (2016) Stan sfery povodzhennja z pobutovymy vidhodamy v Ukrai'ni za 2015 rik [State of the field of household waste management in Ukraine in 2015]. URL: https://www.minregion.gov.ua/wp-content/uploads/2016/04/Zbortpv4-oblasti1.pdf

4. Ministry of Regions. (2021) Stan sfery povodzhennja z pobutovymy vidhodamy v Ukrai'ni za 2020 rik [State of the field of household waste management in Ukraine in 2020]. URL: https://www.minregion.gov.ua/wp-content/uploads/2021/06/rozdil-4-2020_oblasti.pdf

5. Cabinet of Ministers of Ukraine(2004). Postanova № 265 “Pro zatverdzhennja Programy povodzhennja z tverdymy pobutovymy vidhodamy” [Resolution No. 265 "On Approval of the Solid Household Waste Management Program"] . URL: http://zakon1.rada.gov.ua/laws/show/265-2004-%D0%BF

6. Tsymbal B.M.(2017) Pidvyshhennja znosostijkosti shnekovyh ekstruderiv dlja vyrobnyctva palyvnyh bryketiv u kyslotnyh ta luzhnyh seredovyshhah [Increasing the wear resistance of screw extruders for the production of fuel briquettes in acidic and alkaline environments]: abstract dis. … cand. tech. sciences: 05.02.04 – Friction and wear in machines, Kharkiv, 20.

7. Shemshura E.A., Altunina M.S.(2014) Issledovanija nadezhnosti musorovoza kak slozhnoj tehnicheskoj sistemy [Research on the reliability of a garbage truck as a complex technical system]: collection of scientific works SWorld, 4(37), 2, 28-35.

8. Bereziuk O.V.(2021) Naukovo-tehnichni osnovy proektuvannja pryvodiv robochyh organiv mashyn dlja zbyrannja ta pervynnoi' pererobky tverdyh pobutovyh vidhodiv [Scientific and technical grounds of designing drives of working bodies of machines for collection and primary processing of solid household waste]: abstract dis. … doct. tech. sciences: 05.02.02 – Science of Machines, Khmelnytskyi, 44.

9. Altunina M.S. (2015) Sovershenstvovanie sistemy tehnicheskogo obsluzhivanija i remonta kuzovnyh musorovozov [Improving the system of maintenance and repair of body garbage trucks]: abstract dis. … cand. tech. sciences: 05.05.04 – Road, construction and lifting machines, Novocherkassk, 145.

10. Maltsev D.V. (2016) Sovershenstvovanie organizacii perevozochnogo processa tverdyh bytovyh othodov avtomobil'nym transportom [Improving the organization of the transportation process of solid household waste by road]: abstract dis. … cand. tech. sciences: 05.22.10 – Operation of road transport, Orel, 175.

11. Shlyakhovoi V.(2017) Vernym putem idete, musorovozy. Telematika v musorovozah. Osnovnye sredstva [You're on the right track, garbage trucks. Telematics in garbage trucks. Fixed assets], 1, URL: https://os1.ru/article/9607-telematika-v-musorovozah-vernym-putem-idete-musorovozy

12. Bereziuk O.V. (2015) Ogljad konstrukcij mashyn dlja zbyrannja ta pervynnoi' pererobky tverdyh pobutovyh vidhodiv [Review of designs of machines for collection and primary processing of solid household waste]. Herald of mechanical engineering and transport, 1, 3-8.

13. Bereziuk O.V. (2015) Struktura mashyn dlja zbyrannja ta pervynnoi' pererobky tverdyh pobutovyh vidhodiv [Structure of machines for collection and primary processing of solid household waste]. Herald of mechanical engineering and transport, 2, 3-7.

14. Belyaev M.S., Genson E.M. (2020) Opredelenie sootvetstvija fakticheskogo iznosa shin musorovozov normativnomu znacheniju [Determination of compliance of the actual tire wear of garbage trucks with the standard value.]. Chemistry. Ecology. Urbanistics, 2020, 30-33.

15. Chatterjee S., Hadi A.S. (2015) Regression analysis by example. John Wiley & Sons.

Березюк О.В., Савуляк В.І., Харжевський В.О. Динаміка зношеності сміттєвозів у Хмельницькій області.

Стаття присвячена визначенню закономірності, що описує динаміку зношеності сміттєвозів на регіональному рівні за прикладом Хмельницької області. Зношеність автопарку сміттєвозів комунальних підприємств Хмельниччини протягом 2015-2020 років зменшилась з 63 % до 59 %. За допомогою використання методу регресійного аналізу визначено адекватну степеневу закономірність, що описує динаміку зношеності сміттєвозів у регіоні в 2015-2020 рр. Для виконання дослідження використано метод регресійного аналізу результатів однофакторних експериментів та інших парних закономірностей шляхом вибору більш адекватного виду функції із 16 найпоширеніших варіантів за критерієм максимального коефіцієнта кореляції. Регресія проводилась на основі лінеаризувальних перетворень, які дозволяють звести нелінійну закономірність до лінійної. Побудовано графічну залежність, що описує динаміку зношеності сміттєвозів, підтверджено достатню збіжність отриманої закономірності. Зроблено прогноз, що до 2030 року зношеність сміттєвозів у Хмельницькій області, за існуючих темпів спадання, зменшиться до 51,9 %. Виявлено доцільність проведення подальших досліджень з визначення впливу факторів на динаміку зношеності сміттєвозів.

Ключові слова: динаміка, сміттєвоз, зношеність, тверді побутові відходи, регресійний аналіз.

Problems of Tribology, V. 27, No 3/105-2022,76-81

Problems of Tribology
Website: http://tribology.khnu.km.ua/index.php/ProbTrib
E-mail: tribosenator@gmail.com

DOI: https://doi.org/10.31891/2079-1372-2022-105-3-76-81

Influence of temperature on the dynamics of formation of granic sleeps and connected elevation dynamics in sliding conditions

N. Dmytrichenko, A. Savchuk, Y.Turytsia*, A. Milanenko, M.Kosenko

National Transport University, Kyiv, Ukraine
**E-mail:Yuliya_tur@ukr.net*

Received: 29 July 2022: Revised:31 August 2022: Accept:16 September 2022

Abstract

The running-in process is accompanied by a change in microgeometry, as a result of which some constant roughness is established, which is characteristic of given friction conditions, and the physical and mechanical properties of the surface layers also change, since plastic deformations usually predominate in the contact.

The thickness of the surface layers that have undergone changes during external friction depends on the stress state in the zones of their actual contact and heating during friction. The stress state in the zone of actual contact of the bodies is characterized by indentation or crushing of surface microroughnesses, as well as by elastic or plastic states of the latter. Surface heating during friction depends on the thermophysical properties of the contacting bodies and the friction mode. An increase in the temperature of the surface layers causes not only their softening, but also greatly increases the rate of physical and chemical processes in them. This leads to saturation of the surface layers with environmental gas molecules, oxidizing slicks, and also to an increase in the concentration of defects in these layers [1-5].

Key words: lubricating layer, wear, oil, temperature, adsorption layer, viscosity, friction coefficient

Introduction

We studied the lubricating properties of Mobil-1 0w-40 engine oil of a commercial batch and oil, the service life of which was 15 thousand km. As samples, a pair of slip block - roller was used. The sample material is 40X steel. The studies were carried out on the SMC-2 facility, in the start (3 s)–stop (3 s) mode. The cycles followed one after another, without interruption, the total number of cycles in the experiment was N=700. The studies were carried out at bulk temperatures of 20^0C and 120^0C at contact load max = 90 MPa.

In work efficiency of formation of boundary adsorption layers on contact surfaces at variable temperatures and their influence on wear resistance of elements of triboconjugation was investigated.

Lubrication properties of Mobil-1 0w-40 motor oil of commercial batch and oil with the service life of 15 thousand km were investigated. A pair of sliding pad - roller was used as samples. Material of samples - steel 40X. Researches were carried out on the SMC-2 unit, in the start (3 s) - stop (3 s) mode. Cycles followed one after another, without a break, all cycles in the experiment N = 700. Studies were carried out at volumetric temperatures of 20^0C and 120^0C at contact load max = 90 MPa.

The purpose of the work

In this paper, we studied the efficiency of formation of boundary adsorption layers on contact surfaces at variable temperatures and their influence on the wear resistance of triboconjugation elements.

Results of experimental studies

The study of load-carrying capacity of the presented samples of oils has established that in the process of start-up at rotational frequency n > 150 rpm, regardless of oil service life, conditions of hydrodynamic lubrication are realized in the contact at oil volume temperature 20^0C.

Let's follow the formation of non-hydrodynamic component of the lubricating layer thickness in the contact of commercial sample of Mobil-1 oil and the sample which operation period was 15 thousand kilometers at the temperature of 20^0C (Fig. 5.7). Firstly, irrespective of the type of grease, up to N<50 cycles of operating time in 100 % of cycles metal contact of elements of tribocouplings at standstill is observed (Fig. 1,a). With further operating time, due to the intensification of activation processes in the surface layers of the metal during their dynamic loading, their adsorption capacity increases, which leads to the formation of stable boundary layers on the contact surfaces.

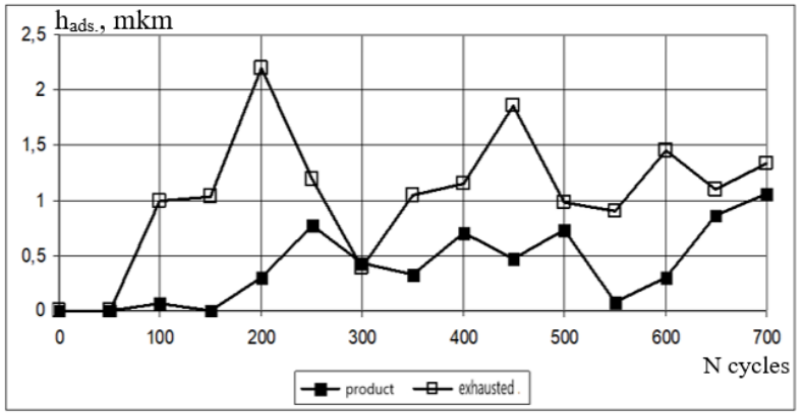

a)

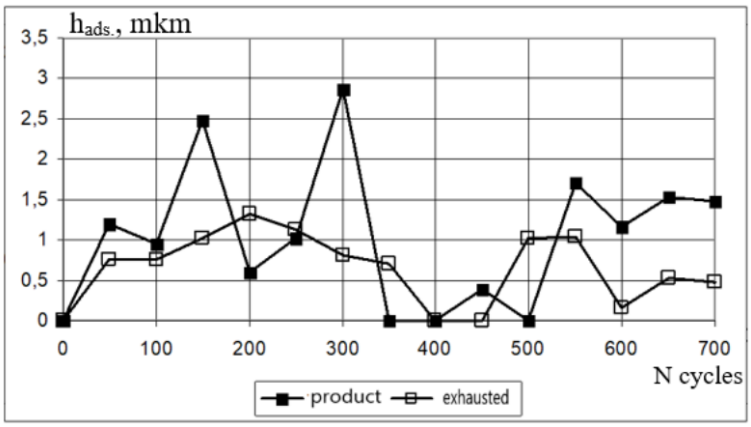

b)

Fig. 1. Dynamics of formation of boundary adsorption layers (had.) with Mobil-1 oil at 20^0C (a) and 120^0C (b) at operating time (N)

Secondly, if a stable boundary film of a lubricant when using a commercial sample of oil is formed at N > 150 cycles, the period of formation of adapted boundary layers for used oil is three times shorter, which is caused, in our opinion, by the accumulation of surface-active substances in the process of oil operation.

Thirdly, there is a clear tendency of increasing the adsorption activity of hydrocarbon components of the oil with the lifetime of 15 thousand km, which is manifested by an increase in the thickness of the boundary adsorption layers by 30-40 %, on the average, in contrast to the similar indicator established for the commercial sample oil. This phenomenon is also intensified by agglomeration of mechanical impurities accumulated during oil operation.

Approbation of the research results

Increasing the volumetric temperature of the oil up to 120^0C leads to significant changes in the efficiency of boundary layer formation by the researched oils.

Firstly, from the first running cycles no metallic contact of surfaces at stopping is observed - up to N < (300 - 400) cycles a stable boundary film is formed, regardless of the type of oil used, reliably separating the contacting surfaces.

Secondly, a period of long breakdown of the lubricating layer at stopping (for commercial and used oil the specified period is 350 < N < 500 and 400 < N < 450 operating cycles, respectively) for both studied oil samples, after which effective formation of limiting adsorb layers in contact Gradual erasure of boundary layers is restored, leading to metallic contact of the surfaces is caused, in our opinion, by high shear rate gradients of the oil layer, reaching $0.7\text{-}10^{-6}$ s^{-1} and $1.6\text{-}10^{-6}$ s^{-1} respectively for commercial and waste oil samples. Triple reduction in the recovery period of the efficiency of formation of limiting films by long-life oil is associated with a higher concentration of surface-active substances in it, characterized by increased adsorption activity.

Third, a greater thickness of the boundary adsorption layers in the contact is traced throughout the 80% cycles of the studies when commercial oil is used. We assume that in this case, the most important parameter influencing the dynamics of boundary layer formation is the viscosity of the lubricant.

According to [6], oil in the initial state is a multicomponent homogeneous system, and in the process of oil operation it transforms into a heterogeneous system containing colloidal and suspended particles of different origin.

Let's consider main physical and chemical properties of Mobil-100-40 oil and their change during operation at 15 thousand km of run (Tab.1).

Table 1

Basic physical and chemical characteristics of Mobil-1 0w-40 engine oil

	Kinematic viscosity $\upsilon_{100}{}^{0}C$	Flash point,^{0}C	Alkaline number, mg KOH/г	Acid number	Ash content	Coking	Active elements of the additive	
							Ca	Zn
Oil sample	13,64	216	10,04	Відсутн.	0,92	1,23	0,32	0,96
Used oil sample (15 thousand km)	14,32 (+5%)	192 (-12%)	6,18 (-39%)	2,38	1,06 (+13%)	2,92 (+68%)	0,32	0,95
Maximum permissible values of the parameter	± 20 – 25% from the commercial oil indicator	< 170	- 50% from the commercial oil indicator	> 2,0	-	> 2,0	-	-

According to the results presented, the commercial synthetic motor oil is characterized by a high quality margin of SAE viscosity class, alkali number, flash point and meets all the requirements for this operational type of oil.

During operation, the oil is aging, which leads to a change in its physical and chemical characteristics. One of the main insufficient parameters is viscosity, however by results of our researches the value of the given parameter is stable enough parameter. This fact contradicts the change of another parameter - flash temperature, which tends to decrease, indicating the presence of two oil aging processes: partial penetration of fuel into the lubricant or partial degradation of hydrocarbon components under the influence of high speed gradients in the contact, which leads to the formation of lighter and volatile compounds. The established contradictions are explained by accumulation of mechanical impurities of organic and inorganic origin in the oil during operation, which are in the dispersed state, which is provided by effective properties of detergent-dispersing additive. The growth of mechanical impurities of organic origin, which indicates chemical transformations of the oil base, causes a significant increase in the acid number and degree of coking of the lubricant; the presence of mechanical impurities of inorganic origin is evidenced by increased ash content and stability of additive active elements (Ca and Zn), despite its intensive actuation, which is explained by effective dispersion of mechanical impurities constantly circulating in the lubricant, with their dilution, and the fact that their dispersion of mechanical impurities in the lubricant is not limited to the operating condition.

Consequently, the accumulation of a significant portion of mechanical impurities in the engine oil leads to significant changes in its initial physical state, which manifests itself in the transformation of a homogeneous multicomponent liquid of commercial oil into a colloidal heterogeneous solution of waste oil. This process causes stabilization of engine oil viscosity during operation, despite the fact

that viscous additive is subject to temperature and mechanical degradation, fuel ingress dilutes oil, formation of light fractions during high-temperature cracking reduces the initial oil viscosity.

Thus, the absolute value of kinematic viscosity of commercial and waste oil does not reflect the change in the physical state of the lubricant, which must be taken into account when analyzing the kinetics of formation of the lubricating layer in the contact.

We assume that the established phenomenon of increase of efficiency of formation of boundary layers in contact in the conditions of increase of volume temperature of the oil at use of a commodity sample Mobil-1 0w-40 reveals potential possibilities both of base components of oil, and polyfunctional components of additives on increase of degree of adsorption. processes on elements of the tribocoupling Application of the used oil in these conditions also provides formation of stable boundary layer, but the basic role in this process belongs According to the work of Wenzel S.V. [7], highly dispersed mechanical impurities, adsorbed on friction surfaces, show effective antifriction and antiwear properties. We found that at the moment of friction coefficient stabilization, corresponding to operating time N > 500 cycles, this parameter for the used oil is 15% lower than the friction coefficient recorded when lubricating with commercial oil (Fig. 2).

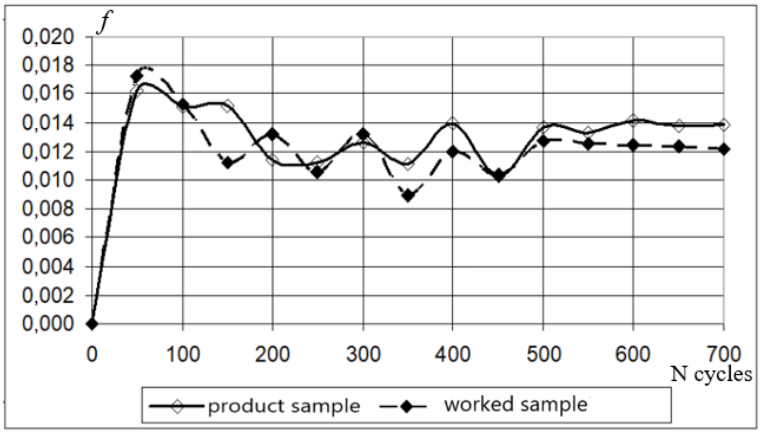

Fig. 2. Kinetics of friction coefficient change at operating time for commercial and used Mobil-1 0w-40 oil at 120^{0}C lubricant volumetric temperature

Note that at 20^{0}C volumetric oil temperature no increase in antifriction properties has been found with used oil (f for used oil is 40% higher than f established in contact with commercial oil lubrication), which is probably due to increased shear stresses in highly dispersed mechanical impurities due to increased thickness of adsorption layers by 30 - 40%, compared to commercial oil (fig. 3).

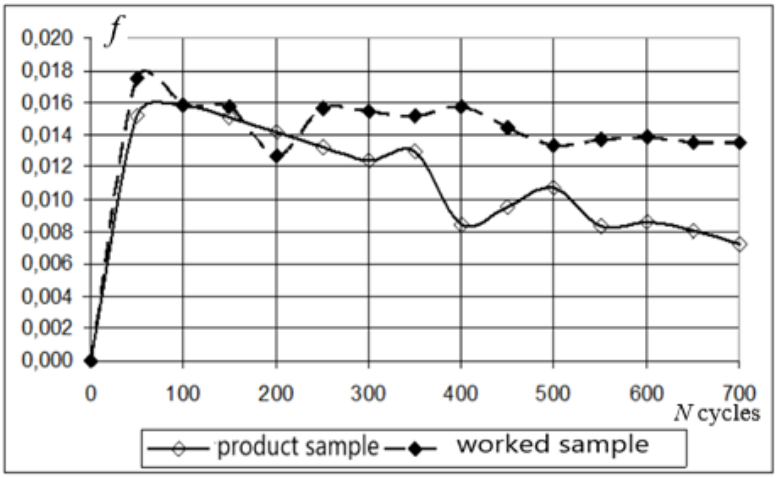

Fig. 3. Dependence of friction coefficient on working life at volumetric temperature of oils 20^{0}C

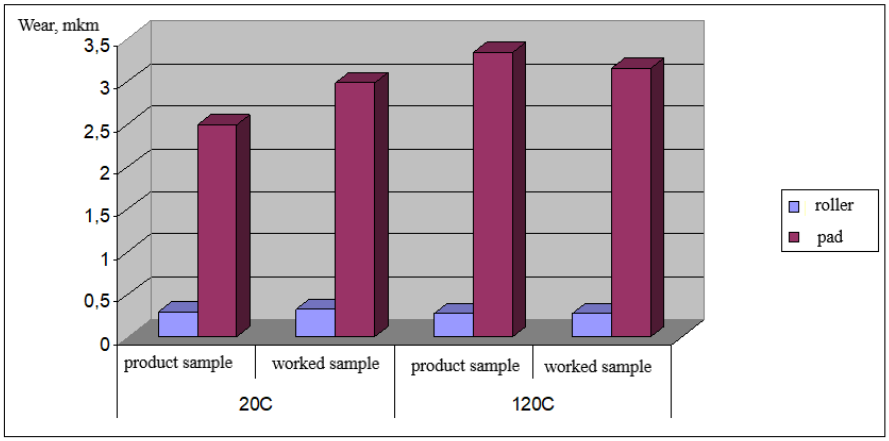

Fig. 4. Linear wear of the Cane friction surfaces (roller - shoe) at 700 operating cycles at volume temperatures of the lubricant 20^0C and 120^0C

The analysis of antiwear properties of oils showed that at 120^0C linear wear of steel 40X is on 5 % lower at use of used oil, and at 20^0C this parameter on 15 % exceeds indicators of wear, established at use of a commercial oil (fig. 4).

Conclusions

Consequently, increase of temperature causes growth of wear at use of commodity sample of Mobil-1 0w-40 oil due to oil "running-in", as a result of which colloid mechanical impurities and oxidation products which lead to stabilization of wear intensity are accumulated in it due to increase of additives activity and oxidation-polymerization processes. At 20^0C the intensity of the given activation processes probably essentially decreases that provides increase of wear resistance of contact surfaces, unlike at lubrication of elements of tribocoupling by the used oil containing the raised concentration of products of oxidation and colloidal mechanical impurity which form low-temperature deposits. intensifying their wear.

References

1.Fuels, lubricants, technical liquids. Assortment and application: Reference ed. / K.M. Badyshova, Ya.A. Bershtadt, M.K. Bogdanov and others - M .: Chemistry, 1989. - 432 p.

2.Technological bases for ensuring the quality of machines / ed. K.S. Kolesnikova - M .: Mashinostroenie, 1990. - 256 p.

3. L.V. Makarova, N.K. Myshkin, V.M. Makarenko, M.S. Semenyuk and others “Integral detector for monitoring the state of the lubricant of tribocouples” Friction and wear, Gomel, volume 29 No. 4, pp.29 -43.

4. Kanarchuk E.A., Kanarchuk V.E. Influence of operating modes on the wear of internal combustion engines. Kyiv, "Naukova Dumka", 1970, 312p.

5. Fundamentals of tribology (wear, friction, lubrication) / under. ed. A.V. Chichinadze. – M.: Mashinostroenie, 2001. – 663 p.

6. Wenzel S.V. The use of lubricating oils in internal combustion engines, 1979, M, 240p.

7. Wenzel E.S. Improving the operational properties of oils and fuels: monograph. - Kharkov, KHNADU, 2010. - 224p.

Дмитриченко М.Ф., Савчук А.М., Туриця Ю.О., Міланенко О.А., Косенко М.І. Вплив температури на динаміку формування граничних плівок та знос контактних поверхонь в умовах ковзання.

В роботі досліджувалась ефективність формування граничних адсорбційних шарів на контактних поверхнях при змінних температурах та їх вплив на зносостійкість елементів трибоспряження.

Дослідження несучої здатності представлених зразків олив встановило, що в процесі пуску, при частоті обертання n > 150 об/хв., незалежно від терміну експлуатації оливи, в контакті реалізуються умови гідродинамічного мащення при об'ємній температурі оливи 20^0C.

Встановлено, що накопичення значної частини механічних домішок в моторній оливі призводить до суттєвих змін її початкового фізичного стану, що проявляється в перетворенні гомогенної багатокомпонентної рідини товарної оливи в колоїдний гетерогенний розчин відпрацьованої оливи. Даний процес обумовлює стабілізацію в'язкості моторної оливи при експлуатації, незважаючи на те, що в'язкістна присадка схильна до температурної та механічної деструкції, попадання палива розріджує оливу, утворення легких фракцій при високотемпературному крекінгу знижує початкову в'язкість оливи. Абсолютне значення кінематичної в'язкості товарної та відпрацьованої оливи не відображує зміну фізичного стану мастильного матеріалу, що необхідно враховувати при аналізі кінетики формування мастильного шару в контакті.

Аналіз протизношувальних властивостей олив показав, що при 120^0C лінійний знос сталі 40Х на 5% нижче при застосування відпрацьованої оливи, а при 20^0C даний параметр на 15% перевищує показники зносу, встановлені при використанні товарної оливи.

Підвищення температури обумовлює зростання зносу при використанні товарного зразка оливи Mobil-1 0w-40 за рахунок „припрацьовування" оливи, в результаті чого, внаслідок підвищення активності присадок та окислювально-полімеризаційних процесів, в ній накопичуються колоїдні механічні домішки та продукти окислення, які призводять до стабілізації інтенсивності зношування. При 20^0C, імовірно, інтенсивність даних активаційних процесів суттєво знижується, що забезпечує підвищення зносостійкості контактних поверхонь, на відміну при змащуванні елементів трибоспряження відпрацьованою оливою, яка містить підвищену концентрацію продуктів окислення та колоїдних механічних домішок, які утворюють низькотемпературні відкладення та спричинюють абразивну дію на контактні поверхні, інтенсифікуючи їх знос.

Ключові слова: мастильний шар, знос, масло, температура, поглинаючий шар, в'язкість, чутливість

***Problems of Tribology**, V. 27, No 3/105-2022, 82-88*

Problems of Tribology
Website: http://tribology.khnu.km.ua/index.php/ProbTrib
E-mail: tribosenator@gmail.com

DOI: https://doi.org/10.31891/2079-1372-2022-105-3-82-88

Study of the Stress-Strain State of the Surface Layer During the Strengthening Treatment of Parts

D.D. Marchenko*, K.S. Matvyeyeva

**Mykolayiv National Agrarian University, Mykolayiv, Ukraine*
E-mail: marchenkodd@mnau.edu.ua

Received: 20 July 2022: Revised: 05 August 2022: Accept:16 September 2022

Abstract

The paper presents experimental studies and obtained statistical models of the influence of processing modes on the quality of the surface layer and cyclic durability of reinforced machine parts. It was established that the main influence on the strengthening effect, the depletion of the plasticity reserve of the metal and the formation of residual stresses are exerted by the effective gap of the cutter, the effective tension and the profile radius of the roller. The results showed that dimensional combined running-in ensures high cyclic durability of strengthened parts under conditions of multi-cycle fatigue load, which reaches 8 million cycles, which is 3.5 times greater than the durability of a non-reinforced part and 1.5 times - the durability of a part strengthened by surface plastic deformation Studies have shown that the greatest cyclic durability of the part is ensured at the minimum values of the effective cutter gap, the maximum values of the profile radius and the value of the effective roller tension of 0.6 mm, which corresponds to the degree of exhaustion of the plasticity reserve by processing with dimensional compatible rolling $\Psi \approx 0.65$. On the basis of the results of theoretical and experimental studies, a methodology and algorithm for the design of processing technology by dimensional combined running-in were developed. A computer program has been developed that allows you to calculate the quality of the surface layer and cyclic durability of the part based on the specified modes, as well as to assign rational processing modes that ensure the specified quality of the surface layer and cyclic durability. Based on the results of research, a technological process of strengthening processing of machine parts by combined dimensional running-in has been developed, which allows forming compressive residual stresses in the surface layer of the processed part, as well as increasing productivity up to 2 times while maintaining or improving the specified quality parameters of the surface layer of the processed part.

Key words: dimensional compatible running-in, stress-strain state, strengthening treatment, surface plastic deformation, residual stresses

Introduction

The urgent task of modern mechanical engineering is to ensure the durability of machine parts, which is largely determined by the quality of the surface layer (SL). The surface layer is formed during the entire technological process, while the phenomenon of technological inheritance (TI) plays an important role.

Improving the quality of the surface layer is possible on the basis of improving the methods of strengthening treatment, as well as identifying the regularities of the TS and their influence on the operational durability of the part, including under the conditions of the application of fatigue loads.

One of the ways to improve the quality of machine parts is the application of technological processes based on combined methods of surface plastic deformation (SPD), including the method of dimensional simultaneous running-in (DSR). The peculiarity of DSR is the original scheme of operation of cutting and deforming tools, according to which, the cutter cuts the plastic wave of metal that occurs in front of the deforming rollers.

This method ensures high accuracy of machine parts, parameters of roughness and strengthening of the surface layer when processing a wide range of important parts, such as rods, shafts, axles, etc., made of reinforcing structural materials and operating under conditions of application of cyclically alternating loads.

In relation to such processes of strengthening treatment, the development of an analytical apparatus is relevant, which allows to calculate the operational durability based on taking into account the entire complex of inherited properties of the surface layer, since the appearance of new materials and the complication of machine operating conditions require a reduction in the terms of structural and technological preparation of the organization by reducing experimental work [1].

Solving this problem is possible on the basis of the disclosure of the consequent physical regularities, both the formation of the state on top of the next layer during processing by dimensional combined rolling, and the transformation of this state during operational fatigue loading of the part. For the study of such regularities, the apparatus of the mechanics of technological inheritance is adapted, based on the accounting of the continuous accumulation of deformations, the exhaustion of the reserve of plasticity and the formation of residual stresses by the metal of the surface layer at the stages of the life cycle (LC) of machine parts, including at the stage of operational fatigue load. The application of the TI mechanics apparatus allows to describe in uniform terms and categories the physical nature of the behavior of metal at the stages of metallurgy and to bring the results of research into a form convenient for engineering use.

Thus, the wide possibilities of the method in terms of ensuring quality and accuracy, on the one hand, and the lack of technological recommendations for ensuring the cyclic durability of strengthened critical parts, on the other hand, restrain the wide application of DSR in industry.

Taking into account the growing requirements for quality and the need to ensure the durability of parts during operation, this work, aimed at the development of analytical apparatus and methods of designing technological processes of strengthening treatment, is relevant.

Literature review

The works of P.G. Alekseeva, M.A. Balter, Y.M. Baratsa, V.F. Bezyazichny, V.M. Braslavskyi, M.S. Drozda, M.M. Zhasimova, S.A. Zaides, A.V. Kyrycheka, E.H. Konovalova, I.V. Kudryavtseva, A.G. Lazutkina, E.M. Verkhivka, L.I. Markus, L.G. Odintsova, D.D. Papsheva, V.V. Petrosova, V.N. Poduraeva, Yu.G. Proskuryakova, O.A. Rosenberga, E.V. Ryzhova, V.M. Smilyanskyi, A.H. Suslova, L.A. Khvorostukhina, P.A. Chepy, P.S. Chistoserdova, L.M. Shkolyara, Yu.G. Schneider, D.L. Yudina, P.I. Lizard and others [2].

One of the effective methods of combined SPD is dimensional run-in, the technological capabilities of which are explored in the works of V.M. Smilyanskyi, V.Yu. Blumenstein, V.A. Vasylieva, V.B. Ignatov and T. Niklevich [3].

The DSR method is quite well studied in terms of ensuring the accuracy and quality of the surface layer. In particular, it was established that it allows to provide within wide limits such quality parameters as roughness (Ra = 0.04...0.8 μm), depth (h = 0.5...15 mm) and degree (δ = 0.2...0.8) strengthening when creating favorable compressive stress patterns.

However, at the same time, the possibilities of dimensionally compatible running-in to ensure the cyclic durability of parts remain unestablished. These capabilities are especially relevant for a wide range of parts operating under fatigue load conditions.

To solve this problem, an analysis of methods for ensuring the quality and durability of strengthened machine parts, features of the formation of final stresses during strengthening processing, as well as an analysis of approaches to accounting for the phenomenon of technological inheritance, outlined in the works of V.I. Averchenkova, I.A. Birgera, V.Yu. Blumenstein, A.S. Vasylieva, A.M. Dalsky, A.I. Kondakva, I.V. Kudryavtseva, A. A. Matalin, A.N. Ovsienko, A.V. Podzeya, E.V. Ryzhova, V.M. Smilyanskyi, A.H. Suslov The formulation of the scientific task of developing a methodology for the design of technological processes of strengthening processing by the RSO method, ensuring the cyclic durability of machine parts and taking into account the appearance of technological inheritance, has been completed [4].

It was established that the apparatus of the mechanics of technological inheritance, developed by V.Yu. Blumenstein, is adapted for solving such a task in the framework of which the formation and transformation of the state of the surface layer at the stages of mechanical processing and subsequent operational fatigue load are considered as a single continuous process of accumulation of deformation and exhaustion of the reserve of plasticity of the metal of the surface layer.

Along with traditional quality parameters, the used apparatus of the mechanics of technological inheritance allows for a thorough description of the regularities of the formation and transformation of the properties of the surface layer at the stages of mechanical processing and subsequent operational fatigue loading in the categories of integral parameters that are uniform for all stress stages: the degree of shear deformation Λ, the degree of depletion plasticity reserve Ψ and residual stress tensor [$T\sigma_{ост}$]. The device allows you to take into account the influence of the accumulated properties of the surface layer on the cyclic durability of the part; at the same time, the latter is understood as the number of load cycles until the plasticity reserve of the metal of the surface layer is completely exhausted and the appearance of a fatigue crack. To calculate the degree of depletion of the plasticity reserve Ψ, the Kalpin-Filippov criterion is used, which takes into account the partial "healing" of the metal defect and the restoration of the plasticity reserve in the zone of change in the sign of deformation [5].

The analysis showed that the use of the apparatus of the mechanics of technological imitation allows to establish the physical regularities of the formation of the surface layer, the processes that occur during the

processing of DSR in the deformed hearth, as well as the regularities of the influence of these processes on the cyclic durability of the part.

Purpose

The purpose of the research is to increase the durability of machine parts strengthened by dimensionally combined running-in based on taking into account the inherited properties of the surface layer.

Research methodology

In order to assess and manage the state of the surface layer in order to ensure the specified cyclic durability of DSR-treated machine parts, the apparatus of the mechanics of technological inheritance was adopted, according to which:

- during the processing of DSR, there is an accumulation of deformations and the exhaustion of the reserve of plasticity, which leads to the formation of a surface layer with defined quality parameters: depth and degree of strengthening, roughness and residual stresses;
- in the process of further operational fatigue loading, the process of accumulation of deformations, depletion of the plasticity reserve and relaxation of residual stresses continues, which leads to a continuous transformation of the loaded state and a change in the degree of strengthening of the surface layer;
- when the limit deformations accumulate to the level of Λp, the plasticity reserve is completely exhausted (Ψ = 1). This state corresponds to complete relaxation of residual stresses ($[T\sigma_{ост}] = 0$) and the appearance of an initial fatigue crack.

In order to structure, systematize and further solve the given problem, a structural-analytical model of the formation of the parameters of the mechanical state of the metal of the surface layer of the part at the stage of dimensional combined running-in was developed, taking into account the phenomenon of technological imitation in the context of ensuring the necessary cyclic durability [6].

The model, built on the basis of CALS - technologies, is based on the idea of the considered process as an information system. The function "Manage the parameters of the mechanical state of the surface layer of the metal at the DSR stage in order to ensure the given cyclic durability of the part" was selected as a high-ranking function. The decomposition of the context diagram made it possible to identify the main parameters for the purpose of controlling the mechanical state of the surface layer and to describe them by a system of kinetic equations.

Research results

The method of dimensional combined running-in is based on plastic wave formation; at the same time, the processing is carried out by two or three rollers, rigidly adjusted to a certain size of the processing of the part. The principle is the presence of a cutter in the zone of wave formation, which partially or completely removes the plastic wave. The tensions of the deforming rollers significantly exceed those adopted for SPD and reach values of 1 mm, however, the destruction of the surface does not occur due to the removal of part of the metal by the cutter in the area of the top of the plastic wave.

When solving the problem of mechanics of cyclic durability, it was accepted:

1. During operation, the part is subjected to multi-cycle fatigue symmetrically changing stress with a scheme of cantilever bending with rotation, fatigue (operational) and residual stress tensors are specified in the Cartesian coordinate system, while the numerical values of the residual stress components decrease in proportion to the number of cycles in accordance with the selected by the law of relaxation.

2. Accumulation of limit deformations, complete exhaustion of the reserve of plasticity and nucleation of a fatigue crack occurs at some point of probable destruction, which can be located both on the surface and at some distance from it; at the same time, there is no point drift in the process of fatigue loading.

3. The end of the stage of cyclic durability corresponds to a certain limiting degree of hardening and hardness (microhardness) of the surface layer at the point of probable destruction, characteristic of the given material, processing modes and load conditions.

Experimental studies were carried out on a 1K62B lathe and screw-cutting machine, equipped with an installation for RSO, as well as on a model 16K20F3 lathe, equipped with a special installation for processing RSO of fatigue samples. The ranges of variation of the processing mode parameters were: feed (S) - 0.07...0.7 mm/rev, part rotation frequency (n) - 100...1200 rpm, profile radius of the roller (R_{pr}) - 2...15 mm , estimated roller tension (h_p) - 0.1...1 mm, actual gap (a_d) - 0...0.2 mm, actual tension (h_d) - 0.05...0.9 mm [7].

The actual geometric parameters of the deformation center were determined by profilography and further processing of the obtained profilograms. To increase efficiency and automate calculations, an algorithm and a program for processing OD profilograms were developed. Their task is to translate the graphic image of the profilogram into the numerical values of the points that make up the OD contour.

Experimental samples were made from steel 45 of one delivery. In order to localize the fatigue crack initiation point, the working surface was made in the form of a combination of a cylindrical part and a fillet. The working part of the fatigue samples, which has a diameter of 15 mm, was subjected to DSR processing on a 16K20F3 machine with different modes. For each series, a sample was made - a witness, on which fixation of the center of deformation was carried out [8]. Based on the obtained deformation rates, the actual parameters of the processing mode, as well as the parameters of the mechanical state of the surface layer, were calculated.

The cyclic durability of the samples was determined on the basis of the proposed calculation-analytical model and fixation of the change in the microhardness of the surface layer during cyclic loading. The distribution of microhardness along the depth of the surface layer was determined in the dangerous section of the samples after stressing with a fixed number of cycles, while the witness samples made it possible to determine the initial distribution of microhardness before fatigue stress [9].

The relationship revealed as a result of experimental and analytical research explains more than 90% of the entire dispersion of experimental data, the relative error of determination does not exceed 15%.

The analysis showed that the actual incisor clearance has the predominant influence on the deformation parameters (Fig. 1, a, b). With a relatively small increase in it, Λ and Ψ grow significantly, since in this case a more deformed metal forms the machined surface.

A significant influence on the parameters of the mechanical condition is also exerted by the profile radius R_{pr} and the effective tension of the roller h_d. It was found that Λ and Ψ when changing R_{pr} have extrema, the position of which is determined by the value of the effective gap (Fig. 1, a). When the effective tension increases, the values of the deformation parameters continuously increase (Fig. 1, b).

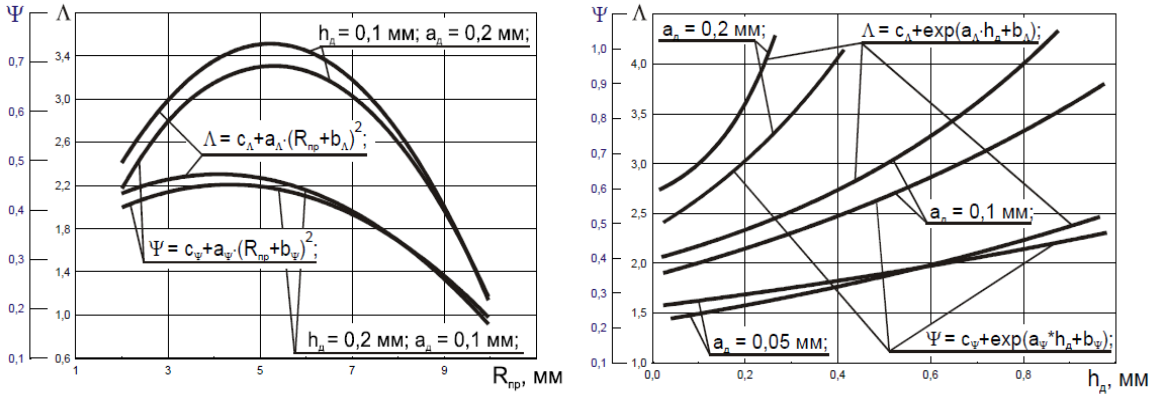

a **b**

Fig. 1. Interrelationships of the accumulated parameters of the mechanical state: a - with profile radius of the roller; b - with real tension

In order to identify the relationships between the residual stresses and the parameters of the mode, a description of the graphs of the OH components in the categories of the coordinates of the characteristic points was carried out. As an example, graphical dependencies for the axial component of residual stresses are considered below (Fig. 2, a, b). It was established that the largest axial compressive stresses on the surface are observed at significant actual tension of about 0.25 mm [10, 11]. Their further decrease with increasing tension is caused by significantly increasing thermal discharge, while the axial compressive stresses in the first extremum continue to increase (Fig. 2, a).

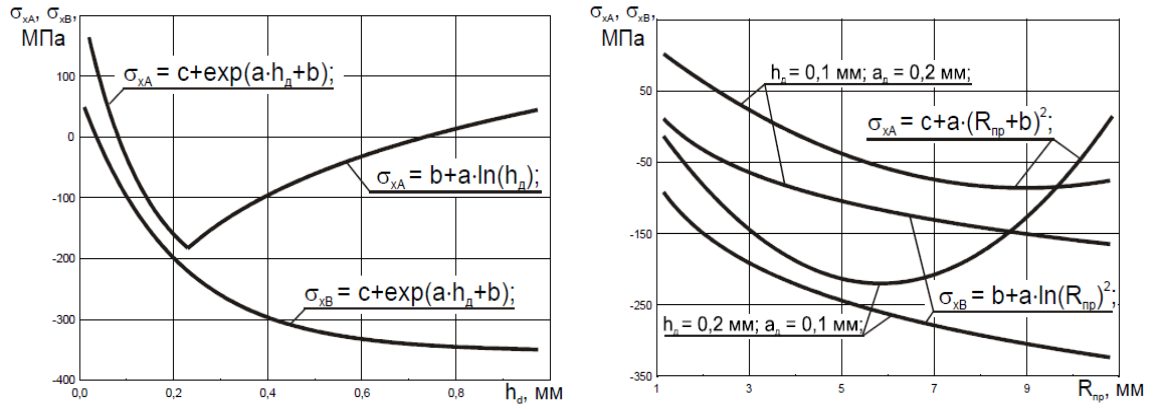

a **b**

Fig. 2. Interrelationships of axial residual stresses on surface and in the first extremum: a - with real tension; b - with the profile radius of the roller

It was established that for each value of the effective tension, there is a value of the profile radius of the roller at which the compressive stresses on the surface of the part are maximum (Fig. 2, b). The maximum values of the axial compressive stresses at the point of the first extremum increase with the increase of both factors and reach values of 400 MPa [12]. The growth of these factors also increases the actual depth of the location of the extremum from the surface of the part. At the maximum values of the effective tension and profile radius of the roller, it reaches values of 6-8 mm.

The conducted experimental studies made it possible to reveal the relationships between the cyclic durability of N_{CD} and the depth of fatigue crack initiation htr with the parameters of the mechanical state of the PS metal and technological factors in the processing of DSR. It was established that the main parameters of the DSR regime have a hereditary influence on the degree of shear deformation accumulated at the stage of cyclic durability $\Delta\Lambda_{ЦД}$, the largest value of which is observed at $h_д$ = 0.6 mm. As the effective gap increases, the value of $\Delta\Lambda_{ЦД}$ decreases, which is caused by a significant increase in the degree of shear deformation accumulated during DSR.

An increase in the effective gap leads to a decrease in the fatigue crack nucleation depth and the exit of the probable fracture point to the surface [13]. This corresponds to the well-known idea that with a further increase in a, there is an accumulation of limit deformations and destruction of the metal surface at the top of the plastic wave already during mechanical processing. An increase in $R_{пр}$ leads to an increase in the crack nucleation depth, while the highest value of $h_{тр}$ is observed at h = 0.6 mm. When $\Delta\Lambda_{ЦД}$ increases, the crack initiation depth increases.

The analysis showed that the maximum cyclic durability was obtained in such modes of DSR, when residual stresses, depth and degree of strengthening did not reach their maximum values.

Conclusions

For the practical use and implementation of the results obtained in the work, an algorithm for calculating the parameters of DSR processing has been developed, which allows:

1. Determine the quality parameters, integral parameters of the mechanical state (Λ, Ψ, $[T\sigma_{ост}]$) and cyclic durability of the part, taking into account the phenomenon of technological inheritance, based on the given value of the mode parameters.

2. According to the given value of the parameters of the quality and durability of the part under conditions of application of fatigue loads, determine the optimal processing modes.

The program "Calculation of the inherited parameters of the dimensional combined running-in process" is intended for the automated calculation of the accumulation of deformation, the exhaustion of the plasticity reserve and the residual stress tensor and the appointment of rational processing modes that provide the best surface properties. It allows you to calculate DSR parameters in three ways:

The 1st method is practical: calculation based on the experimentally obtained geometric profile of the deformation center, which can be obtained with the help of the program "Processing of profilograms of deformation foci during dimensionally shifted rolling and surface plastic deformation".

The 2nd method is analytical: the starting points are the technological parameters set on the machine during the processing of the part by the DSR method.

The 3rd method is inverse analytical: the initial data are the values of the parameters of the quality of the surface layer, which must be obtained during the processing of DSR, as well as the values of technological factors acting as limitations.

Structural and calculation-analytical models were developed and the physical regularities of the formation of the quality of the surface layer were revealed, taking into account the phenomenon of technological inheritance. It has been found that compared to traditional surface plastic deformation, dimensionally coupled rolling provides higher quality and allows to accumulate more deformation without destroying the surface layer.

An analytical model of the formation of residual stresses has been developed, which is presented in the form of a tensor, which is the sum of the tensor of elastic-plastic stresses, as well as the tensors of elastic and thermal unloading stresses. The nature of the distribution of residual stress components along the depth of the surface layer has been established. The calculations showed that the axial component of the residual stresses, which reaches 400 MPa and the depth of spread of compressive stresses up to 10 mm, is characterized by the greatest stress values.

References

1. Archard J.F. Contact and rubbing of flat surfaces. J Appl Phys 1953; 24: 981–988.

2. Lai F.Q., Qu S.G., Yin L.M., et al. Design and operation of a new multifunctional wear apparatus for engine valve train components. Proc IMechE, Part J: J Engineering Tribology 2018; 232: 259–276.

3. Lewis R., Dwyer-Joyce R.S. Wear of diesel engine inlet valves and seat inserts. Proc IMechE, Part D: J Automobile Engineering 2002; 216: 205–216.

4. Worthen R.P., Rauen D.G. Measurement of valve temperatures and strain in a firing engine. SAE paper 860356, 1986.

5. Forsberg P., Debord D., Jacobson S. Quantification of combustion valve sealing interface sliding – a novel experimental technique and simulations. Tri Int 2014; 69: 150–155.

6. Mascarenhas L.B., Gomes J.D., Beal V.E., et al. Design and operation of a high temperature wear test apparatus for automotive valve materials. Wear 2015; 342–343: 129–137.

7. Marchenko D.D., Matvyeyeva K.S. Improving the contact strength of V-belt pulleys using plastic deformation. Problems of Tribology. Khmelnitsky, 2019. Vol 24. No 4/94 (2019). S. 49–53. DOI: https://doi.org/10.31891/2079-1372-2019-94-4-49-53.

8. Chun K.J., Kim J.H., Hong J.S. A study of exhaust valve and seat insert wear depending on cycle numbers. Wear 2007; 263: 1147–1157.

9. Marchenko D.D., Matvyeyeva K.S. Investigation of tool wear resistance when smoothing parts. Problems of Tribology. Khmelnitsky, 2020. Vol 25. No 4/98 (2020). S. 40–44. DOI: https://doi.org/10.31891/2079-1372-2020-98-4-40-44

10. Dykha A.V. Marchenko D.D., Artyukh V.A., Zubiekhina–Khaiiat O.V., Kurepin V.N. Study and development of the technology for hardening rope blocks by reeling. Eastern–European Journal of Enterprise Technologies. Ukraine: PC «TECHNOLOGY CENTER». 2018. №2/1 (92) 2018. pp. 22–32. DOI: https://doi.org/10.15587/1729-4061.2018.126196.

11. Blum M., Jarczyk G., Scholz H., et al. Prototype plant for the economical mass production of TiAl-valves. Mat Sci Eng A-Struct 2002; 329–331: 616–620.

12. Dykha A.V., Marchenko D.D. Prediction the wear of sliding bearings. International Journal of Engineering and Technology (UAE). India: “Sciencepubco–logo” Science Publishing Corporation. Publisher of International Academic Journals. 2018. Vol. 7, No 2.23 (2018). pp. 4–8. DOI: https://doi.org/10.14419/ijet.v7i2.23.11872.

13. Marchenko D.D., Artyukh V.A., Matvyeyeva K.S. Analysis of the influence of surface plastic deformation on increasing the wear resistance of machine parts. Problems of Tribology. Khmelnitsky, 2020. Vol 25. No 2/96 (2020). S. 6–11. DOI: https://doi.org/10.31891/2079-1372-2020-96-2-6-11.

Марченко Д.Д., Матвєєва К.С. Дослідження напружено-деформованого стану поверхневого шару при зміцнюючій обробці деталей

У роботі представлені експериментальні дослідження та отримані статистичні моделі впливу режимів обробки на якість поверхневого шару і циклічній довговічності зміцнених деталей машин. Встановлено, що основна впливу на зміцнюючий ефект, вичерпання запасу пластичності металу і формування залишкових напружень надають дійсний зазор різця, дійсний натяг і профільний радіус ролика. Результати показали, що розмірне поєднане обкатування забезпечує високу циклічну довговічність зміцнених деталей в умовах багатоциклового втомного навантаження, що досягає 8 млн. циклів, що в 3,5 рази перевищує довговічність не зміцненої деталі і в 1,5 рази - довговічність деталі, зміцненої поверхневим пластичним деформуванням. Дослідження показали, що найбільша циклічна довговічність деталі забезпечується при мінімальних значеннях дійсного зазору різця, максимальних значеннях профільного радіусу і значенні дійсного натягу ролика 0,6 мм, що відповідає ступеню вичерпання запасу пластичності обробкою розмірним сумісним обкатуванням $\Psi \approx 0{,}65$. На основі результатів теоретичних і експериментальних досліджень розроблено методику та алгоритм проектування технології обробки розмірним поєднаним обкатуванням. Розроблено програму для ЕОМ, що дозволяє розрахунковим шляхом визначати якість поверхневого шару і циклічну довговічності деталі, виходячи із заданих режимів, а також призначати раціональні режими обробки, що забезпечують задану якість поверхневого шару і циклічну довговічність. На основі результатів досліджень розроблено технологічний процес зміцнюючої обробки деталей машин комбінованим розмірним обкатуванням, який дозволяє формувати стискаючі залишкові напруження в поверхневому шарі обробленої деталі, а також збільшити продуктивність до 2 разів при збереженні або поліпшенні заданих параметрів якості поверхневого шару обробленої деталі.

Ключові слова: розмірне сумісне обкатування, напружено-деформований стан, зміцнююча обробка, поверхнева пластична деформація, залишкові напруження

Problems of Tribology, V. 27, No 3/105-2022,89-95

Problems of Tribology
Website: http://tribology.khnu.km.ua/index.php/ProbTrib
E-mail: tribosenator@gmail.com

DOI: https://doi.org/10.31891/2079-1372-2022-105-3-89-95

Microstructure and wear resistance of modified surfaces obtained by ion-plasma nitriding of 40XH2MA steel

I.V. Smyrnov[1], A.V. Chornyi[1], V.V. Lysak[1], O.S. Drobot[2], P.V. Kaplun[2*], M.M. Poberezhnyi[2], A.V. Rutkovskyi[3]

[1]National Technical University of Ukraine "Igor Sikorsky, Polytechnic Institute", Ukraine
[2]Khmelnitskyi National University, Ukraine
[3]G. S. Pisarenko. Institute for Problems of Strength of the National Academy of Sciences of Ukraine
**E-mail:kaplunpavel@gmail.com*

Received: 27 July 2022: Revised:03 Septembert 2022: Accept:18 September 2022

Abstract

The article is devoted to the analysis of wear resistance of diffusion coatings, which were applied by ionic nitriding on steel 40XH2MA. There is a comparison of the technological efficiency of the results. The parameters of technological modes used in the process of application are presented, with the list of equipment and stages. The authors conduct the comparative analysis of chemical composition, microstructure, metallographic and tribological studies. They study the wear kinetics of 40XH2MA steel with nitrided coatings as well as provide practical recommendations on the use of hardened samples in dry friction conditions.

Key words: structural steels, physical and mechanical properties, ionic nitriding, technology, diffusion coatings, wear.

Problem statement

In recent years, many industries have established a tendency to use ion nitriding as an energy- efficient, environmentally friendly method of chemical-thermal hardeningof machine parts, cutting and stamping tools.To a large extent, this is facilitated by the creation of modern high-tech automated equipment, which made it possible to get rid of significant disadvantages of gas nitriding, such as duration, labor intensity of the process, instability of the results, low strength properties of the nitrided layer, etc.

Nitriding refers to surface modification processes that increase the local concentration of nitrogen in the metal structure. Many metals and alloys have shown the capacity for nitriding, that is, ability to increase hardness and wear resistance as a result of saturation with nitrogen in the amount from 5 to 50 atomic percent.

The most effective technological process of surface hardening is the method of ion nitriding in hydrogen-free media, which is well studied and is widely used for modification of metal materials. Unlike nitriding in hydrogen-containing media, in this case, there is no weakening of the base caused by the harmful effects of hydrogen on the metal, electricity and gas consumption is reduced, nitriding time is shortened, the absence of toxic ammonia makes this method environmentally friendly.

Literature review

Many scientific papers and monographs of both Ukrainian and foreign scientists are devoted to the processes and technologies of ion-plasma nitriding [1-5]. Of particular interest are publications from the countries where these technologies are highly developed and the production of industrial equipment is established, these are the Austrian company "RÜBIG", the German companies "ELTROPULS" and "PLATEG-PULSPLASMA", the Bulgarian company "IONITECH", the Brazilian company "NINRION" and others.

In the Institute for Problems of Strength named after H.S. Pysarenko, the technology of modification of the surface of structural elements of general engineering was developed by the method of vacuum ion-plasma

gas-thermocyclic nitriding, which is based on the theory of thermal fatigue, abnormal mass transfer under mechanical load and the effect of discrete energy input. This technology has a number of advantages: only the surface layer of the part is heated by glow discharge energy; cyclic heating and cooling cause thermal stress in the surface layer, which accelerates diffusion processes and, consequently, reduces processing time; discrete energy input and heating only the surface layer reduce energy consumption by up to 10 times [6].

A promising direction of controlling the structure and service properties of working surfaces is the use of pulsed plasma technologies. The National Technical University of Ukraine "Ihor Sikorsky Kyiv Polytechnic Institute" conducts research on ion-pulse high-frequency nitriding. This approach is based on a combination of a pulsed discharge for creating a plasma flow of diffuser elements and a pulsed biasing of the substrate potential for ion implantation or modification of a surface with the transition to the batch pulsed excitation mode of induction discharge.The pulsed modulation (periodic interruption) of gas discharge current or voltage of substrate negative biasreduces the average power of the thermal load on electrodes (cathode, anode, electrodes of separators, screens, etc.). This mode significantly reduces the operating temperature and makes it possible to modify surfaces and/or apply coatings on heat-sensitive substrates, such as hardened steels without the risk of overheating [7].

Thus, further study of surface modification by ion-plasma nitriding for improving its functional properties is relevant and appropriate in the case of specific implementation.

The aim of the work is to analyze and study the microstructures of modified surfaces using different technologies of ion-plasma nitriding for enhancing the wear resistance of parts and structural elements made of 40XH2MA steel.

Materials and methods

In the work, to study nitriding processes, structural alloyed high-quality steel 40XH2MA (ДСТУ 7806:2015) was used, which is used for the manufacture of heavily loaded critical parts – disks, cam clutches, gears, connecting rods, valves, crankshafts, etc.

According to the quality certificate, this steel has the following composition: 0,41%C, 0,31%Si; 0,57%Mn; 0,003%S; 0,017%P; 0,8%Cr; 1,37%Ni; 0,07%W; 0,01%V; 0,21%Mo, 0,18%Cu; 0,001%Ti; 0,016%Al; 0,009%N. The actual composition of the steel was determined during the study of microstructures, and it is slightly different from the data on the certificate, which may be due to the elimination of elements in the sample content, the results are shown in Table 1.

Table 1

The actual composition of the steel

Element	At. No.	Netto	Mass [%]	Mass Norm. [%]	Atom [%]	abs. error [%] (1 sigma)	rel. error [%] (1 sigma)
C	6	1559	0.40	0.40	1.83	0.00	0.00
Si	14	375	0.15	0.17	0.33	0.05	33.26
Cr	24	1468	1.07	1.18	1.25	0.08	7.68
Mn	25	1119	1.06	1.18	1.18	0.09	8.69
Fe	26	73421	86.07	95.56	94.20	2.40	2.78
Ni	28	513	0.82	0.92	0.86	0.10	11.94
Mo	42	793	0.53	0.59	0.34	0.08	15.13
		Sum	**90.11**	**100.00**	**100.00**		

Before nitriding, all samples were subjected to normalization with heating to 850±10°C for 15 min followed by cooling in air.

The study of microstructure, chemical composition was carried out using a scanning electron microscope VEGA3 manufactured by TESCAN; optical images of the microstructure were taken using a microscope manufactured by CARL ZEISS, JENA. The microhardness of the nitrided surface was measured by a PMT-3 microhardness tester with a load on the indenter of 20 g. Wear resistance of the samples testedby the method of friction plane on plane in conditions of dry friction metal on metal, with the sample reciprocating movement according to the scheme shown in figure 1. The friction samples were in the shape of bars with the following dimensions: length – 20 mm, width – 10 mm, thickness – 6 mm;the samples were cut from the original round samples with a diameter of 33 mm before and after nitriding.

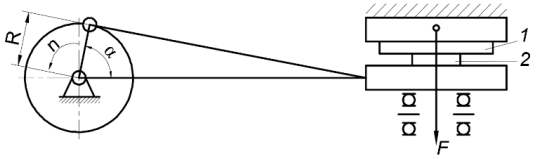

Fig. 1. Kinematic diagram of the friction unit 1 - counterbody, 2 - test sample

The hardened steel U13 with hardness of 70 HRC served as the counter body, the pressure in the contact zone of the counter body on the sample was 10 kPa. Friction of each sample was carried out for 6 hours, graphs were built based on the dependence of mass loss on the distance covered and time.

Results

In accordance with the set goal, the surfaces of samples with nitrided layers, which were obtained by three technologies of ionic nitriding, were studied in the work.

By the first technology, nitriding was applied using an experimental nitriding unit U1 designed by Podilskyi Scientific Physics and Technology Center of the Khmelnytskyi National University in the following modes: T = 560°C; P = 160 Pa; τ = 300 min; 75%N_2+25%Ar . The part was placed in a sealed chamber on a special device to which the negative pole of the power supply was connected, and the walls of the chamber were connected to the positive pole. Air was pumped out of the chamber to a pressure of 1.33 Pa, then the chamber was filled with pure Ar to a pressure of 1330 Pa, pumped out again to 1.33 Pa, and a constant voltage was applied to the electrodes using a special power supply to excite the glow discharge. The ion cleaning process was started at the voltage up to 1200 V for 30...60 minutes. Then the voltage was reduced to 500...1200 V, and the pressure was increased to operating pressure.

The process was carried out in the mode of anomalous glow discharge, where the surface of the part participates in the discharge as a cathode electrode and is covered with a layer of plasma. The density of current supplied to the part is up to 20 mA/cm^2. The temperature of the sample during nitriding was regulated by changing the parameters of the power supply mode and did not exceed 560 ° C, the control was carried out using a pyrometer F.08196.Ar purity at the initial stage was 99.993%.

By the second technology, nitriding was applied using the VIPA-1 unit designed by the H.S. Pysarenko Institute for Problems of Strength of the National Academy of Sciences of Ukraine. The technological process is as follows. The part is placed in a sealed container and connected to the negative pole of the current source, and the container walls are connected to the positive pole. Air is pumped out of the container to a pressure of 1.33 Pa, the container is purged with working gas for 5...15 minutes at a pressure of 1330 Pa, then it is pumped out again to a pressure of 1.33 Pa, a pulsating voltage of 1100...1400 V is applied to the electrodes using a special power supply and a glow discharge is excited. At this stage, cathodic spraying is carried out for 5...60 minutes, during which the part is cleaned. Then the voltage is reduced to operating voltage and the pressure is increased to 25...250 Pa. At these parameters, the actual process of diffusion saturation with nitrogen is carried out, and the voltage of 1000...1200 V is pulsating with a current pulse duration t = 10...20 ms and a pulse period T = 40 ms. Meanwhile, the filling factor Q, which is equal to the ratio of the value of the pulse period T to the duration t of a single pulse, is in the range of 2...4 because at Q < 2 arc discharges which cause damage to the surface of the workpiece may occur and at Q > 4 the efficiency of ion treatment decreases.

In the process of diffusion saturation, there is a cyclic termination of the reaction gas supply to the vacuum chamber in the ratio of 80%Ar + 20%N_2 with a half-cycle duration of 15...30 min, while the temperature of nitrogen saturation and denitration (resorption) is different – higher or lower than the eutectoid transformation temperature (591ºC) [8].

The process of nitriding by the third technology was carried out on an experimental vacuum unit, which was additionally equipped with a special source of the regulated constant voltage, a high-frequency generator and a pulse modulator made on vacuum electronic devices GU-81M. Due to the properties of their characteristics, these devices automatically limit the current to the load to a specified value and interrupt the arcing process, which is accompanied by explosive local destruction of the cathode surface.

The process was carried out in the mode of anomalous glow discharge, under which the entire surface of the cathode electrode (in our case, the part) participates in the discharge and is covered with plasma glow (Fig.2). The voltage for such discharge is hundreds of volts, and the current density on the part is up to 10 mA/cm^2. The operating parameters were set in the following range: voltage – 0.8-1.0 kV, pulse frequency – 10 Hz; pulse ratio– 1.5-2; working gas pressure in the chamber – 250-350 Pa, process length – 5-6 hours. The sample temperature during nitriding was regulated by changing the parameters of the pulse power supply mode and did not exceed 580°C. A mixture of 75%N_2 and 25%Ar was used as working gas, and pure Ar was used to clean the surface at the initial stage.

The use of pulse mode with a frequency of 10kHz ensures the stability of the process of diffusion saturation of the surface without electrical breakdowns and arcing, thus, in accordance with the volt-ampere characteristic of the electric discharge, the mode of anomalous glow discharge is realized. An important role in this process, as well as in the second technology, is played by the pulse density, the decrease in which leads to the localization of the amount of plasma, which can be compensated by increasing the voltage, but it causes overheating on the sample surface, which can lead to undesirable structural transformations.

Thus, the glow discharge burning occurred uniformly around the perimeter of the samples (Fig. 2), which provided the uniform thickness of the diffusion layer.

Fig. 2. Burning process of anomalous glow discharge in pulse mode. 1 - anode, 2 - cathode (part), 3 - anode glow, 4 - cathode glow.

Figure 3 shows electron pictures of sample surfaces after nitriding under the modes corresponding to the three described technologies. Table 2 shows the results of chemical analysis of sample surfaces in different zones formed during the nitriding process.

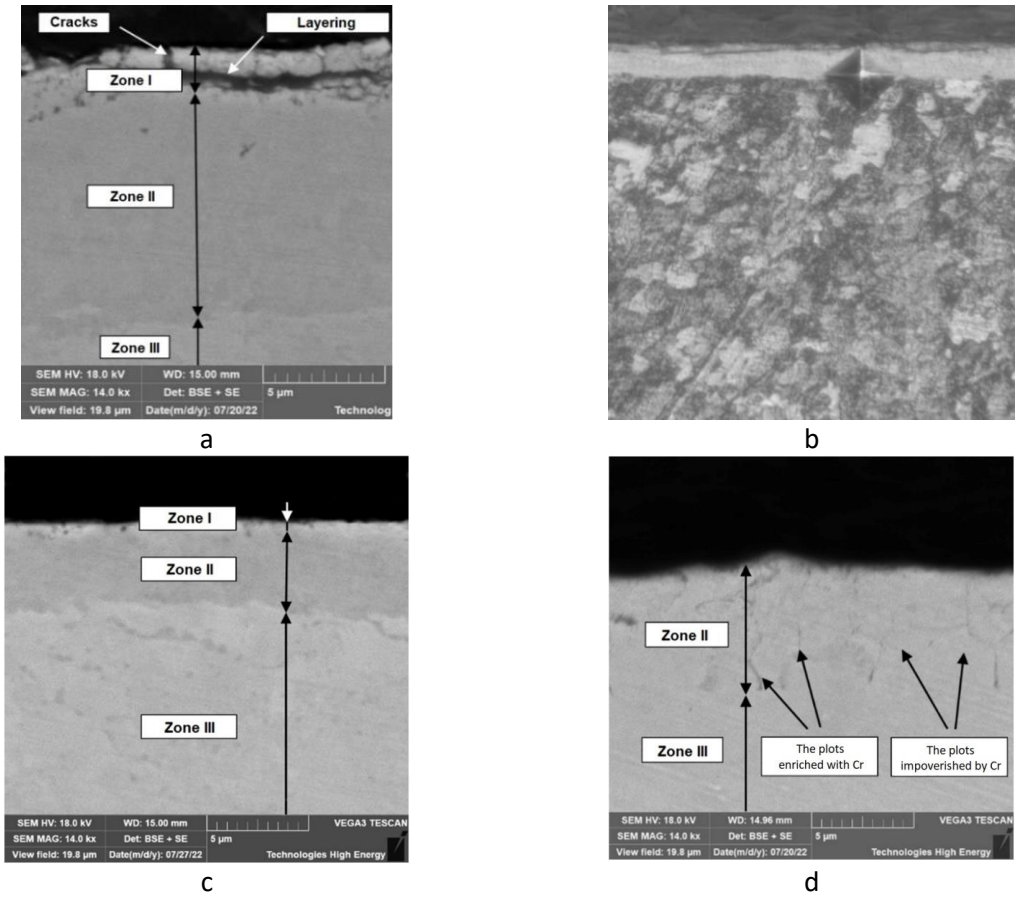

Fig. 3. Electronic pictures of the sample surface after nitriding: a, b - sample №1 by the first technology, c - sample №2 by the second technology, d - sample №3 by the third technology

Table 2

The results of chemical analysis of sample surfaces

Sample №	Analysis zone	Composition of elements, mas. %						
		N	Si	Cr	Mn	Fe	Ni	Mo
1	Zone I	6,13	0,63	1,58	–	90,8	0,86	–
	Zone II	4,76	0,19	1,12	–	93,02	0,91	–
	Zone III	1,71	0,4	2,83	–	94,09	0,74	–
2	Zone II	5,55	0,3	1,02	1,03	89,28	1,19	–
	Zone III	2,20	0,15	1,03	1,11	93,83	1,00	0,28
3	Zone II	5,9	0,32	0,58	0,63	90,75	1,42	–
	Zone III	3,27	0,25	0,52	1,07	93,4	0,99	0,1

Analysis of the results of determining the chemical composition of the nitrided layer showed that the structure is layered and consists of two zones: nitride, where the γ′- phase was formed, and nitrogenous ferrite. Alloying elements chromium and nickel dissolve in ferrite, increase the solubility of nitrogen in the α-phase forming special nitrides. Being released in a finely dispersed state, these nitrides contribute to enhancing the hardness of the nitrided layer, mainly in the lower layer of the saturated zone. Chromium, as a transition element, actively interacts with nitrogen and increases the solubility of nitrogen in the α-phase. Zone I with γ′-phase is very thin and brittle, microcracks and delamination are found (Fig.3 a).

After nitriding on the surface of sample No. 1 in zone I, the nitrogen concentration reaches 6.13 wt.%, respectively 18.05 atm% (Table 2). According to the iron-nitrogen diagram (Fig. 4), at a nitrogen concentration of about 20 atm%, iron nitride Fe4N will be formed, which causes the maximum hardness of the surface at the level of 805 MPa.

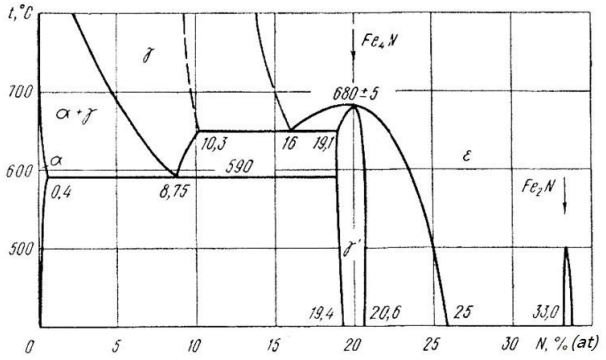

Fig. 4. Iron-nitrogen diagram

The amount of chromium in zone I increased to 1.58 mas.%, respectively to 1.25 atm% in comparison with its average amount in steel before nitriding of 1.18 mas.% (Table 1), and nickel, on the contrary, decreased from 0.92 mas. %, respectively from 0.86 atm %, in the initial state (Table 1) to 0.86 mas. %, respectively to 0.61 atm % after nitriding.

In zone II, the chemical composition of the nitrided surface differs from both the initial and the nitrided one: the nitrogen amount reaches 4.76 mas.% (16.6 atm %), and the alloying elements chromium and nickel show different activity. The amount of chromium decreased to 1.12 mas.% (1.05 atm %), and the amount of nickel decreased to 0.91 mas.% (0.76 atm %) (Table 2). Zone III, where the nitrided layer was formed, also underwent changes in the chemical composition: the amount of nitrogen decreased to 1.71 mas. % (6.47 atm %), and the amount of chromium increased to 2.83 mas. % (2.88 atm%). The amount of nickel remained at 0.74 mas.% (0.67 atm %), which is less than the average amount of nickel in steel before nitriding of 0.92 mas.% (Table 2). Thus, the microanalysis data indicate that the chemical composition of the saturated layer did not change in a uniform manner. Nitrogen has the highest concentration at a distance of 6-7 mcm from the surface (Fig. 5), chromium is more actively involved in the formation of the surface layer, where its concentration increased to 1.58 mas.% (1.25), and nickel remained in the deeper layers of the samples.

The surface nitrided layer reaches 200 mcm, and the hardened zone reaches 300 mcm. In the case of the indenter pyramid hitting the boundary between the white nitrided layer and the base with a load on the indenter of 100 g, the microcracks and delamination are not found (Fig. 3, b).

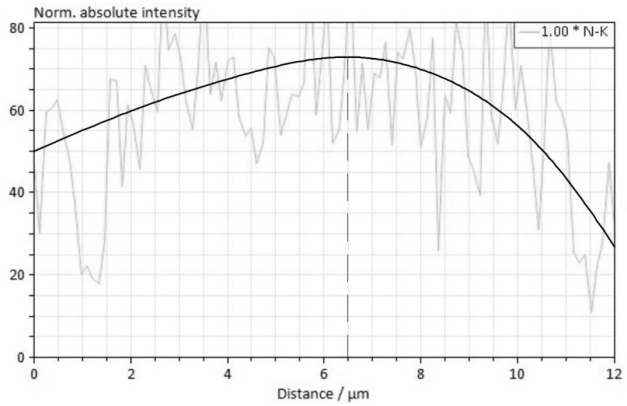

Fig. 5. Change of nitrogen concentration inwards from the surface of sample №1

The analysis of nitrogen distribution in sample No. 2 shows a slight increase in concentration to 5.55 mas. %, respectively to 18.77 atm% in zone II and to 2.20 mas. % (8.13 atm%) in zone III (Table 2). However, there is a significant decrease in the nitride zone I and the transition zone II from 10 mcm to 5 mcm (Fig.3, c), a small amount of molybdenum of 0.28 mas.% is observed, which may be due to the chemical heterogeneity of the steel bar from which the samples were cut. The distribution of nitrogen in sample No. 3 is similar to sample No. 2 in zone II in the amount of 5.9mas.%, respectively of 18.8 atm% and 3.27 mas.% (11.69 atm%) in zone III, there is also a small amount of molybdenum which is 0.1 mas.%. At the same time, zone I is absent, which can be explained by the absence of γ′-phase formations. The sample is different from the previous samples due to uneven redistribution of chromium (Fig. 6), with enrichment at the grain boundaries in the amount of 2.44 mas.% respectively of 2.13 atm and depletion in the grains to 0.52 mas.% respectively to 0.5 atm (Table 2, Fig. 3, d).

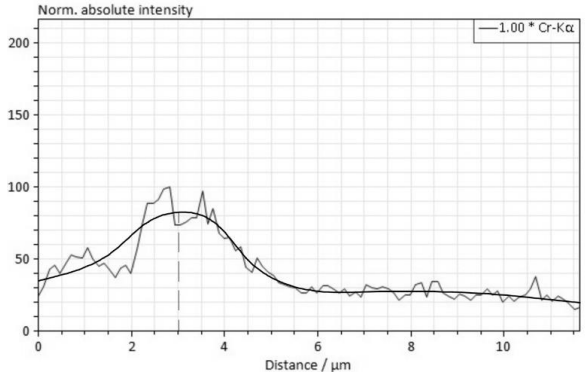

Fig. 6. Change of chromium concentration inwards from the surface of sample№3

The results of the analysis show the difference of microstructures and chemical composition in the surface zones of the nitrided surface of the samples treated by different technologies.The size, presence or absence of the nitride zone I with high nitrogen concentration and, accordingly, the maximum hardness on the surface are of particular importance; the redistribution of chromium in near-surface layers is also important, which in turn is reflected in the wear results shown in figure 7.

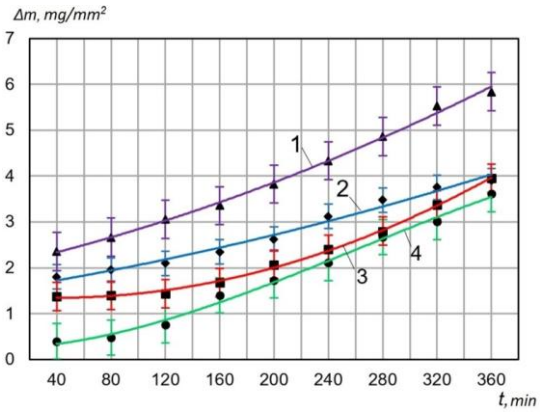

Fig. 7. Wear kinetics of samples from 40XH2MA steel in the initial state and after ionic nitriding.
1 – virgin sample; 2 – nitrided sample №3; 3 – nitrided sample №2; 4 – nitrided sample №1.

Based on the graphs shown in figure 7, it can be concluded that sample №1 nitrided by the first technology has the highest wear resistance, which is particularly apparent in the first minutes of friction, after wear of the nitride zone with maximum hardness, the mass loss of the sample increases uniformly. Sample No. 3 has almost the same wear at the beginning and at the end of the tests compared to sample No. 2, however, the wear changes uniformly with time as in the case of the non-nitrided sample, which can be explained by the more homogeneous structure of the nitrided layer. In general, after 360 minutes of testing, the wear resistance of all nitrided samples is 50-70% higher than that of the virgin non-nitrided sample.

Conclusion

The microstructural studies of the modified surfaces of 40XH2MA steel samples showed the difference in the structure and chemical composition of nitrided layers obtained by different ion-plasma nitriding technologies.

The size and presence on the surface of nitride zone with the formation of γ′-phase at the nitrogen concentration of 18-20 atm%, which along with high hardness has defects such asmicrocracks and delaminations, is of particular importance. Reduction of this zone, up to its complete elimination, is facilitated by the use of gas-thermocyclic and pulsed high-frequency ion-plasma nitriding technologies.

Tests under conditions of metal on metal dry friction showed that the wear resistance of all nitrided samples processed by the above technologies is 50-70% higher than that of the virgin non-nitrided sample.

References

1. Kaplun V.G., Kaplun P.V. Ion nitriding in hydrogen-free media. – Khmelnytsky: KhNU, 2015. – 318 p.

2. Pastukh I.M. Theory and practice of hydrogen-free nitriding in the glow discharge. – Kharkov: NSC KIPT, 2006. – 361 p.

3. Berlin E.V., Koval N.N., Seidman L.A. Plasma chemical-thermal surface treatment of steel parts. Moscow: Technosphere, 2012. – 464p.

4. DavidPye. PracticalNitridindandFerriticNitrocarburizing. – ASM InternationalPark, Ohio. – 2003. – PP. 256

5. HosseinAghajani, SahandBehrangiPlasma Nitriding ofSteels. – SpringerInternationalPublishing. – 2016.- PP.187.

6. On the advantages of vacuum nitriding technology / B.A. Lyashenko, A.V. Rutkovsky // Equipment and tools. – 2005. – Issue 12. – PP. 20-21.

7. The Power of Puled Plasma Ion Nitriding / David Pye // Heat treating progress. – July/August 2009. – P. 37-40.

8. Improved method of vacuum gas-thermocyclic ion-plasma nitriding of drill string elements / B.O. Chernov, A.V. Rutkovsky, M.Y. Tkach // Exploration and development of oil and gas fields. – 2014. № 1(50). – PP. 44-50.

Смирнов І.В., Чорний А.В., Лисак В.В., Дробот О.С., Каплун П.В., Побережний М.М., Рутковський А.В. Мікроструктура та зносостійкість модифікованих поверхонь отриманих іонно-плазмовим азотуванням сталі 40ХН2МА

Стаття присвячена аналізу зносостійкості дифузійних покриттів,що були нанесенні іонним азотуванням на сталь 40ХН2МА. Проведено порівняння технологічної ефективності результатів. Приведені параметри технологічних режимів, що використовувались в процесі нанесення, вказаний перелік обладнання та етапи. Проведено порівняльний аналіз хімічного складу, мікроструктури, металографічних та трибологічних досліджень. Вивчена кінетика зношування сталі 40ХН2МА з азотованими покриттями, що були нанесені. Надані практичні рекомендації щодо використання зміцнених зразків в умовах сухого тертя.

Ключові слова: конструкційні сталі, фізико-механічні властивості, іонне азотування, технологія, дифузійні покриття, знос.

Problems of Tribology , V. 27, No. 3/105-2022, 96-107-

Problems of Tribology
Website: http://tribology.khnu.km.ua/index.php/ProbTrib
E-mail: tribosenator@gmail.com

DOI: https://doi.org/10.31891/2079-1372-2022-105-3-96-107

Improvement of tribological characteristics of coupling parts "shaft-sleeve" with polymer and polymer-composite materials

V.V. Aulin, S.V. Lysenko, A.V. Hrynkiv, M.V. Pashynskyi

Central Ukrainian National Technical University , Ukraine
**E-mail: AulinVV @gmail.com*

Received: 31 July 2022: Revised:10 Septembert 2022: Accept:22 September 2022

Abstract

The article provides an analytical justification of the flow of tribological processes of coupling of "shaft-sleeve" parts, which simulates the functioning of sliding bearings and cylindrical joints of machines. The main attention is paid to such characteristics as contact pressure, static and dynamic forces, the criterion of the product of the total pressure on the sliding speed, the work of friction forces and its transition into thermal energy in the friction zone for polymer (based on polyamide P-68) and polymer-composite coatings (based on P-68 with kaolin filler) on the working surfaces of the parts. A comparative analysis of the functioning and tribological characteristics of the couplings of parts without coatings is presented.

Experimentally, on the basis of tests of samples on the МИ-1М friction machine, a significant reduction in wear and an increase in the relative wear resistance of samples with polymer-composite coatings in the modes of friction without lubrication (by 1.3...1.4 times) and marginal friction (in 1.2...1.3 times), as well as a decrease in the temperature in the friction zone (365 K and 347 K) compared to the polymer coating.

Keywords: tribological characteristics, polymer material, polymer-composite material, conjugation of parts, heat resistance

Introduction

The coupling of parts, nodes, systems and aggregates of machines in agricultural production [1,2] work in difficult conditions of sign-changing cyclic and dynamic load, increased dustiness, interaction with active and aggressive working (technological) environments, and therefore do not produce the planned resource and 80...90% of their failures are caused by friction and wear. The development of methods and measures to increase their wear resistance, such as tribotechnical systems, control of processes and states, require the identification of patterns of interaction, the mechanism of friction and wear, a set of characteristics and properties of materials.

Among the main directions of increasing the wear resistance of tribocouplers of parts, the following deserve attention: improvement of the design of parts and their joints; use of advanced materials and working (technological) environments; development of effective technologies for strengthening, restoration and modification of materials of parts, modification of working (technological) environments with substances (fillers, additives, additives, etc.) and treatment with physical fields (electric, magnetic, electromagnetic, laser and ultrasonic radiation, etc.); improvement of technologies of accelerated practice of conjugations of parts; improvement of operating conditions and selection of rational modes of their operation; development of new tribotechnical methods and technologies for ensuring reliable operation of parts, their couplings and machines as a whole [3].

The performance of restored external cylindrical surfaces of machine parts with polymer (PC) and polymer-composite coatings (PCC) largely depends on ensuring reliable heat removal from the friction zone into the part and the environment, because the operational heat resistance of polymers is very low (kapron – 383 K, polyamide P-68 – 403 K, fluoroplastic-4 – 413 K) [4,5].

The intensity of heat dissipation is determined both by the geometry and phase ratio of the PCC components, and by the thermophysical characteristics of the coating materials and conjugated parts [6].

At the same time, the task of PCC efficiency is realized from both theoretical and experimental points of view, i.e. the friction conditions and such tribotechnical characteristics of the working surfaces of the parts as wear, friction coefficient and temperature in the friction zone are determined. It matters on which surfaces of the parts' conjugations the PC and PCC were formed. Most often, PC and PCC are applied to the working surfaces of the coupling of "shaft-sleeve" parts, that is, direct and reverse pairs. If PC or PCC is applied to the shaft, the tribocoupling is a reverse pair. The theoretical substantiation of the evaluation of the tribotechnical characteristics of the surfaces of the tribocoupling parts requires the use of the theoretical provisions of B.I. Kostetskyi [7,8], as well as the establishment of the balanced mode of tribocoupling "shaft-sleeve" friction.

Literature review

It is known [9-11] that sowing machines work in conditions of direct contact with the soil and high dustiness, which causes intensive wear of their parts: quick failure of cuffs and seals is observed; shafts coupled with bushings [1,2]; axes of ninety- and forty-toothed cogs; tension sprocket and marker, drive shafts of fat seeding machines; conjugation "thirteen-tooth gear shaft"; gear mechanism shafts, etc. Analysis of the nature of the wear of the shafts of sowing machines shows that they are subject to mainly abrasive wear (fig. 1).

a **b**

Fig. 1. General view of the operation of the drive shafts of the fat seeder (a) and the transmission mechanism (b) when the ССТ-12Б 480 на seeder is working

According to the statistical data on the wear of the shafts of sowing machines, it was determined that the distribution of the amount of wear most closely corresponds to the normal law and the Weibull-Hnedenko law [12, 13]. The limit value of the wear of the shafts leads to the occurrence of excess force during their rotation in the bushings, as a result of which the cotter pins are cut or the connecting brackets of the drive of the seeding device are broken, which leads to the complete loss of performance of the seeding machines. The analysis of studies on the amount and nature of wear of the shafts of sowing machines [7, 14] shows that they have low wear resistance and require strengthening during manufacture.

The wear resistance of moving couplings of parts, including the "shaft-sleeve", is one of the most important factors limiting the reliability of machines. The speed of their wear depends on the following factors: load (contact pressure), temperature (volume average and contact), type and mode of movement, rotation frequency, aggressive action of working (technological) and external environments. To ensure their efficiency, the rational choice of the material of the parts, the physico-chemical and mechanical properties of their surface layers, the rheological and physico-chemical characteristics and properties of the working (technological) environment, etc., are of decisive importance.

The analysis of the constructions of movable conjugations of parts that create direct and reverse pairs - tribotechnical systems [15] allows us to identify four conditions of their existence (table 1).

Table 1

Conditions of existence of direct and reverse TTS and their characteristics

The type of movable conjugations of parts	The ratio of the hardness of the materials of the parts*	The ratio of areas of friction zones of parts surfaces*
Straight	$H_p > H_н$	$S_p > S_н$
Back by materials	$H_p < H_н$	$S_p > S_н$
Inverse by geometry	$H_p > H_н$	$S_p < S_н$
Reversible in terms of materials and geometry	$H_p < H_н$	$S_p < S_н$

*H_p, $H_н$, S_p, $S_н$ – *hardness* and areas of friction zones of moving and stationary parts .

Direct tribocoupling of parts is a widespread construction, in which the material of the moving part has a higher hardness and a larger area of the friction zone, and the stationary part has a correspondingly lower hardness and a smaller area of the friction zone. The intensity of wear of hard and soft materials of reverse tribocoupling parts is the same in terms of materials and geometry. They are characterized by the "cutter" effect, that is, the process of introducing a solid layer with a smaller friction area. Schemes of reverse and direct tribocoupling of parts, when they are strengthened by RS and RSS, are shown in fig. 2.

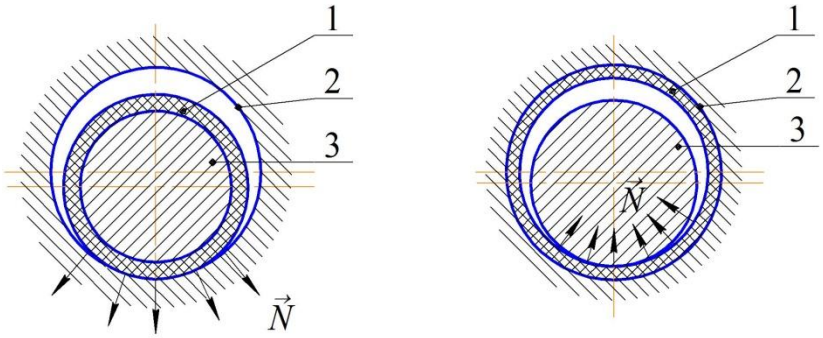

a b

Fig. 2. Schemes of reverse (a) and forward (b) tribocoupling of parts: 1 – layer of PC or PCC; 2 – sleeve; 3 - shaft.

The displayed different nature of force influence in the reverse and forward tribocouplers determines the difference in the conditions of their friction and wear. This is evidenced by the analysis of the operation of "shaft-hub" couplings, characteristic of seeders [1,2] and other machines [16-21] .

Purpose

The purpose of this work is a theoretical-experimental comparative tribological study of the coupling of "shaft-sleeve" parts reinforced with polymer (polyamide P-68) and polymer-composite coatings (based on polyamide P-68 with kaolin filler).

Results

The tribocoupling of the "shaft-hub" parts, which simulate such friction nodes as sliding bearings and cylindrical joints, is schematically depicted in fig. 3.

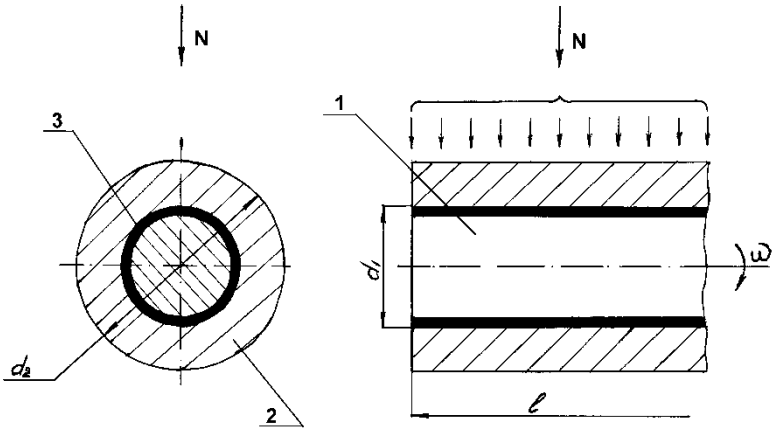

Fig. 3. Scheme of contact tribocoupling of parts with a polymer coating: 1 - shaft; 2 - sleeve; 3 – polymer coating.

The contact pressure in the tribocoupling of parts can be estimated by the formula [22,23]:

$$P_{st} = 0{,}8\left(\frac{N}{l \cdot K_{\Sigma}} \cdot \frac{\delta}{d_1(d_1 - \delta)}\right)^{1/2}, \quad (1)$$

where N – the normal load; d_1 – the diameter of the cylindrical surface; l – the length of the cylindrical surface; δ – thickness of the polymer layer; K_{Σ} – the total elastic constant for the case of contact of deformable conjugate parts.

$$K_{\Sigma} = K_1 + K_2, \quad (2)$$

where K_1, K_2 – the elastic constant for the material of the shaft and sleeve, respectively.

$$K_1 = \frac{1-\mu_1^2}{E_1};\ K_2 = \frac{1-\mu_2^2}{E_2}, \quad (3)$$

where μ_1, μ_2, E_1, E_2 – are Poisson's coefficients and modulus of elasticity, respectively, of the material of the shaft and sleeve.

Substituting (2) and (3) into (1), we obtain the value of the static force in the friction node:

$$P_{st} = 0{,}8\left(\frac{N \cdot \delta \cdot E_1 \cdot E_2}{l \cdot d_1 (d_1 + \delta) \cdot \left[E_1 (1-\mu_2)^2 + E_2 (1-\mu_1)^2 \right]} \right)^{1/2}. \quad (4)$$

During the oscillating motion of the tribocoupling of parts (fig. 4), loaded by an external force, it can be exposed to the conditioned loads generated by the inertia of the oscillating masses.

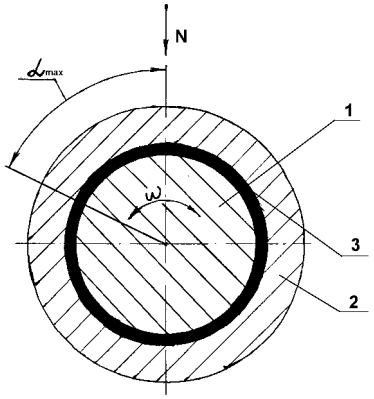

Fig. 4. Scheme of tribocoupling of parts in the oscillation mode: 1 – shaft; 2 – sleeve; 3 – coating.

When increasing the frequency and amplitude of the oscillating motion, the tribocoupling parts are loaded with inertial forces comparable in magnitude to the specified external load.

The lines of action of static and dynamic forces practically coincide [24,25]. At the same time, the amount of the total load acting is equal to:

$$P_\Sigma = P_{st} + P_a \sin \omega t, \quad (5)$$

where P_{st} – the value of the static force determined by expression (4); P_a – the amplitude value of the inertial force.

The relative speed of displacement of the working surfaces of the tribocoupling parts reaches its maximum value when the inertial forces are equal to zero, that is, the phase shift between speed and load fluctuations is equal to 90 °.

Accordingly, the sliding speed is described by a function

$$V = V_a \cos \omega t = \cos \alpha, \quad (6)$$

and the product of the total load on the sliding speed, respectively, is a function of α:

$$P_\Sigma V = V_\alpha \left(P_{st} \cos \alpha + \frac{P_a}{2} \sin \alpha \right). \quad (7)$$

It is worth noting that when using the criterion $P_\Sigma V$, it is necessary to take into account the fact that when the value of the friction coefficient depends on the sliding speed, this affects the heat release in the friction zone, and, therefore, the temperature of the friction surfaces.

To determine the value of the angle $\alpha = \alpha_m$ at which the criterion $P_\Sigma V$ reaches its maximum value, function (7) is differentiated by α_a, and the resulting expression is set to zero and we obtain:

$$\alpha_a = \arcsin \left[-\frac{P_{st}}{4P_a} + \left(\frac{P_{st}^2}{16P_a^2} + \frac{1}{2} \right)^{1/2} \right]. \quad (8)$$

introduce the coefficient η that characterizes the ratio of the product of the load on the sliding speed, taking into account inertial forces, to the product of the static load on the amplitude value of the sliding speed:

$$\eta = \frac{(P_\Sigma V)_{\max}}{P_{st} V_{\max}} = \cos \alpha_a + \frac{P_a}{P_{st}} \sin 2\alpha_a. \quad (9)$$

According to expression (9), when testing bearings for wear, their parameter data were limited so that the magnitude of the inertial force did not exceed one third of the load. At the same time, the criterion $P_\Sigma V$ increases by less than 5%, and therefore it is possible to accept $\eta \approx \cos \alpha_a$.

The magnitude of the amplitude value of the inertial (dynamic) force acting on the tribocoupling unit of the parts is determined by the formula:

$$P_a = \frac{I \cdot \omega^2 \cdot \alpha^2}{S_a}, \tag{10}$$

where I – the moment of inertia of the parts set in motion by the friction node relative to the rocking axis; S_a – the amplitude of swinging of the tribocoupler of parts during oscillations.

In the general case, considering that the friction zone in the tribocoupling of parts extends to part of the surface of the shaft coating S_{tr}. At the same time, the force of friction is equal to:

$$F_{tr} = P_a \cdot f_{tr} \cdot S_{tr}, \tag{11}$$

where f_{tr} – coefficient of friction. With dry friction in the coupling of polymeric materials with steel, the coefficient of friction for kapron is 0.115; for polyamide P-68 - 0.115, and for fluoroplastic-4 - 0.105.

The maximum surface area of the friction zone for a full period is equal to:

– for rotational movement:

$$S_{tr} = \pi d_1 l; \tag{12,a}$$

– for oscillating motion:

$$S_{tr} = 2d_1 \cdot l \cdot \alpha_a, \tag{12, b}$$

where α_a is the amplitude of the angle of deviation from the initial position (Fig. 4), expressed in radians.

Based on the previous one, with a fixed friction process $F_{tr} = const$, the work of friction forces for a full period can be estimated by the formula:

$$A_{tr} = \Omega \cdot d_1 \left(\frac{N \cdot \delta \cdot E_1 \cdot E_2 \cdot l \cdot d_1}{(d_1 + \delta) \cdot \left[E_1 (1 - \mu_2)^2 + E_2 (1 - \mu_1)^2 \right]} \right)^{1/2}, \tag{13}$$

where Ω – the coefficient that takes into account the nature of the movement ($\Omega = 7{,}9$ – for rotational movement; $\Omega = 3{,}2\alpha_a^2$ – for oscillatory movement, α_a, rad).

Based on the second law of thermodynamics, the work of external friction is described by the equation:

$$A_{tr} = Q + \Delta E, \tag{14}$$

where Q – the thermal energy into which the work of external friction was transferred; ΔE is the amount of energy absorbed by the surface layers of conjugated parts.

Well known [26,27] that in a real process, the work of external friction is not completely transformed into thermal energy, and therefore the energy is ΔE not equal to zero. The ratio $\frac{\Delta E}{A_{tr}}$ is, in general, a value that depends on the properties of the constituent tribocouples of materials, the nature of their interaction, the mode of friction and the working environment.

When the friction conditions change, the energy characteristics of this coupling of parts and their ratio also change. If $\frac{Q}{A_{tr}} \to \max$, or $\frac{\Delta E}{A_{tr}} \to \min$, then this characterizes the transitional process from unsteady to steady friction, and, therefore, wear processes when the friction surfaces are not worn. If the friction surfaces of the restored parts are worked in and given the necessary physical and mechanical properties, then already at the first stage of the friction process, the following ratios are realized:

$$\frac{Q}{A_{tr}} \approx 1; \qquad \frac{\Delta E}{A_{tr}} \to \min.$$

The regime of stable friction is also observed when the tribotechnical characteristics of tribocouplers have linear dependencies [7,8]. At the same time, the rate of wear is minimal and sinusoidally fluctuates near some constant value. A dynamic balance of friction and wear processes is also observed here. The specified conditions are the most desirable for tribocoupling parts of nodes, systems and machine assemblies. Under these conditions, their service life will be maximum. Modes of sharp changes in friction characteristics are also observed, in which the work of friction forces increasingly turns into energy absorbed by the surface layers of materials of tribocoupler parts. At the same time: $\frac{\Delta E}{A_{tr}} \to \max$ or $\frac{Q}{A_{tr}} \to \min \to 0$. This leads to a complete change in their physical properties, the nature and type of connections between the conjugated parts. As a result of established friction, wear of parts and dynamic self-regulation in the system of formation and destruction of secondary structures occurs.

Given the given materials of the tribocoupled parts, the nature of the interaction and the working medium, there is a region of change in the friction mode, in which the integral over the volume of the deformed surface layers takes a minimum value:

$$\int_V \frac{\Delta E}{A_{tr}} dV \to \min \tag{15}$$

For polymer-metal couplings, stable friction is observed almost at the beginning of the process, that is, it can be assumed that $A_{tr} \approx Q$ in the friction zone in one revolution, according to expression (13), the amount of thermal energy will be released:

$$Q = \Omega \cdot d_1 \left(\frac{N \cdot E_1 \cdot E_2 \cdot d_1 \cdot \delta}{l(d_1 + \delta) \cdot \left[E_1 (1 - \mu_2)^2 + E_2 (1 - \mu_1)^2 \right]} \right)^{1/2}. \tag{16}$$

First of all, let's consider the process of heat removal from the tribo-coupling zone of "shaft-sleeve" parts with the corresponding materials (fig. 5). We also assume that the isothermal surfaces in the triboconjugation of parts and the temperature will be a function of only one coordinate *h* - along the normal to the isothermal surfaces.

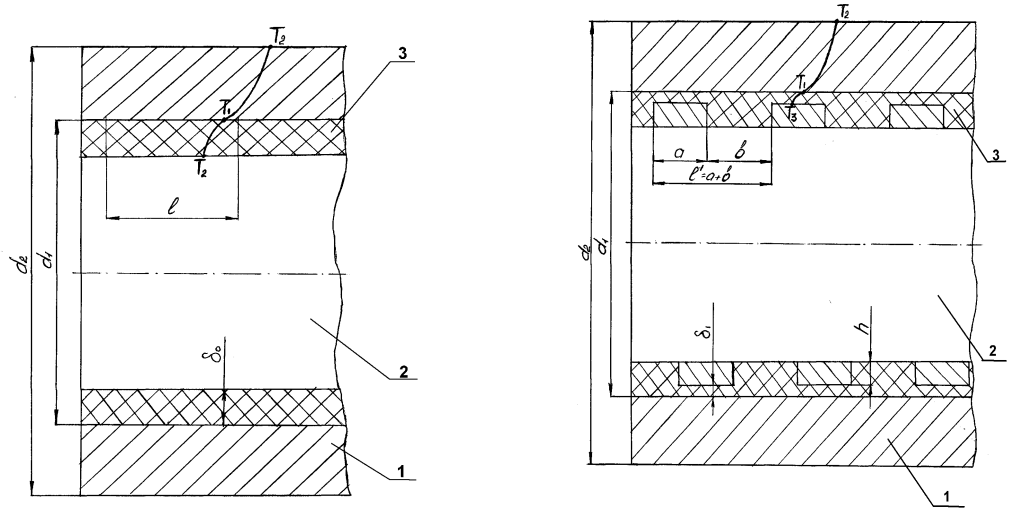

a **b**

Fig. 5. Scheme of removal of thermal energy from the friction zone for PC (a) and PCC (b): 1 - sleeve; 2 - shaft; 3 – coating.

According to the Fourier law [28,29], the heat flow through the cylindrical surface of the sleeve can be determined by the expression:

$$Q = -\lambda \frac{dT}{dh} \cdot S(h), \tag{17}$$

where $Q = const$ for any isothermal surface; $S(h)$ – heat energy removal surface; λ – thermal conductivity of the part material.

Having integrated equation (17), having previously divided the variables, within the limits of h from h_1 to h_2 and to T – from T_1 to T_2, we have:

$$Q = \frac{\lambda (T_1 - T_2)}{\int_{h_1}^{h_2} \frac{dh}{S(h)}}, \tag{18}$$

where T_1, T_2 – the temperatures in the friction zone and on the outer surface of the sleeve, respectively.

Let's enter the notation

$$\int_{h_1}^{h_2} \frac{dh}{S(h)} = N_{h_1}^{h_2}, \tag{19}$$

where $N_{h_1}^{h_2}$ is the thickness of the wall along which heat dissipation is observed.

Considering (19) in (18), we have:

$$Q = \lambda(T_1 - T_2)/ N_{h_1}^{h_2}. \tag{2 0}$$

If equation (17) is integrated from h_1 to h and from T_1 to T:

$$\frac{Q}{\lambda}\int_{h_1}^{h}\frac{dh}{S(h)} = -\int_{T_1}^{T} dT, \tag{ 21}$$

then we get the following temperature distribution:

$$T = T_1 - \frac{Q}{\lambda} N_{h_1}^{h}. \tag{2 2}$$

Substituting the value Q from expression (20), we have:

$$T = T_1 - (T_1 - T_2)\frac{N_{h_1}^{h}}{N_{h_1}^{h_2}}. \tag{23}$$

If we enter the dimensionless temperature $\theta = \dfrac{T - T_1}{T_1 - T_2}$, then the temperature distribution according to expression (23) will take the form:

$$\theta = 1 - \frac{N_{h_1}^{h}}{N_{h_1}^{h_2}}. \tag{24}$$

Let the stationary process of heat conduction be carried out in a cylindrical wall (sleeve) with an inner radius r_1 and an outer radius r_2 and through a polymer coating on the cylindrical surface of the shaft (Fig. 5).

Boundary conditions are set on the sleeve surfaces

$$T|_{r=r_1} = T_1;\ T|_{r=r_2} = T_2, \text{ or } \theta|_{r=r_1} = 1;\ \theta|_{r=r_2} = 0. \tag{25}$$

Based on equations (21) and (22) and fig. 4, we have:

$$h = r; h_1 = r_1; h_2 = r_2; S(h) = 2\pi r l. \tag{26}$$

According to expression (19), the reduced thicknesses of the heat sink walls are equal to:

$$N_{h_1}^{h} = \int_{r_1}^{r}\frac{dr}{2\pi r l} = \frac{1}{2\pi l}\ln\frac{r}{r_1}, \tag{27}$$

$$N_{h_1}^{h_2} = \frac{1}{2\pi l}\ln\frac{r_2}{r_1}. \tag{28}$$

Taking into account the obtained parameters (27) and (28), the expression for the heat flow diverted from the friction zone by the bushing has the form:

$$Q_b = \frac{2\pi l\lambda_1(T_1 - T_2)}{\ln\dfrac{r_2}{r_1}}. \tag{29}$$

Then the distributions of temperature (23) and dimensionless temperature (24) will be converted into expressions, respectively:

$$T = T_1 - (T_1 - T_2)\frac{\ln(r/r_1)}{\ln(r_2/r_1)}; \tag{30}$$

$$\theta = 1 - \frac{\ln(r/r_1)}{\ln(r_2/r_1)}. \tag{31}$$

If you enter dimensionless coordinates:

$R = \frac{r}{r_1}$, and $\frac{r_2}{r_1} = K_R$, expression (31) can be written in the form:

$$\theta = 1 - \frac{\ln R}{\ln K_R} = 1 - \frac{2\lambda \ln R}{2\lambda \ln K_R} = \frac{\ln R}{2\lambda \xi_{to}}, \tag{32}$$

where $\xi_{to} = \frac{\ln(K_R)}{2\lambda}$ is the linear thermal resistance of the cylindrical wall.

The amount of thermal energy from the friction zone of the tribocoupling parts is removed both through the sleeve and through the polymer coating on the cylindrical surface of the shaft.

Estimate these heat flows as you can according to the obtained expressions (29) and (16), based on the thermal energy released in the friction zone.

Let the amount of heat be removed through the sleeve

$$Q_b = \gamma Q, \tag{33}$$

where γ – the coefficient that takes into account part of the heat removed through the sleeve from the friction surface. Part of the heat dissipated through the polymer coating on the cylindrical surface of the shaft is equal to:

$$Q_{pc} = (1-\gamma)(1-\beta)Q, \tag{34}$$

where β – is the coefficient that takes into account part of the thermal energy dissipated in the tribo coupling of parts.

Let us have a section of the shaft *l* with a uniform polymer coating of thickness δ_p (fig. 3).

Then, according to expressions (18), (29) and (34), the heat flow is transferred to the shaft with a polymer coating:

$$Q_{pc} = (1-\gamma)(1-\beta)\frac{2\pi l_p \lambda_2 (T_1 - T_2)}{\ln \frac{d_1}{d_1 - 2\delta_p}}, \tag{35}$$

where λ_2 – the thermal conductivity of the polymer material.

In case of combined PCC:

$$Q_{pcc} = (1-\gamma)(1-\beta)\frac{2\pi(a\lambda_3 + b\lambda_2)(T_1 - T_2)}{\ln \frac{d_1}{d_1 - 2\delta_{PCC}}}, \tag{36}$$

where *a* – the length of the metal section of PCC with thermal conductivity λ_3, *b* – the length of the polymer section of PCC with thermal conductivity λ_2, δ_{PCC} – the thickness of PCC.

On the МИ-1М friction machine, in accordance with the standard methodology [ ] , studies of the wear characteristics of the friction surfaces were carried out (PC – pure polymer coatings (polyamide P-68), PCC – polymer-composite coatings based on P-68, cast iron СЧ18, steel 45) without lubrication and with extreme friction from specific load and sliding speed.

Experimental values of the values of linear wear depending on the duration of tests without lubrication and

with extreme friction are presented in Figs. 6 and 7.

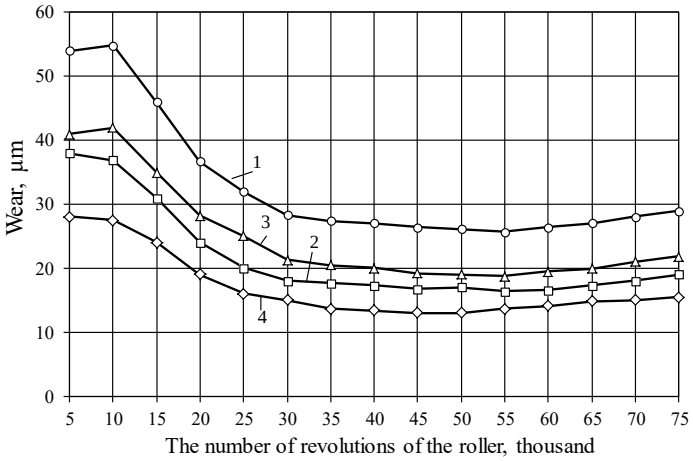

Fig. 6. Dependence of the amount of wear of tribo-coupling friction surfaces of "roller-pad" samples without lubrication depending on the duration of the test (P = 1.5 MPa, V = 0.5 m/s). Tribocoupling of materials: 1 – "cast iron-PC", 2 – "cast iron-PCC", 3 – "steel-PC", 4 – "steel-PCC".

The tests were carried out at a specific load of 0.5 MPa and a sliding speed of 0.5 m/s without lubrication and at extreme friction. The linear wear of the samples was determined after every 5000 revolutions, which corresponded to 628 m of friction path. The total duration of the tests included both a run-in period and a period of steady wear.

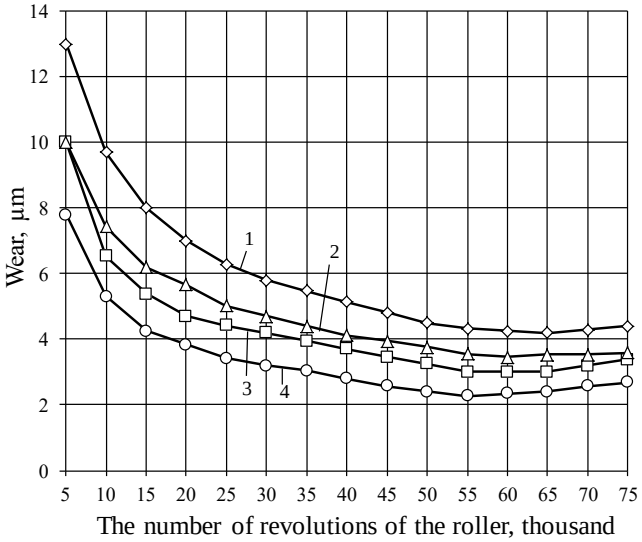

Fig. 7. Dependence of the amount of wear of the "roller-pad" tribocoupling surfaces at the limit friction depending on the duration of the test (P = 1.5 MPa, V = 0.5 m/s). Tribo-coupling of materials: 1 – "cast iron-PC", 2 – "cast iron-PCC", 3 – "steel-PC", 4 – "steel-PCC".

In each test, linear wear, friction moment and temperature in the friction zone were determined. In comparative tests, it was determined that after 50,000 revolutions, the wear process both under conditions of extreme friction and without lubrication occurs with constant intensity. Therefore, the wear results obtained after 50,000 revolutions of the roller were used for a comparative assessment of the wear resistance of the surfaces of the studied samples.

In order to evaluate the wear resistance during the period of established wear, the criterion is the relative wear resistance, which is determined by the ratio:

$$\gamma = \frac{U_e}{U_a},$$

where U_e – the linear wear of the reference surface for a certain number of revolutions of the roller, μm; U_a – absolute wear of the tested surface for the same number of roller revolutions, μm. The indicated values were determined during the period of established wear, that is, from 50,000 to 75,000 roller revolutions, according to the data shown in the graphs. Cast iron was used as the standard for determining the relative wear resistance of

tribocoupling samples. The results of relative wear resistance at friction without lubrication and at limit friction are presented in table 2.

Table 2

Relative wear resistance of surfaces in friction without lubrication and in extreme friction during the period of established wear (P=1.5 MPa, V = 0.5 m/s)

Surface	Relative wear resistance,γ	
	without lubrication	marginal friction
PC	3.11	2.00
PCC	4.66	3.33
Cast iron СЧ18	1.00	1.00
Steel 45	1.36	1.25

The results given in the table. 2 show that the relative wear resistance of PCC samples in the mode of friction without lubrication is 1.5 times greater than the relative wear resistance of PC samples and 3.4 times greater than that of steel 45 samples. For limit friction, the relative wear resistance is respectively greater than 1, 3 and 2.7 times.

Differences are also observed in the nature of the wear of the conjugated surfaces. The results of experimental studies of the wear of the roller and pad for the tested samples under friction without lubrication and under extreme friction are given in table 3.

Table 3

The nature of the wear of the coupled surfaces in friction without lubrication and in marginal friction during the period of established wear (P=1.5 MPa, V = 0.5 m/s)

The studied surface	Amount of wear, μm					
	without lubrication			marginal friction		
	roller	pin feather	couple	roller	pin feather	tribocoupling of samples
Cast iron-PC	27	32	59	5	11	16
Cast iron-PCC	18	26	44	3	9	12
Steel-PC	20.8	24.6	45.4	3.8	8.5	12.3
Steel-PCC	13.9	20	33.9	2,3	6.9	9.2

The analysis of the experimental data showed that it is characteristic for the studied samples: the pad wears out more intensively compared to the roller. The total wear of "cast iron-PCC" and "steel-PCC" friction pairs is 1.3...1.4 times less than the wear of "cast iron-PC" and "steel-PC" pairs in friction conditions without lubrication and 1.2 ...1.3 times less when working in conditions of extreme friction.

The presence in the friction zone of a polymer material with a high molecular weight and a low activation energy of mechanodestruction [5,30-32] has a favorable effect on the reduction of the working-in time of the couplings, which increases the degree of dispersion of the micro-uniformities of the surface being worked-in.

Thus, polymer materials applied to the surface to be restored help speed up the run-in process, reduce initial wear, and, as research shows, surface roughness decreases.

The study of temperature changes in the friction zone was carried out by comparing heat dissipation with pure polymer and polymer-composite coatings. The temperature was measured according to the method described in [3]. In addition, the intensity of heat removal from the friction zone was studied.

The results of measurements of the temperature of the examined surfaces of the samples and its theoretical assessment are given in table 4.

Table 4

Temperature in the friction zone (P=1.0 MPa, V = 0.5 m/s)

Surface	Temperature, *K*			
	Experimental data		Theoretical evaluations	
	without lubrication	marginal friction	without lubrication	marginal friction
PC	378	364	376	361
PCC	365	347	363	344
Cast iron СЧ18	388	375	384	371
Steel 45	385	372	383	368

According to the data in the table, the heat resistance of PCC is higher than pure polymeric PC, which indicates the feasibility of using the developed technological process to increase the wear resistance and heat resistance of the range of parts that work as sliding bearings.

For polymer materials, there is a fairly clear relationship between the friction coefficients and the temperature in the contact zone: lower temperatures correspond to a lower value of the friction coefficient and vice versa. The temperature arising as a result of friction changes the elastic and strength properties of the polymer

surface layers of tribocouples of samples and parts. This affects the change of the actual contact area of the surfaces and the force of friction, and, therefore, the coefficient of friction.

The change in temperature observed in the friction zone is due to the more intense heat dissipation of polymer-composite coatings compared to pure polymer ones.

Conclusions

1. Analytical expressions for static, dynamic and total forces were obtained for tribocoupling of "shaft-sleeve" parts. The assessment of the work of forces and thermal energy in the tribocoupling of parts is determined for the established friction process.

2. From a theoretical point of view, the effectiveness of heat dissipation from a polymer-composite coating in comparison with polymer coatings has been proven. Patterns of change in thermodynamic and dimensionless temperature changes were found for the investigated coatings.

3. A study of the wear of the working surfaces of the "roller-pad" samples was carried out on the МИ-1М friction machine. Polymer coatings, polymer-composite coatings, cast iron СЧ-18, steel 45 were subjected to research. The dependence of the wear of the conjugation of the samples on the number of revolutions of the roller in the modes without lubrication and with extreme friction was determined. It is shown that the relative wear resistance of PCC samples in the mode of friction without lubrication is 1.5 times greater than that of PC and 3.4 times greater than that of samples made of steel 45. For extreme friction, the relative wear resistance is correspondingly greater by 1.3... 2.7 times.

4. The results of temperature measurements in the friction zone of the sample joints indicate that the heat resistance of the polymer-composite coating based on polyamide P-68 with kaolin filler is higher than the pure matrix polymer material both in the mode without lubrication and in the mode of marginal friction.

References

1. Sysolin P.V., Salo V.M., Kropivnyi V.M. (2001) Silskohospodarski mashyny: teoretychni osnovy, konstruktsiia, proektuvannia [K.:Urozhai]. – 384 s.

2. Sisolin P.V., Pogorelyiy L.V. (2005). Pochvoobrabatyivayuschie i posevnyie mashinyi: istoriya, mashinostroenie, konstruirovanie [K.: Feniks] – 264s.

3. Aulin V.V. Trybofizychni osnovy pidvyshchennia znosostiikosti detalei ta robochykh orhaniv silskohospodarskoi tekhniky [dys. ... d-ra tekhn. nauk : 05.02.04]. – 360 s.

4. Beloysov V.Ya. (1984). Dolgovechnost detaley mashin s kompozitsionnyimi materialami [LvIv: Vischa shkola]. – 180 s.

5. Mashkov Yu.K. (2013). Tribofizika metallov i polimerov: monografiya [Omsk: OmGTU] – 240 s.

6. Vanin G.A. (1985). Mikromehanika kompozitsionnyih materialov: monografIya [K.: Nauk. dumka] – 304s.

7. Kostetskiy B.I. (1970). Trenie, smazka i iznos v mashinah [K.: "Tehnika"] – 304 s.

8. Kostetskiy B.I. (1976). Poverhnostnaya prochnost materialov pri trenii [Kiev: "Tehnika"] – 296 s.

9. Dobrovolskiy A.G., Koshelenko P.I. (1989). Abrazivnaya iznosostoykost materialov [K.: Tehnika] – 128 s.

10. Severnev M.M., Podlekarev N.N., Sohadze V.Sh., Kitikov V.O. (2011). Iznos i korroziya selskohozyaystvennyih mashin [Minsk: Belarus. navuka]. – 333 s.

11. Ikramov U. (1979). Mehanizmyi i priroda abrazivnogo iznashivaniya [Tashkent: FanUzSSR]. – 132 s.

12. Bershadskiy L.I. (1981). Samoorganizatsiya i nadezhnost tribosistem [Kiev] – 35 s.

13. Kuzmenko A.G. (2011). Nadezhnost uzlov treniya po prochnosti i iznosu: monografiya [Hmelnitskiy:HNU]. – 391s.

14. Dykha O.V. (2018). Rozrakhunkovo-eksperymentalni metody keruvannia protsesamy hranychnoho zmashchuvannia tekhnichnykh trybosystem. Monohrafiia. [Khmelnytskyi: KhNU]. – 197 s.

15. Voitov V.A., Yakhno O.M., F.Kh. Ali Saab. (1999). Pryntsypy konstruktyvnoi stiikosti vuzliv tertia hidromashyn proty spratsiuvannia: monohrafiia [K]. – 192 s.

16. Aulin V.V., Derkach O.D., Kabat O.S., Makarenko D.O., Hrynkiv A.V., Krutous D.I. (2020). Application of polymer composites in the design of agricultural machines for tillage [Problems of Tribology, V.25, No2/96]. P. 49-58.

17. Aulin V., Kobets A., Derkach O., Makarenko D., Hrynkiv A., Krutous D., Muranov E. (2020. Design of mated parts using polymeric materials with enhanced tribotechnical characteristics [Eastern-European Journal of Enterprise Technologies. Vol. 5 (12-107)]. P. 49-57.

18. Kabat O., Makarenko D., Derkach O., Muranov E. (2021). Determining the influence of the filler on the properties of structural thermal-resistant polymeric materials based on Phenylone C1 [Eastern-European Journal of Enterprise Technologies, 5(6 (113)]. P.24-29.

19. Aulin V.V., Hrynkiv A.V., Smal V.V., Lysenko S.V., Pashynskyi M.V., Katerynych S.E., Livitskyi O.M. (2021). Basic approaches and requirements for the design of tribological polymer composite materials with high-modulus fillers [Problems of Tribology, V.26, No 4/102). P. 51-60.

20. Liushuk O.M. (2021). Kompleksnyi pidkhid pidvyshchennia dovhovichnosti ta znosostiikosti robochykh orhaniv gruntoobrobnykh mashyn [avtoref. dys. ... kand. tekhn. nauk: 05.05.11]. – 52 s.

21. Borak K.V. (2021). Rozrobka polimermatrychnykh multynapovnenykh kompozytsiinykh materialiv fryktsiinoho pryznachennia z kompleksom kerovanykh vlastyvostei [dys. ... kand. tekhn. nauk : 05.02.01]. – 162 s.

22. Kuzmenko A.G., Dyiha A.V., Babak O.P. (2011). Kontaktnaya mehanika i iznosostoykost smazannyih tribosistem. Teoreticheskaya i eksperimentalnaya tribologiya: v 12 t.; t. 8 (1): monografiya. [Hmelnitskiy: HNU]. 250 s.

23.Kuzmenko A.H., Dykha O.V. (2005). Doslidzhennia znosokontaktnoi vzaiemodii zmashchenykh poverkhon tertia: monohrafiia [Khmelnytskyi: KhNU]. 183 s.

24. Aulin V., Derkach O., Makarenko D., Hrynkiv A., Pankov A., Tykhyi A. (2019). Analysis of tribological efficiency of movable junctions "polymeric-composite materials – steel" [Eastern-European Journal of Enterprise Technologies. Vol. 4 (12-100)]. P. 6-15.

25. Savuliak V.I. (2004). Naukovi zasady formuvannia na splavakh zaliza kompozytsiinykh metalokarbidnykh shariv zi stabilnymy strukturamy ta pidvyshchenymy trybotekhnichnymy kharakterystykamy [avtoref. dys... d-ra tekhn. nauk: 05.02.01]. 39 s.

26. Bondarenko V.P. (1987). Tribotehnicheskie kompozityi s vyisokomodulnyimi napolnitelyami [K.: Nauk. dumka]. 232 s.

27. Kondrachuk M.V., Khabutel V.F., Pashechko M.I., Korbut Ye.V. (2009). Trybolohiia [K.: Vyd-vo Natsionalnoho Aviatsiinoho universytetu «NAU-druk»] – 232 s.

28. Bondarenko V.P. (1987). Tribotehnicheskie kompozityi s vyisokomodulnyimi napolnitelyami [K.: Nauk. dumka]. 232 s.

29. Luchka M.V. (1998). Pokryttia hradiientnoho typu poverkhni trybokontaktu kovzanniam [K]. - 53 s.

30. Chernets M.V., Klimenko L.P., Pashechko M.I., Nevchas A. (2006). Tribomehanika. Tribotehnika. Tribotehnologii : monografIya: v 3 t. T. 1. Mehanika tribokontaktnogo vzaimodeystviya pri skolzhenii [Nikolaev : NGGU im. P.Mogili]. - 476 s.

31. Aulin V.V., Derkach O.D., Makarenko D.O., Hrynkiv A.V. (2018). Vplyv rezhymiv ekspluatatsii na znoshuvannia detalei, vyhotovlenykh z polimerno-kompozytnoho materialu [Problemy trybolohii. №4]. S.65-69.

32. Sorokov S. (2003). Klasternyi pidkhid do rozrakhunku fizychnykh kharakterystyk kompozytnykh materialiv [Lviv: In-t fizyky kondens. system NANU]. 23 s.

Аулін В.В., Лисенко С.В., Гриньків А.В., Пашинський М.В. Покращення трибологічних характеристик спряження деталей "вал-втулка" полімерними та полімерно-композиційними матеріалами

В статті дано аналітичне обґрунтування протікання трибологічних процесів спряження деталей "вал-втулка", яке моделює функціонування підшипників ковзання і циліндричні шарніри машин. Основна увага приділена таким характеристикам як контактний тиск, статичному та динамічному зусиллям, критерію добутку сумарного тиску на швидкість ковзання, роботи сил тертя й її переходу в теплову енергію в зоні тертя для полімерних (на основі поліаміду П-68) і полімерно-композиційних покриттів (на основі П-68 з наповнювачем каоліну) на робочих поверхнях деталей. Наведено порівняльний аналіз функціонування і трибологічних характеристик спряжень деталей без покриттів.

Експериментально, на основі випробувань зразків на машині тертя МИ-1М, доведено істотне зменшення зносу та підвищення відносної зносостійкості зразків з полімерно-композиційними покриттями в режимах тертя без змащення (в 1,3...1,4 рази) і граничному терті (в 1,2...1,3 рази), а також зменшення температури у зоні тертя (365 К і 347 К) у порівнянні з полімерним покриттям.

Ключові слова: трибологічна характеристика, полімерний матеріал, полімерно-композиційний матеріал, спряження деталей, термостійкість.

Problems of Tribology, *V. 27, No 3/105-2022*

Problems of Tribology
Website: http://tribology.khnu.km.ua/index.php/ProbTrib
E-mail: tribosenator@gmail.com

Myroslav Vasyliovych Kindrachuk

to the 75th anniversary of the birth

September 21 marks the 75th birthday of Doctor of Technical Sciences, Professor, Corresponding Member of the National Academy of Sciences of Ukraine Myroslav Vasyliovych Kindrachuk. Born in the village Kotykyvka, Horodenkiv district, Ivano-Frankivsk region.

In 1971, M.V. Kindrachuk graduated from the Kyiv Polytechnic Institute. The beginning of his career was connected with the Kyiv Automatic Machine Tool Plant named after M. Gorky (1971 - 1989) - first a technologist of the thermal workshop, then an engineer of the Central factory laboratory, then he was transferred to the position of deputy chief metallurgist for heat treatment. Scientific activity began in 1973. During the period of study in a targeted postgraduate course at the Department of Aviation Materials Science of the Kyiv Institute of Civil Aviation Engineers. Since 1989 after 2003 - scientific and pedagogical activity is connected with the engineering and physics faculty of NTUU "KPI", where he went from a senior researcher to a professor of the "Metal science and heat treatment" department, and since 2004 with the National Aviation University.

In 1982, he defended his candidate's dissertation in technical sciences in the specialty "Friction and wear in machines", and in 1996 he defended his doctoral dissertation in the specialties " Metal science and heat treatment of metals" and "Friction and wear in machines". In 1997 received the academic title of professor.

M.V. Kindrachuk is a well-known scientist in the field of tribotechnical materials science. With his direct participation, based on the theoretical ideas of the structural theory of wear resistance of materials, the theory and practice of creating new alloys and methods of obtaining optimal surface structures using concentrated energy sources are being developed. A new conceptual approach to the creation of composite alloys and gradient coatings of the eutectic type with high tribotechnical properties is proposed. The approach consists in optimizing alloy parameters, as well as technological features of coating application based on analysis of the stress-strain state of the composition during friction, thermodynamic analysis and mathematical modeling of the relationship between friction and wear processes with external load parameters. Kindrachuk M.V. conducts extensive scientific and organizational activities, is the initiator of cooperation with institutes of the National Academy of Sciences of Ukraine, leading scientific and research and research and production organizations and enterprises. He is the editor-in-chief of the scientific and technical journal "Friction and Wear Problems". He was the head of a number of international scientific and technical projects.

The results of scientific and practical activities of Kindrachuk M.V. were reflected in more than 500 works, including 27 monographs and textbooks, 70 author's certificates and patents. He is the author of the scientific discovery "The phenomenon of thermal stabilization in metal-polymer friction pairs". 3 doctoral and 14 candidate dissertation were prepared and defended under his supervision. He was awarded the State Prize of Ukraine in the field of science and technology.

***Problems of Tribology**, V. 27, No 3/105-2022*

Problems of Tribology
Website: http://tribology.khnu.km.ua/index.php/ProbTrib
E-mail: tribosenator@gmail.com

INFORMATION ABOUT JOURNAL"PROBLEMS OF TRIBOLOGY"

POLICY (GOAL AND TASKS)

"Problems of Tribology (Problems of Tribology)" - an international scientific journal.

Along with the main task of collecting information from tribology, the journal also performs organizational and coordinating functions:

- coordination of scientific and technical work in the field of tribology;
- organization of conferences, sympsiums;
- organization of work on the creation of databases and expert systems in the field of tribology;
- the organization of communications and information exchange between specialists in the field of tribology internationally.

2. The journal contains articles directly or indirectly related to tribology, including:

- theoretical problems (physics, chemistry, mechanics, mathematics)
- experimental methods and research results;
- contact mechanics, friction, wear, lubrication, durability and reliability of friction units of machines and units;
- scientific, technical and production problems of manufacturing, repair, improving the quality, reliability and durability of friction;
- technological and structural methods of improving wear resistance, frictional and anti-friction properties of friction units;
- problems of tribo materials science;
- methodological and methodological issues of training specialists in tribology.

3. The main requirements of the article is the novelty and completeness of information.

Articles of theoretical content should include theoretical explanation (possibly in the form of an annex to the article) to assess the scientific novelty of the publication.

Experimental articles should contain complete information about the methodology, conditions and results of the experiment.

Technological profile articles should contain a description of the technology as much as possible. If it is impossible to disclose "know-how", the method of obtaining the necessary detailed information must be indicated.

4. All articles are reviewed by a closed double review for compliance with the topics and level requirements. At the same time, the authors are fully responsible for the content of the articles.

5. Due to the international nature of the journal it is preferably submit articles in English.

REQUIREMENTS TO THE ARTICLES

In order to publish an article in the journal authors should submit it by e-mail.

Text of an article should be laid out on A4 format (210 x 297 mm) page with the following margins set: left and right – 2.0 cm, top and bottom – 2.5 cm. Use the font Times New Roman throughout, single-spacing, 10-point type and 1.0 cm indention for body text. Use lower-case bold 14-point type for headings. Put subheadings in bold.

Article structure:

– Universal Decimal classification index (in the upper left corner).

– Initials and surnames of all authors (no more than 4 people) and the article title (up to 10 words) in Ukrainian, Russian and English (one-column format).

– Abstract (200–300 words, only commonly accepted terminology) in Englishshould be structured and contain the following elements: purpose, methodology, findings, originality, practical value, keywords (6–8 words), one-column format. The abstract should not repeat the heading of the article.

– Body text.

– Reference list.

– Abstracts and keywords (up to 6–8words) in the Ukrainian and Russian languages;

Each article should include the following sections:

– An introduction, indicating article's scientific problem.

– An analysis of the recent research and publications.

– Unsolved aspects of the problem.
– Objectives of the article.
– Presentation of the main research and explanation of scientific results.
– Research conclusions and recommendations for further research in this area.
– The title and number of the project in terms of whichthe presented results were obtained and Acknowledgements to the organizations and/or people contributing to or sponsoring the project (at the discretion of the author)

The recommended length of articles (including text, tables, and figures) is 6–9 pages. Figures should not exceed 25 % of length of an article. The text should be laconic, and should not contain duplicated information. No running titles and section brakes should be applied in the file.

Figures must be provided both in color and grayscale. They must be included in the text after corresponding references and given as separate files TIFF, JPG. EPS (300 dpi). The preferable width for the figures is 8.15 cm; not more than 17 cm for maps, charts, etc. All figures should be placed within the text, not in tables. Lettering, lines and symbols must be readable. Captions under the figures should contain order number and description of the figure and should be put in Italics. Placing the figure numbers and captions inside figures is not allowed.

Equationsshould be entered using Microsoft Word for Windows Editor plug-in or Microsoft Equation, 10-point type. The equations sited in the text are to be numbered in order of their appearance in the text (number in brackets with right justify). Equations should be column width (<8 cm). Long formulas should be divided into parts of 8 cm width. Before and after each formula there should be one empty line. Physical quantities should be measured in SI units. An integer part should be separated from a decimal by a dot.

Tablesmust be in portrait orientation, have titles and be numbered. Preferably tables should not exceed 1 page in length; width should make 8.15 cm or 17 cm. It is recommended to use 8–9-point type (not smaller than 6-point type for big data).

References(no more than 15 items, published not earlier than 5 years before, no more than 20%of self-citations) should be listed in the order of appearance in the text of the article. The in-text references should be given in square brackets.

Also the author should submit the following data about all authors of the article: surname, name and patronymic, academic degree, academic rank, place of employment (complete name of organization), position, city, country, phone number, e-mail and authors' ORCID identifier, in a separate file in English, Ukrainian and Russian (one-column format, comma-separated).

REVIEW PROCEDURE

All manuscripts are initially treated by editors to assess their compliance with the requirements of the journal and the subject.

After the editor decision the manuscripts are sent to at least two external experts working in this area. **The manuscript goes double-blind peer review**, neither the authors nor the reviewers do not know each other.

Review comments transmitted to the author, together with a recommendation for a possible revision of the manuscript. Publishing editor reports to the authors about adopting manuscript without require revision or authors are given the opportunity to review the manuscript and submit it again, or manuscript rejected.

EDITORIAL ETHICS

Principles of professional ethics in the work of the editor and publisher

The editor of a peer-reviewed journal is responsible for deciding which of the articles submitted to the journal should be published. The validation of the work in question and its importance to researchers and readers must always drive such decisions.

- An editor should make decisions on which articles to publish based on representational faithfulness and scholarly importance of the proposed work.
- An editor should be alert to intellectual property issues and must not to publish information if there are reasons to think that it is plagiarism. ·
- An editor should evaluate manuscripts for their intellectual content without regard to race, gender, sexual orientation, religious belief, ethnic origin, citizenship, social set-up or political philosophy of the authors.
- Unpublished materials disclosed in a submitted manuscript must not be used in an editor's own research without the express written consent of the author. Privileged information or ideas obtained through peer review must be kept confidential and not used for personal advantage.
- An editor should take reasonably responsive measures when ethical complaints have been presented concerning a submitted manuscript or published paper, in conjunction with the publisher (or society). Every reported act of unethical publishing behavior must be looked into, even if it is discovered years after publication.

Publishers should provide reasonable practical support to editors and define the relationship between publishers, editor and other parties in a contract.

- Publishers should protect intellectual property and copyright.

- Publishers should foster editorial independence.
- Publishers should work with journal editors to set journal policies appropriately and aim to meet those policies, particularly with respect to editorial independence, research ethics, authorship, transparency and integrity (for example, conflicts of interest research funding, reporting standards), peer review and the role of the editorial team beyond that of the journal editor, appeals and complaints.
- Publishers should communicate and periodically review journal policies (for example, to authors, readers, peer reviewers).
- Publishers should assist the parties (for example, institutions, grant funders, governing bodies) responsible for the investigation of suspected research and publication misconduct and, where possible, facilitate in the resolution of these cases.
- Publishers are responsible for publishing corrections, clarifications and retractions.

Ethical principles in the reviewer work

Peer review assists the editor in making editorial decisions and through the editorial communications with the author may also assist the author in improving the paper. That is why actions of a reviewer should be unbiased.

- Any manuscripts received for review must be treated as confidential documents. They must not be shown to or discussed with others except as authorized by the editor.
- Reviews should be conducted objectively. Personal criticism of the author is inappropriate. Referees should express their views clearly with supporting arguments.
- Unpublished materials disclosed in a submitted manuscript must not be used in a reviewer's own research without the express written consent of the author. Privileged information or ideas obtained through peer review must be kept confidential and not used for personal advantage.
- Any selected referee who feels unqualified to review the research reported in a manuscript or knows that its prompt review will be impossible should notify the editor and excuse himself from the review process.

Principles that should guide the author of scientific publications

Authors realize that they are responsible for novelty and faithfulness of research results.

- Authors of reports of original research should present an accurate account of the work performed as well as an objective discussion of its significance. Underlying data should be represented accurately in the paper. A paper should contain sufficient detail and references to permit others to replicate the work. Fraudulent or knowingly inaccurate statements constitute unethical behavior and are unacceptable.
- An author should ensure that they have written entirely original works, and if the author has used the work and/or words of others, then this has been appropriately cited or quoted. Plagiarism in all its forms constitutes unethical publishing behavior and is unacceptable.
- Proper acknowledgment of the work of others must always be given. Author should cite publications that have been influential in determining the nature of the reported work. Information obtained privately, as in conversation, correspondence, or discussion with third parties, must not be used or reported without explicit, written permission from the source. Information obtained in the course of confidential services, such as refereeing manuscripts or grant applications, must not be used without the explicit written permission of the author of the work involved in these services.
- An author should not in general publish manuscripts describing essentially the same research in more than one journal or primary publication. Submitting the same manuscript to more than one journal concurrently constitutes unethical publishing behavior and is unacceptable. In general, an author should not submit for consideration in another journal a previously published paper.
- All those who have made significant contributions should be listed as co-authors. Where there are others who have participated in certain substantive aspects of the research project, they should be acknowledged or listed as contributors. The corresponding author should ensure that all co-authors have seen and approved the final version of the paper and have agreed to its submission for publication.
- When an author discovers a significant error or inaccuracy in their own published work, it is the author's obligation to promptly notify the journal editor or publisher and cooperate with the editor to retract or correct the paper. If the editor or the publisher learns from a third party that a published work contains a significant error, it is the obligation of the author to promptly retract or correct the paper or provide evidence to the editor of the correctness of the original paper.

CONTACTS

International scientific journal “Problems of Tribology”,
Khmelnitsky National University,
Institutskaia str. 11, Khmelnitsky, 29016, Ukraine
phone +380975546925
E-mail: tribosenator@gmail.com
Internet: http://tribology.khnu.km.ua